

Detecting prompt and afterglow jet emission of gravitational wave events from LIGO/Virgo/KAGRA and next generation detectors

Ravjit Kaur ^{1,2,*} Brendan O'Connor, ^{3,†} A. Palmese ^{3,4,‡} and Keerthi Kunnumkai³

¹*Department of Astronomy, University of California Berkeley,
501 Campbell Hall 3411, Berkeley, CA 94720-3411, USA*

²*Department of Astronomy and Astrophysics, University of California Santa Cruz, 1156 High St, Santa Cruz, CA 95064, USA*

³*McWilliams Center for Cosmology and Astrophysics, Department of Physics,*

Carnegie Mellon University, Pittsburgh, PA 15213, USA

⁴*Department of Physics, University of California Berkeley,*

366 LeConte Hall MC 7300, Berkeley, CA 94720, USA

(Dated: October 15, 2024)

Following the wealth of new results enabled by multimessenger observations of the binary neutron star (BNS) merger GW170817, the next goal is increasing the number of detections of electromagnetic (EM) counterparts to gravitational wave (GW) events. Here, we study the detectability of the prompt emission and afterglows produced by the relativistic jets launched by BNS mergers that will be detected by LIGO-Virgo-KAGRA (LVK) during their fifth observing run (O5), and by next generation (XG) GW detectors (Einstein Telescope and Cosmic Explorer). We quantify the impact of various BNS merger and jet afterglow parameters on the likelihood of detection for a wide range of telescopes, focusing on the impact of the observer's viewing angle θ_v and the jet's core half-opening angle θ_c . We find that during the LVK O5 run, the *James Webb Space Telescope* (JWST) is expected to reach the largest number of afterglow detections, up to 32% of BNS mergers with 27% detectable on timescales > 10 d. Overall the detection of 20–30% of events is possible across the EM spectrum with the available instruments, including the *Chandra X-ray Observatory*, the *Nancy Grace Roman Space Telescope*, the Square Kilometer Array (SKA), and the Very Large Array (VLA). In the XG era, afterglows for 20–25% of events will be detectable with *AXIS*, *Athena*, *Lynx*, *UVEX*, *JWST* and the next generation VLA (ngVLA), reaching beyond redshift $z \gtrsim 1$. We also find that the majority of detected afterglows are expected to accompany prompt gamma-ray emission detectable by the *Neil Gehrels Swift Observatory*, the *Space-based multi-band astronomical Variable Objects Monitor* (SVOM), and the *Transient High-Energy Sky and Early Universe Surveyor* (THESEUS), with at least $\sim 6\%$ of afterglows being orphan.

I. INTRODUCTION

Over the past decade, gravitational wave (GW) observations have unlocked a new view of the Universe, unleashing a fruitful period of multimessenger astrophysics. Made possible by the Advanced LIGO (Laser Interferometer Gravitational-Wave Observatory; [1]), Virgo [2], and KAGRA [3], GW discoveries allow for observations of astrophysical phenomena that cannot often be studied by other means. The first (and thus far, only) multimessenger detection of a GW merger is the binary neutron star (BNS) merger GW170817 [4], detected by LIGO/Virgo in GWs, and followed by multiple EM counterparts. A short duration gamma-ray burst (GRB) was detected by both the *Fermi Gamma-Ray Space Telescope* [5] and *INTEGRAL* [6], followed by subsequent detections in X-ray, ultraviolet, optical, infrared, and radio wavelengths of both the kilonova [7–24] and jet afterglow [25–40]. This multimessenger event addressed critical open questions regarding jet launching and jet structure, the production of heavy elements, the neutron star equation of state, and the expansion of the Universe [for a review see, e.g., 41, 42].

The detection of future EM counterparts to GW events, like GW170817, are crucial to continue advancing our knowledge

of these topics, and to provide an accurate measurement of the Hubble constant independent of the cosmic distance ladder [e.g., 43–51]. However, in order to identify a counterpart and maximize the scientific output of a discovery, we require sensitive telescopes at a variety of wavelengths to detect the counterpart across the EM spectrum (radio to X-rays). Given the tail of relatively small GW localization regions (< 100 deg² for a significant fraction of events; e.g. [52, 53]) expected during the fifth LIGO-Virgo-KAGRA (LVK) observing run (O5, starting $\sim 2027^1$), this observing run will provide a prime opportunity for counterpart discovery. However, the ideal strategy to implement (cadence, sensitivity, filters), and telescopes to use, is still partially an open question for both kilonovae [e.g., 54–66] and afterglows [e.g., 67–79].

The ground-breaking detection of GRB 170817A [5, 6] following GW170817 [4] demonstrated conclusively that BNS mergers are capable of launching highly collimated, highly relativistic outflows. The interaction of the relativistic jet with the surrounding environment causes a forward shock that produces non-thermal synchrotron radiation across the EM spectrum [80–83], called the “afterglow” [84–87]. In typical observations of cosmological GRBs, we see them on-axis (aligned with our line of sight) where the observer's viewing angle θ_v is less than the jet's core half-opening angle θ_c [88, 89]. In this case, both the afterglow and prompt

* ravkaur@ucsc.edu

† boconnor2@andrew.cmu.edu; McWilliams Fellow

‡ palmese@cmu.edu; NASA Einstein Fellow

¹ <https://observing.docs.ligo.org/plan/>

gamma-ray emission is dominated by the jet’s core. However, in the case of GW170817, the jet was observed at a large angle ($\sim 15 - 30$ degrees) with respect to the jet’s axis [33, 40, 47, 90–98], revealing new information about the angular structure of the jet and showing that in the nearby Universe the detection of lower luminosity emission from the jet’s “wings” is possible. Future afterglow observations in conjunction with GWs will reveal the structure and half-opening angle of short GRB jets [99–104].

As the GW amplitude is anisotropic and larger for on-axis events [e.g., 105], which we define here as $\theta_v < \theta_c$ with respect to GRB afterglows and as an inclination angle of $\iota \approx 0$ for GW mergers, this introduces a Malmquist bias that, for an isotropic distribution of viewing angles, leads the events detected in GWs by current advanced detectors to most likely be detected with $\theta_v \approx 35$ deg [106]. If we assume a typical jet core half-opening angle of $\theta_c \approx 6$ deg [107, 108] this naively implies that half of the events will have viewing angles larger than $\theta_v/\theta_c \gtrsim 6$, similar to the inferred value for GW170817 of $\theta_{\text{obs}}/\theta_c \approx 5 - 6$ [33, 47, 90–93, 96, 97]. As the afterglow of GW170817 was difficult to detect with current instruments at high signal-to-noise over a long period of time, requiring only the handful of most sensitive instruments at each wavelength (i.e., *Chandra*, *HST*, VLA), we can expect that GW mergers during LVK O5 (and A#; McIver et al. in prep.) and next-generation detector runs, when the detection horizon increases substantially, will be more difficult to detect given they are likely at $\gg 40$ Mpc. However, the increase in distance is timed with the launch or commissioning of next generation telescopes at all wavelengths. Here we seek to quantify the ability to detect the off-axis afterglows of BNS mergers using the more sensitive suites of instruments available in the coming decade(s).

As for far off-axis observers the time of the peak $t_p \propto (\theta_v/\theta_c)^2$ and flux at peak $F_p \propto (\theta_v/\theta_c)^{-2p}$ are modified significantly compared to the on-axis expectations [109–113], we expect a similar Malmquist bias toward viewing angles closer to their jet’s core, which are also more likely to be the GW mergers detected at larger distances. At cosmological distances current short GRB observations are dominated by the on-axis sample [$\theta_v < \theta_c$; 89], but the additional information from the GW merger as a trigger time and localization may allow for this population to be extended to larger viewing angles. Though we note that the lack of clearly off-axis GRBs at cosmological distances may be due to a reduced prompt gamma-ray efficiency outside the narrow core of these jets [89, 99]. In this case an off-axis GRB would appear as an orphan afterglow [70, 90, 109, 114–126].

The uncertain viewing angle derived for the majority of GW mergers with current generation detectors [e.g., 127] complicates searches for afterglows as the likely peak time $t_p \propto (\theta_v/\theta_c)^2$ is not well constrained by the initial information. However, refined GW analysis following the identification of a kilonova and redshift z can allow for accurate determinations of the viewing angle [e.g., 127], aiding in afterglow searches. In the absence of a clear narrow-field localization for the merger from either the prompt gamma-ray detection of a GRB as in GW170817, or from a kilonova detection in wide-

field searches [e.g., 59], the efficient way to search for the afterglow is with wide-field pointed instruments at late times (e.g., *ULTRASAT* or *Einstein Probe*) or in upcoming surveys (e.g., the Vera Rubin Observatory or the Square Kilometer Array).

In this paper, we simulate the likelihood of detecting an afterglow counterpart to GW events during LVK O5 and with respect to next-generation (XG) detectors, such as Cosmic Explorer (CE; [128]) and Einstein Telescope (ET; [129]), expected to start operations in the late 2030s. We simulate the likelihood of detection over all wavelengths for a range of telescopes (radio to X-ray). We consider both small and large Field of View (FoV) telescopes, to take into account the case where a KN or sGRB is identified and pointed searches deep-field can occur, as well as the case in which the afterglow is the only EM counterpart to be detected. We use realistic GW sky localizations, distances, and viewing angles expected for O5 and next-generation to simulate afterglow lightcurves for comparison to the different telescope sensitivities. Additionally, we look at the impact of jet opening angle on detectability of the afterglow.

The paper is laid out as follows. In §II, we discuss the GW simulations, the parameters used for the jet afterglow simulations, and the telescopes and sensitivities considered in this work. In §III, we present our findings and compare the detectability across all telescopes and wavelengths. Lastly, in §IV, we discuss implications of these findings and possibilities for future work. Throughout this work we assume the Planck Collaboration results [130] under a flat Λ CDM cosmology.

II. SIMULATIONS

A. GW simulations

We produce realistic simulations of GW events with LVK O5 sensitivities, as well as next-generation CE [128] and ET [129] detector sensitivities. We use BAYESTAR, a rapid sky localization code to localize the sky area [131], tools from LALSuite [132] to make simulations of GW events, and the public software `ligo.skymap` to generate and visualize the GW skymaps. The mass and spin distributions for the O5 simulations are chosen as described in [133–135]. We use the population posterior samples from Farah *et al.* [135] to draw masses. We uniformly distribute the mass and spin samples in comoving volume and isotropically distribute them in the orbital orientation and sky location. We draw 10^5 samples from the distribution, which include binary neutron star (BNS) mergers, binary black hole (BBH) mergers, and neutron star-black hole (NSBH) mergers. We filter these events to satisfy our detection criteria for LVK O5 (network SNR > 8), assuming the detector sensitivities from <https://dcc.ligo.org/LIGO-T2000012-v1/public> (A+ for the two LIGO detectors, `avirgo_O5low_NEW.txt` for Virgo, `kagra_128Mpc.txt` for KAGRA), and a 70% duty cycle for each detector. We then filter by mass to extract the BNS mergers: mergers with a primary and secondary mass below $3M_\odot$

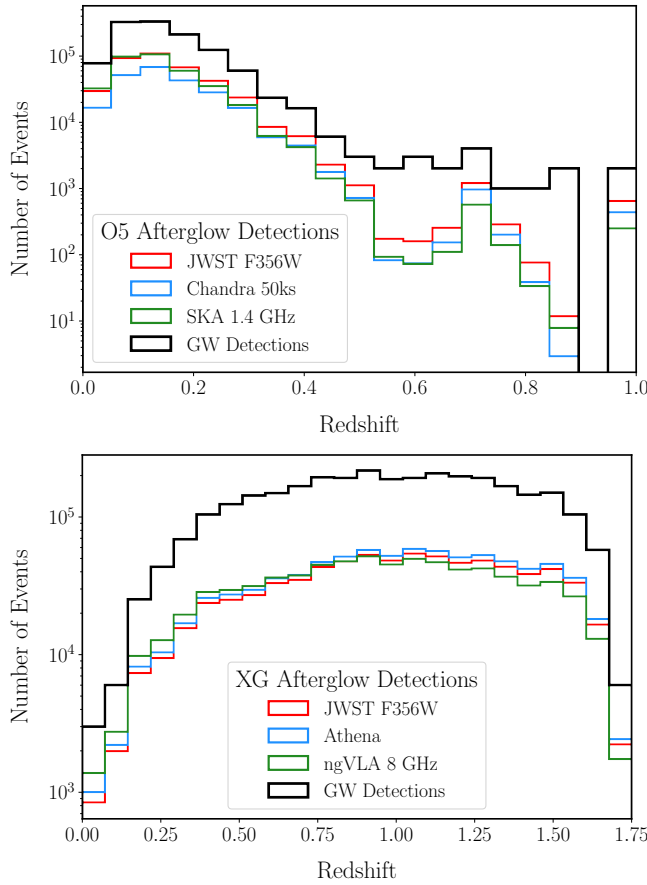


FIG. 1. Redshift distribution of all simulated NS mergers, where for each GW event, see §II A, we simulated 1,000 afterglows. Events with GW detections are shown in black, and the distribution of those events that had an afterglow detectable by instruments in X-ray (blue), UVOIR (red), and Radio (green) are also shown. The top figure displays these distributions for O5, and the bottom for XG.

are considered to be BNSs. Through this process, we obtain 1,166 BNS GW events for O5. For more details about the O5 simulations see Kunnumkai *et al.* [65, 66].

For next generation detectors, we do not use the [135] population posterior samples as we would need to extrapolate those to significantly larger redshifts compared to O5, which may not be realistic to assume. Instead, we assume a Gaussian distribution centered at $1.5 M_{\odot}$ with standard deviation $1.1 M_{\odot}$, consistent with the [133] parametric fits results. The redshift distribution follows the cosmic star formation density [136]. This time, we inject 10^6 events to ensure that we have enough samples at all redshifts, given that the observable volume is larger. We assume 1 CE and 1 ET detector, using the sensitivity curves from [137]² for a baseline 40 km CE facility and the ET-D design from [138]. We require an SNR threshold of 4 for single detectors, and a minimum network

SNR of 12 for detection. We require an event to be detected by 2 detectors and assume a duty cycle of 70% for both ET and CE. We have 169,560 detected BNS GW events for this next-generation network. We select a random sub-sample of 3,000 events, comparable to the number for O5, in order to use within this work. We show the redshift distribution of our GW detections in Figure 1. The distance and viewing angle of all simulated events for O5 and XG are shown in Appendix A (see Figures 10 and 11).

B. Multi-wavelength telescopes and instrument sensitivities

The afterglow of a binary neutron star merger can be discovered through three routes: *i*) the rapid identification (< 1 d) of either an X-ray, optical, or radio afterglow following a joint GW-GRB trigger, *ii*) localized late-time ($\sim 10 - 100+$ d) observations following the detection of a kilonova in wide-field searches after the initial localization of either a GW or joint GW-GRB with a large sky localization, *iii*) late-time observations covering the localization of either a GW or GRB in the event a kilonova was not discovered (i.e., no arcsecond localization is available). The first method depends largely on the viewing angle θ_v with respect to the jet's core half-opening angle θ_c , as their ratio θ_v/θ_c dictates the behavior of the afterglow lightcurve [e.g., 171]. The second method depends largely on source visibility to telescopes in either the Northern or Southern hemispheres or to space-based observatories (e.g., *Roman*, *ULTRASAT*) to discover the kilonova and allow for well-localized and sensitive late-time observations (e.g., VLA, Chandra, JWST) to detect the afterglow peak (for an off-axis merger). The third method requires wide-field survey instruments to perform the follow-up using a similar tiling strategy as carried out at earlier times for kilonovae. In this case the exact strategy and timing of the observations to best catch the peak is unclear initially, and largely depends on the unknown viewing angle.

As there are multiple methods, strategies, and telescopes to localize and detect the EM counterpart of a BNS merger, we focus simply on the ability of a variety of telescopes to detect the afterglow, as opposed to their likelihood to localize and then characterize the afterglow behavior. We consider a range of telescopes that will be available during LVK O5 and mission concepts that may exist at the same time as XG detectors. We consider both sensitive narrow-field instruments and wide-field survey telescopes covering a range of wavelengths (X-ray, ultraviolet, optical, infrared, and radio) in our analysis. The telescopes and their assumed sensitivities are listed in Table I.

1. LVK O5

For LVK O5 we consider a majority of telescopes that are already currently active and likely to still be operational in ~ 2027 . At X-ray wavelengths these include the *Chandra X-ray Observatory* [139], the eROSITA instrument onboard the *Spectrum-Roentgen-Gamma* mission [140], *Neil Gehrels*

² <https://dcc.cosmicexplorer.org/cgi-bin/DocDB>ShowDocument?docid=T2000017>

TABLE I. The X-ray, ultraviolet, optical, infrared, and radio wavelength instruments and their compiled parameters used throughout this work. The run column depicts whether the instrument was considered for our O5 runs, XG runs, or both, according to whether it will be operational during the correct time frame. The % afterglows detected columns refer to the results for simulation Run 1 (§II C) We count an afterglow event as detected by a specific instrument if the simulated lightcurve flux values for that event are at any point greater than the sensitivity for that instrument. X-ray sensitivities are reported at 1 keV assuming a photon index of $\Gamma = 1.7$.

Telescope		Exposure Time	Sensitivity (mJy)	Field of View	Run	% Afterglows Detected (O5)	% Afterglows Detected (XG)	References
X-ray	Frequency (keV)							
<i>Chandra</i>	0.5-8	50 ks	4.4×10^{-7}	9.7 arcmin ²	O5	20.1	–	[139]
eROSITA	0.2-2.3	1.6 ks	2.2×10^{-6}	0.833 deg ²	O5	16.7	–	[140]
<i>Einstein Probe</i>	0.5-2	1.5 ks	1.4×10^{-5}	3600 deg ²	O5	13.2	–	[141, 142]
<i>Swift/XRT</i>	0.3-10	5 ks	4.8×10^{-5}	23.6' \times 23.6'	O5	11.0	–	[143]
<i>SVOM/MXT</i>	0.2-10	10 ks	9.5×10^{-5}	1.1° \times 1.1°	O5	9.7	–	[144]
<i>Athena</i>	0.2-10	50 ks	5.9×10^{-9}	40' \times 40'	XG	–	26.8	[145, 146]
<i>AXIS</i>	0.2-10	50 ks	9.6×10^{-9}	0.125 deg ²	XG	–	25.5	[147]
<i>Lynx</i>	0.5-2	100 ks	1.9×10^{-9}	0.105 deg ²	XG	–	30.3	[148]
UVOIR	Frequency (Hz)							
<i>ULTRASAT</i> (NUV)	1.3×10^{15}	900 s	4.4×10^{-3}	204 deg ²	O5	9.6	–	[149]
<i>UVEX</i> (NUV)	1.3×10^{15}	900 s	5.8×10^{-4}	12 deg ²	O5, XG	13.4	8.8	[150]
Rubin (g-band)	6.2×10^{14}	30 s	4.8×10^{-4}	9.6 deg ²	O5, XG	14.8	10.3	[151]
Rubin (i-band)	4.0×10^{14}	30 s	1.1×10^{-3}	9.6 deg ²	O5, XG	13.8	8.9	[151]
Rubin (g-band)	6.2×10^{14}	180 s	1.4×10^{-4}	9.6 deg ²	O5, XG	17.3	13.1	[151]
Rubin (i-band)	4.0×10^{14}	180 s	3.2×10^{-4}	9.6 deg ²	O5, XG	16.2	11.8	[151]
<i>Euclid</i> (H-band)	1.7×10^{14}	360 s	9.1×10^{-4}	0.57 deg ²	O5, XG	15.3	10.4	[152]
<i>Roman</i> (R-band)	4.9×10^{14}	67 s	1.2×10^{-4}	0.28 deg ²	O5, XG	18.0	13.9	[153, 154]
<i>Roman</i> (J-band)	2.3×10^{14}	67 s	2.3×10^{-4}	0.28 deg ²	O5, XG	17.8	13.5	[153, 154]
<i>JWST</i> (F150W)	2.0×10^{14}	7000 s	6.9×10^{-6}	9.7 arcmin ²	O5, XG	28.4	22.3	[155]
<i>JWST</i> (F356W)	8.5×10^{13}	7000 s	5.3×10^{-6}	9.7 arcmin ²	O5, XG	32.4	24.6	[155]
ELT (J-band)	2.3×10^{14}	5 hr	1.3×10^{-5}	78.5 arcmin ²	O5, XG	25.6	20.4	[156]
ELT (H-band)	1.9×10^{14}	5 hr	5.8×10^{-6}	78.5 arcmin ²	O5, XG	15.3	22.9	[156]
Radio	Frequency (GHz)							
ALMA	97.5	1 hr	3.0×10^{-2}	–	O5	13.9	–	[157]
ALMA	187	1 hr	6.5×10^{-2}	–	O5	10.6	–	[157]
ALMA	324	1 hr	2.2×10^{-1}	–	O5	6.5	–	[157]
ATCA	2.1	2 hr	3.6×10^{-2}	–	O5	17.4	–	[158]
ATCA	5.5	2 hr	2.4×10^{-2}	–	O5	18.2	–	[158]
ATCA	9	2 hr	2.4×10^{-2}	–	O5	17.6	–	[158]
VLA	6	2 hr	7.0×10^{-3}	–	O5	25.5	–	[159]
VLA	10	2 hr	7.5×10^{-3}	–	O5	23.9	–	[159]
VLA	22.25	2 hr	1.3×10^{-2}	–	O5	29.4	–	[159]
SKA	1.4	1 hr	6.0×10^{-3}	–	O5, XG	30.4	9.5	[160, 161]
SKA	9	1 hr	3.6×10^{-3}	–	O5, XG	28.5	11.2	[160, 161]
SKA	12.5	1 hr	3.6×10^{-3}	–	O5, XG	27.7	11.0	[160, 161]
ngVLA	2.4	1 hr	7.2×10^{-4}	–	XG	–	22.1	[162, 163]
ngVLA	8	1 hr	4.2×10^{-4}	–	XG	–	23.8	[162, 163]
ngVLA	16	1 hr	4.8×10^{-4}	–	XG	–	21.9	[162, 163]

Swift Observatory [172] X-ray telescope (XRT; [173]), *Space-based multi-band astronomical Variable Objects Monitor* (SVOM; [174, 175]) Microchannel X-ray Telescope (MXT; [144]), and the Wide-field X-ray Telescope (WXT) on the

Einstein Probe [142]. At ultraviolet wavelengths we consider the *Ultraviolet Transient Astronomy Satellite* (ULTRASAT, \sim 2026; [149]) and the *Ultraviolet Explorer* (UVEX, \sim 2030; [150]), while at optical and near-infrared wavelengths we have

TABLE II. The gamma-ray satellites and their compiled parameters used throughout this work to consider joint GRB and GW detections. For simplicity we consider each of these satellites for both LVK O5 and XG detector runs as representative gamma-ray sensitivities in these eras.

Telescope	Energy (keV)	Flux Limit (erg/cm ² /s)	Run	% GRBs Detected (O5)	% GRBs Detected (XG)	References
<i>Swift</i> -BAT	15-150	2×10^{-8}	O5, XG	27.9	19.8	[164]
<i>Fermi</i>	50-300	2×10^{-7}	O5, XG	19.8	7.1	[165]
<i>SVOM</i>	4-150	2×10^{-8}	O5, XG	29.4	21.2	[166]
<i>Daksha</i>	20-200	4×10^{-8}	O5, XG	25.9	16.5	[167, 168]
<i>THESEUS</i>	2-10,000	3×10^{-8}	O5, XG	30.1	23.2	[169, 170]
<i>COSI</i>	200-1,000	6×10^{-7}	O5, XG	15.2	2.7	<i>COSI</i> ^a

^a Level 2 requirements document, J. Tomsick private communication.

included the *James Webb Space Telescope* [JWST; 155], *Euclid* [176], the *Nancy Grace Roman Space Telescope* (*Roman*, \sim 2026; [177]), the *Vera Rubin Observatory's Legacy Survey of Space and Time* (LSST, \sim 2025; [151]), and the *Extremely Large Telescope* (ELT, \sim 2028; [156]). At radio wavelengths we include the *Very Large Array* [VLA; 159], the *Australia Telescope Compact Array* [ATCA; 158], the *Atacama Large Millimeter Array* [ALMA; 157], and the *Square Kilometer Array* (SKA, \sim 2029; [161]).

The typical exposure times and sensitivities for each instrument are compiled in Table I and are tabulated from the literature for mission concepts or using the instrument exposure time calculators for active missions (e.g., *Chandra*, *Swift*, JWST, VLA, and ATCA). Field of views (FoVs) for the instruments are also tabulated in Table I.

This study is not a comprehensive list of all available instruments that will be available for use during LVK O5. Moreover, a handful of these missions, which cannot be predicted, may still be operational in the mid- to late-2030s when XG detectors are expected to come online. However, the expectation is that current mission concepts will replace them in sensitivity, and thus we consider the majority of these instruments only for LVK O5.

2. XG detectors

For XG detector runs, the majority of instruments we consider are currently only mission concepts (though some are actively being developed) that may be active in the mid- to late-2030s as a representative case for the available instruments in the XG era. The only currently operational missions we consider for the XG era are *Euclid* and JWST, though we tentatively include Rubin in this category as well given its rapidly approaching start date. In the XG era the LSST is likely complete (after its 10 yr run) and more Rubin Observatory time may be available to dedicate to GW and GRB follow-up. We therefore consider also the potential for longer exposures (e.g., 180 s) in each filter [e.g., 60].

For potential future missions we consider *Athena* [\sim 2037; 145, 146, 178], *AXIS* [\sim 2032; 147], and *Lynx* [\sim 2036; 148] at X-ray wavelengths and the next-generation VLA (ngVLA, \sim 2035; [68, 162, 163]) at radio wavelengths. At ultraviolet

and near-infrared wavelengths we also consider *UVEX*, *Roman*, and thirty meter class telescopes such as the ELT.

While the available missions during XG detector runs are not clear and can change with time, these instruments offer a range of possible sensitivities during this timeframe across the EM spectrum.

3. Gamma-ray satellites

We consider a range of available gamma-ray satellites that currently exist and which are likely to exist during LVK O5. The available missions at the time XG detectors will be operational are not known, and we consider the current available detectors and some likely mission concepts as characteristic gamma-ray detector sensitivities for missions to launch in the mid- to late-2030s. Sensitive and large field-of-view gamma-ray telescopes are required to increase the chance for joint GRB and GW detections, which in turn greatly increase the chances of identifying an additional EM counterpart, namely a kilonova or jet afterglow.

For current instruments we consider the *Swift* Burst Alert Telescope [BAT; 179], the *Fermi Gamma-ray Burst Monitor* [180], and *SVOM/ECLAIRs* [166, 181]. As proposed mission concepts we consider *Daksha* [76, 167, 168] and the *Transient High-Energy Sky and Early Universe Surveyor* [THESEUS; 169, 170]. We also consider the Compton Spectrometer and Imager [*COSI*; 182–184] which has planned launch in \sim 2027. We note that there are a number of other currently proposed mission concepts that may be selected or that already have been selected, and that our study is not a comprehensive analysis of all available or potential instruments, see, e.g., *AMEGO-X*, *StarBurst*, *MoonBEAM*, and many others.

C. Afterglow simulations

1. Afterglowpy

We use the publicly available `afterglowpy` package³ [v0.8.0; 97, 171] to simulate GRB jet afterglow lightcurves over a range of afterglow parameters and jet structures. We apply `specType=0`, corresponding to synchrotron radiation from a forward shock [81–83] without the inclusion of inverse Compton effects [185–189]. We consider only jets propagating into a uniform density environment, typical of short GRBs [107, 190]. The generated afterglow depends on the following parameters: the observer’s viewing angle, θ_v ; the isotropic equivalent kinetic energy of the jet’s core, $E_{\text{kin},0}$; the jet’s core half-opening angle, θ_c ; the jet truncation angle outside of which the energy is 0, θ_w ; the circumburst density, n ; the electron energy distribution index, p ; the fraction of energy that goes into relativistic electrons, ϵ_e ; the fraction of energy that goes into magnetic energy, ϵ_B ; the luminosity distance to the source, d_L ; and the corresponding redshift z .

We consider GRB jets with both a power-law (PLJ; `jetType=4`) and Gaussian (GJ; `jetType=0`) angular kinetic energy structure $E_{\text{kin}}(\theta)$. These are defined by [171]:

$$\text{GJ: } E_{\text{kin}}(\theta) = E_{\text{kin},0} \exp\left(-\frac{1}{2} \frac{\theta^2}{\theta_c^2}\right) \quad \text{for } \theta \leq \theta_w, \quad (1)$$

$$\text{PLJ: } E_{\text{kin}}(\theta) = E_{\text{kin},0} \left(1 + \frac{1}{b} \frac{\theta^2}{\theta_c^2}\right)^{-b/2} \quad \text{for } \theta \leq \pi/2, \quad (2)$$

where $\theta_w \leq \pi/2$ is the truncation angle of the GJ and b is the power-law slope of the PLJ outside of the core. We apply a typical truncation angle of $\theta_w = 4.9\theta_c$, but also consider $\theta_w = 3\theta_c$ as a test of this assumption’s impact on our results. The truncation angle is an arbitrary parameterization of a sharp cutoff to the energy profile, observed in some numerical simulations [e.g., 191], which also serves to decrease the calculation time in `afterglowpy` for material that does not influence the observed lightcurve. In general θ_w is unconstrained in afterglow modeling, though we adopt values similar to those derived for GW170817 [e.g., 97]. We note that the PLJ model, for essentially all values of b , allows for more energetic material outside the jet’s core than the GJ model. Both the PLJ and GJ models in `afterglowpy` have been used to model the full lightcurve of GW170817 [e.g., 97, 171, 192, 193]. For the PLJ model, Ryan *et al.* [97] found a power-law slope of $b \approx 9 - 10$ was able to match the data and we adopt similar values here.

By default `afterglowpy` does not include an angular profile for the bulk Lorentz factor Γ (see Appendix B for a discussion), and generally adopts an infinite bulk Lorentz factor at all angles, leading to a deceleration radius of zero; i.e., material at all angles is in the deceleration regime (where $\Gamma(\theta) \propto E(\theta)^{1/2}$; [171]) and has skipped the initial coasting

phase (where $\Gamma = \text{constant}$). For on-axis observers there is no change to the lightcurve if observations only occur after the (on-axis) deceleration time $t_{\text{dec},0}$ [194–197]. This is the case for cosmological short GRBs, even those with rapid follow-up (< 100 s) by *Swift*, which are almost always observed in the deceleration regime, see discussions in O’Connor *et al.* [89, 190].

However, the angular Lorentz factor profile also dictates when material at different angles becomes de-beamed to the observer, and, therefore, can significantly impact the observed lightcurve for off-axis observers (Appendix B) and the inferred afterglow detectability. Therefore, we adopt an angular profile for the Lorentz factor that is the same as the energy profile (Equations 1 and 2) such that

$$\frac{\Gamma(\theta)-1}{\Gamma_0-1} = \frac{E_\gamma(\theta)}{E_{\gamma,0}}, \quad (3)$$

where Γ_0 is the initial bulk Lorentz factor at the jet’s core. This setup, defined within `afterglowpy` [171] through the `GammaEvenMass` flag (Appendix B), provides identical mass loading throughout the jet. We adopt an initial bulk Lorentz factor at the jet’s core of $\Gamma_0 = 300$ throughout this work [197].

2. Connecting to GW simulations

From our GW simulations outlined in §IIA we have produced a realistic population of GW events for both O5 and XG detector runs containing 1,166 and 3,000 BNS mergers for O5 and XG, respectively. For each of these events we obtain the inclination angle ι and luminosity distance d_L , which we convert to a redshift z assuming a flat Λ CDM *Planck* cosmology [130]. Given the inclination angle, ι , we can determine the viewing angle with respect to the jet’s axis, which we assume is aligned with the binary’s orbital angular momentum axis (which may not always be the case, see, e.g., [198] for a discussion). The viewing angle is then:

$$\theta_v = \min(\iota, \pi - \iota). \quad (4)$$

In this work, we assume that all simulated BNS launch a successful relativistic jet [e.g., 199]. We also consider the afterglow and jet structure to be independent of the compact object masses as with only a single multimessenger event these properties are not suitably connected to observations.

3. Afterglow parameter distributions

Here we outline our choices of afterglow parameter distributions that are typically found from afterglow modeling of short GRBs. The two main cases of afterglow parameters we consider are shown in Table III. For the slope p of the electron’s power-law energy distribution $N(E) \propto E^{-p}$ we adopt a uniform distribution between $U[2.1, 2.8]$. The density of the surrounding uniform environment is taken to be

³ <https://github.com/geoffryan/afterglowpy>

TABLE III. The afterglow parameter cases assumed throughout this work. Here $U[x_1, x_2]$ refers to a uniform distribution between x_1 and x_2 , and $N[y_1, y_2]$ refers to a normal distribution with median y_1 and standard deviation y_2 .

Label	p	$\log(n/\text{cm}^{-3})$	$\log \varepsilon_e$	$\log \varepsilon_B$	$\log \varepsilon_\gamma$
Case 1	$U[2.1, 2.8]$	$N[-3, 1]$	$N[-0.82, 0.15]$	$N[-3, 1]$	$N[-0.82, 0.15]$
Case 2	$U[2.1, 2.8]$	$U[-4, 0]$	$U[-2, -0.5]$	$U[-4, -0.5]$	–

TABLE IV. The simulation setups performed in this work. The same setups were used for both LVK O5 and XG detectors. Here G16 refers to the energy distribution derived from Ghirlanda *et al.* [200] while F15 refers to the inferred kinetic energy distribution from Fong *et al.* [107]. The “narrow” distribution of core angles refers to the log-normal distribution while RE22 refers to the inferred core angle distribution from Rouco Escorial *et al.* [108].

Label	Structure	Afterglow	$E_{\text{kin},0}$	θ_c	θ_w
Run 1	GJ	Case 1	G16	RE22	$\min(4.9\theta_c, \pi/2)$
Run 2	GJ	Case 1	G16	RE22	$\min(3\theta_c, \pi/2)$
Run 3	GJ	Case 1	G16	Narrow	$\min(4.9\theta_c, \pi/2)$
Run 4	PLJ	Case 1	G16	Narrow	–
Run 5	GJ	Case 2	F15	RE22	$\min(4.9\theta_c, \pi/2)$

a normal distribution in \log_{10} , with mean and standard deviation $\log(n/\text{cm}^{-3}) = -3 \pm 1$ and is based on observations of short GRB afterglows [107, 190]. The low density matches the expected distribution of interstellar medium (ISM) densities [190, 201] at their typically large host galaxy offsets [202–205]. We also adopt a lognormal distribution for the microphysical parameters of $\log \varepsilon_e = -0.82 \pm 0.15$ [206–208] and $\log \varepsilon_B = -3 \pm 1$ [209–211]. In order to test our base assumptions on these parameters (Table III) we also consider uniform distributions in $\log(n/\text{cm}^{-3}) = U[-4, 0]$, $\log \varepsilon_e = U[-2, -0.5]$, and $\log \varepsilon_B = U[-4, -0.5]$. This is discussed further in §III A.

For the jet’s core half-opening angle we adopt the probability distribution of opening angles derived in [108] based on late-time X-ray observations of short GRBs and the corresponding constraints to the time of their jet break [109, 212–215]. As we have selected a truncation angle θ_w for the GJ structure that depends on the core angle, e.g., $\theta_w = 4.9\theta_c$, we must set $\theta_w \leq \pi/2$ as an upper limit for the small sample of wide jets ($\theta_c > 15$ deg; 0.26 rad) derived in [108]. In order to test the impact of the tail of wide core angles we also utilize a distribution of narrow opening angles described by a normal distribution with mean and standard deviation of $\log(\theta_c/\text{rad}) = -1 \pm 0.15$. This distribution is centered at around 6 deg (0.1 rad) and chosen to match the approximately Gaussian distribution of core angles when excluding those with wide jets [107, 108]. A major reason for this choice is that extremely wide jets (with opening angles as wide as 30 deg; 0.5 rad) will be detectable at extreme viewing angles covering all the way out to $\theta_v \approx \pi/2$ ⁴, and we wish to ensure that this small sample of events (which are quite different from the inferred core angle for GW170817 of $\sim 3 - 5$ deg; 0.07 rad) do not significantly impact our results. We discuss this further in §III A.

In order to determine the isotropic equivalent core kinetic energy $E_{\text{kin},0}$ of the jet as input for `afterglowpy` we employ two methodologies. The first is to adopt the observed distribution of short GRB isotropic equivalent core gamma-ray luminosities $L_{\gamma,0}$ from Ghirlanda *et al.* [200] and convert them to energies $E_{\gamma,0} = L_{\gamma,0} T_{90}$ assuming a short GRB rest-frame duration of $T_{90} = 0.2$ s. The kinetic energy $E_{\text{kin},0} = E_{\gamma,0}(1 - \varepsilon_\gamma)/\varepsilon_\gamma$ is then computed assuming a gamma-ray efficiency ε_γ that is sampled from a normal distribution with mean and standard deviation -0.82 and 0.15 in $\log \varepsilon_\gamma$ [206, 207, 217]. We set a lower bound to the gamma-ray efficiency of 1%. The second method is to utilize the inferred core kinetic energies from short GRB afterglow modeling. In this case the kinetic energies are taken to be a normal distribution in $\log(E_{\text{kin},0}/\text{erg})$ with mean 51.6 and standard deviation 0.5 [107, 108]. Both of these methods obtain very similar energy distributions for short GRBs; the main difference being the low energy tail inferred by Ghirlanda *et al.* [200] (see also [218, 219]).

4. Afterglow detectability

For every simulated BNS merger (§II A) we perform a simple Monte Carlo simulation by sampling from the distribution of afterglow parameters $N = 1,000$ times. This leads to $\sim 1.1 \times 10^6$ and 3.0×10^6 simulated lightcurves for O5 and XG, respectively. We compute the afterglow lightcurves between observer frame times of 10^{-2} d and 6.5 yr after merger in 100 log-spaced steps. The afterglow fluxes are computed at each frequency corresponding to every telescope we are considering for detectability. A table containing the list of telescopes, their effective frequencies, sensitivities, and whether they are expected to be available in O5 or next-generation is shown in Table I. For each event we determine the detected fraction by comparing the afterglow lightcurve to these detector sensitivity limits at a given frequency. We perform this detectability simulation for five different setups outlined in Table IV.

⁴ We performed tests including a counter-jet within `afterglowpy` [e.g., 97, 216], but found the impact on afterglow detection to be negligible.

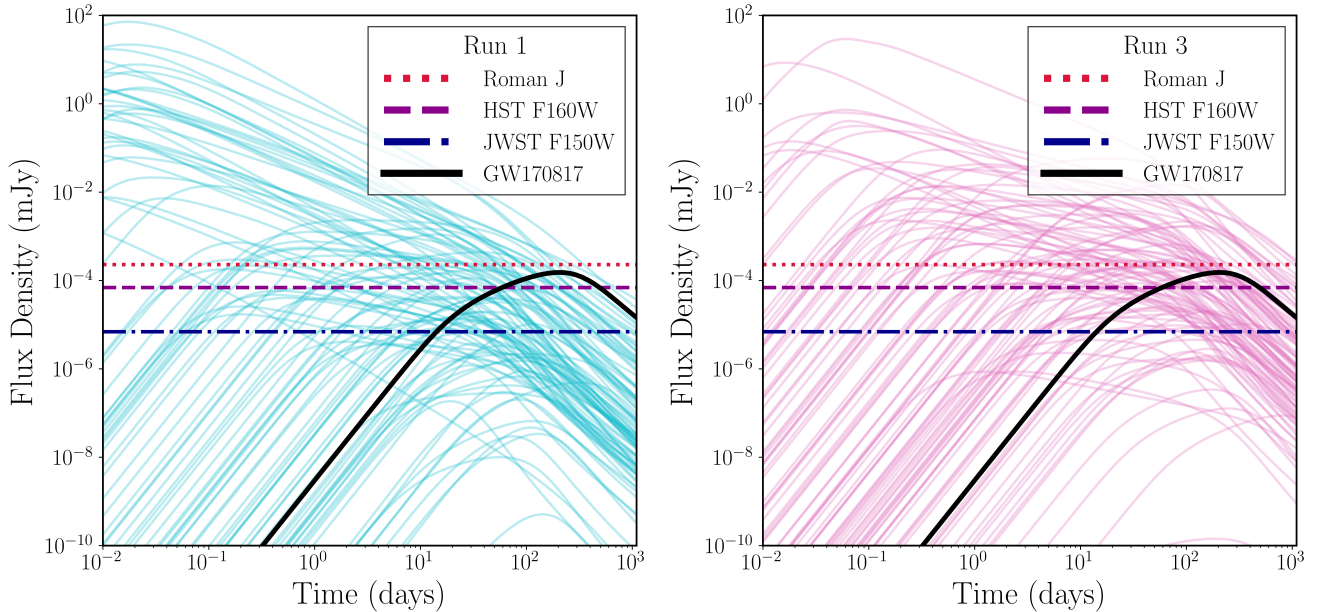


FIG. 2. 100 simulated afterglowpy lightcurves at near-infrared wavelengths showing the impact of afterglow parameter assumptions for a simulated GW event with fixed $d_L = 130$ Mpc, $\theta_v = 0.36$ rad (20 deg). The afterglow parameters are sampled from Case 1 as outlined in §II C 3. Run 1 is shown on the left in cyan, and Run 3, using the narrow distribution for θ_c , is shown on the right in pink. A lightcurve simulated from the GW170817 parameters is shown in the thick black line [97]. The sensitivities of a few instruments, *Roman*, *HST*, and *JWST*, are shown by the dashed horizontal lines.

An example of the different possible lightcurves that are generated for a single GW event (fixed viewing angle and distance) are displayed in Figure 2. In Figure 3 we show the total afterglow detection percentage as a function of instrument (described in Table I) and parameter assumptions in different simulation runs (described in Table IV). While Figure 3 does not account for the exact time of detection, we show how the time after merger impacts detectability in Figure 4. This is discussed further in §III.

We do not account for the impact of dust extinction on optical and infrared sensitivity or hydrogen gas absorption to X-rays. Furthermore, we have not accounted for telescope observing constraints or the location of the simulated BNS on the sky with respect to the telescopes, Sun, or Moon. We do however discuss the detectability timescales and peak times as a function of viewing angle in §III. Our study is strictly based on the ability for a given telescope sensitivity to detect an afterglow, and we leave afterglow characterization and detection rates to future work.

5. Gamma-ray detectability

While we do not require that the prompt gamma-ray emission is detectable in order for the afterglow to be detectable, we also track this information in our Monte Carlo simulations and consider the probability of a joint detection (GRB and afterglow; as all simulated events already have a GW detection based on §II A) during LVK O5 and XG runs. In §II C 3 we outlined two methods for determining the core kinetic en-

ergy: *i*) using the observed broken power-law gamma-ray luminosity function [200] and applying a gamma-ray efficiency or *ii*) adopting the inferred core kinetic energies from afterglow modeling efforts [107, 108]. In order to convert the latter method to a core gamma-ray energy $E_{\gamma,0}$, we apply a gamma-ray efficiency in reverse such that $E_{\gamma,0} = E_{\text{kin},0}\varepsilon_{\gamma}/(1-\varepsilon_{\gamma})$. In this case we consider a 50% gamma-ray efficiency as found by Fong *et al.* [107], which yields $E_{\gamma,0} = E_{\text{kin},0}$.

As we adopt the same energy structure (Equations 1 and 2) for both the gamma-ray energy and kinetic energy, effectively we have assumed in this case that the gamma-ray efficiency is constant with angle. This provides an upper bound on the number of joint detections as the efficiency is expected to decrease with angle [89, 99]. In addition, a decreasing Lorentz factor with angle can cause other issues for gamma-ray production, such as an increasing optical depth [e.g., 220] or rapidly decreasing the dissipation radius [e.g., 221, 222], both of which can potentially lead to a cutoff in gamma-ray production at large angles [$\theta_{\text{obs}}/\theta_c > 2$; 99, 220, 222]. For simplicity, we neglect the effects of these mechanisms in this work.

The observed line-of-sight (isotropic equivalent) gamma-ray energy $E_{\gamma}(\theta)$ depends on the viewing angle θ_v/θ_c for both the GJ (Equation 1) and PLJ (Equation 2). We consider only the jet's line-of-sight contribution to the prompt gamma-ray emission and do not account for de-beamed emission from the core [15, 223]. This choice has a negligible impact as the line-of-sight structured jet energy dominates over the de-beamed emission.

However, we do consider the addition of a quasi-isotropic

cocoon producing gamma-rays through shock breakout [224–230]. We adopt the analytic model presented by Duffell *et al.* [225], as previously adopted for similar gamma-ray detectability studies of short GRBs [e.g., 76, 199, 231]. We adopt a cocoon breakout efficiency of $\eta_{\text{br}} = 10^{-3}$ and a peak energy for the cocoon of 100 keV. This leads to typical isotropic-equivalent energies of $\approx 10^{47}$ erg for the cocoon. We only apply the cocoon model for events simulated for LVK O5, as the further distances of events in XG do not allow for the detection of a cocoon.

The jet’s core energy $E_{\gamma,0}$ is converted to the line-of-sight energy $E_{\gamma}(\theta_v)$, which is taken to be in the rest frame 1–10,000 keV energy range. This energy $E_{\gamma}(\theta_v)$ is then transformed to a line-of-sight gamma-ray fluence $\phi_{\gamma}(\theta_v)$ in different (observer frame) energy ranges $[e_{\text{low}}, e_{\text{high}}]$ corresponding to the telescopes we consider here (see Table I). For simplicity, and due to the short duration of the GRBs considered here, we consider equivalent fluence sensitivity limits to the flux limits displayed in Table I. In order to determine the fluence in the observer frame bandpass we apply a bolometric correction:

$$k_{\text{bol}} = \frac{\int_{1\text{keV}}^{10\text{MeV}} N(E) E dE}{\int_{(1+z)e_{\text{low}}}^{(1+z)e_{\text{high}}} N(E) E dE}, \quad (5)$$

where $N(E)$ represents the prompt emission energy spectrum, defined by a Band function [232]. The prompt emission spectral parameters are taken to be the observed values for *Fermi* short GRBs [233], where the low energy spectral slope is $\alpha = -0.5 \pm 0.4$ and (observer frame) peak energy at the jet’s core is a normal distribution of $\log E_{\text{p},0} = 2.9 \pm 0.2$ keV. We fix the high energy spectral slope to $\beta = -2.25$.

We also assume that the peak energy is constant in the comoving frame. The peak energy at a given viewing angle $E_{\text{p}}(\theta_v)$ is then given by $E_{\text{p}}(\theta_v) = E_{\text{p},0}\Gamma(\theta_v)/\Gamma_0 = E_{\text{p},0}E_{\gamma}(\theta_v)/E_{\gamma,0}$ [76], where the Lorentz factor profile $\Gamma(\theta)$ is taken to be the same as the energy profile (Equation 3). As such the peak energy is independent of assumptions for the initial Lorentz factor Γ_0 .

The observed gamma-ray fluence can be computed as $\phi_{\gamma}(\theta_v) = (1+z)E_{\gamma}(\theta_v)/(4\pi d_L^2 k_{\text{bol}})$. If a given GRB has a fluence higher than the sensitivity $\phi_{\gamma,\text{lim}}$ of the considered telescopes (Table I) in their observer frame bandpass $[e_{\text{low}}, e_{\text{high}}]$ we consider it a detection. In Figure 5 we show the prompt gamma-ray detection percentage as a function of instrument (Table II) and run (Table IV). The joint gamma-ray and afterglow detection probability is discussed in §III.

III. RESULTS AND DISCUSSION

A. Impact of afterglow parameter and jet structure assumptions

Here we discuss the impact of our assumptions used in the five simulations (Table IV) on the afterglow detectability. There are a number of assumptions that have to be made to perform this study, such as: *i*) the distribution of jet core

half-opening angles θ_c , which largely dictate detectability and are unknown a priori, *ii*) the jet structure and truncation angle θ_w of the jet, and *iii*) the distribution of jet kinetic energies, microphysical parameters, and surrounding environmental densities. Each of these are relatively unknown and display a broad diversity. We utilize available constraints from the observed population of cosmological short GRBs [e.g., 107, 108, 190] that are used to construct our simulation setup.

We find that the most critical assumption for detectability is the core half-opening angle, which is unconstrained for the vast majority of cosmological short GRBs and based on only around a dozen measurements [107, 108, 234–249]. We have tested two different distributions for the core angle, which we refer to as “narrow” (a log-normal distribution centered at 6 deg, 0.1 rad) or the observed distribution from Rouco Escorial *et al.* [108], which we refer to as RE22 (see Table IV). The RE22 distribution has a similar median value (6 deg; [108]), but has a small fraction (a tail) of wide jets with half-opening angles $> 10–30$ deg (0.17–0.5 rad). In Figures 2 and 6 we compare the results between Run 1 and Run 3, which differ only in the distribution adopted for θ_c .

Figure 6 clearly shows that the detectability of afterglows (based on *JWST* but this applies to all instruments) is significantly biased towards small values of the ratio θ_v/θ_c . As Run 1 produces a larger fraction of wider jets, with larger core angles, the ratio θ_v/θ_c peaks at systematically smaller values where afterglows are easier to detect. This is reflected in the higher detection percentage of Run 1 versus Run 3 for all instruments and wavelengths (Figure 3). The detected fraction of afterglows decreases rapidly for $\theta_v/\theta_c > 2$ (see also Figure 7) where for a GJ the energy along the line-of-sight has decreased by a factor of ~ 8 . This trend is the same for both Run 1 and Run 3, and thus the major indicator of the difference in detected fraction is the number of afterglows with $\theta_v/\theta_c < 2$. This is also reflected in the observed population of cosmological GRBs which are limited to smaller viewing angles [e.g., $\theta_v/\theta_c < 2$; 89, 99]. Here we have shown that the small handful of short GRBs with wide jets [108, 234, 238, 249] inferred based on their jet break times (or lack of a jet break to late-times) can have a large impact on the expected detection rate of the entire population.

In afterglowpy the other relevant parameter dictating the structure of a GJ is the jet’s truncation angle θ_w . We have tested the impact of our assumption by varying this value between Run 1 and Run 2 (which both adopt the RE22 distribution for θ_c). In Run 1 we take $\theta_w = 4.9\theta_c$ whereas in Run 2 we truncate the jet at smaller angles $\theta_w = 3\theta_c$ outside of which there is no material along the line-of-sight (for $\theta_v > \theta_w$). Figure 3 shows that this has no impact on afterglow detection. This is because far off-axis afterglow detection is generally dependent on the peak flux of the afterglow, and independent of the early afterglow behavior (and is only dependent on emission from the jet’s core; Appendix B), which is modified by this change in θ_w .

We also briefly tested the impact of jet structure. The difference between simulation Run 3 and Run 4 is the use of a GJ for Run 3 (and all other runs) and PLJ with $b = 10$ [97] for Run 4. From Figure 3 we see that the PLJ (Run 4) is slightly

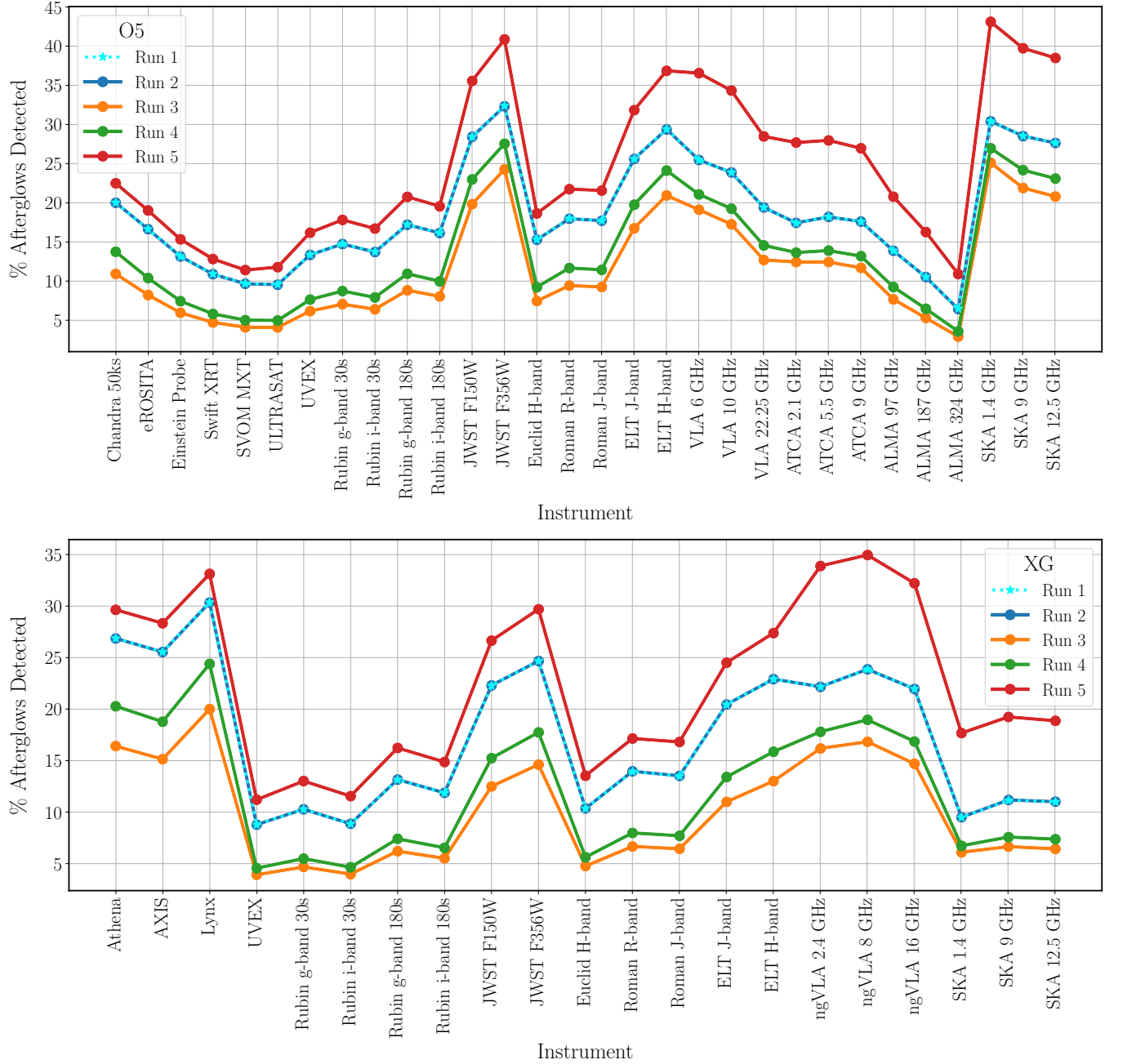


FIG. 3. Total percent of afterglows detected by each instrument for O5 (top) and XG (bottom) over all simulated times between 10^{-2} d and 6.5 yr after the merger. We show how these detections change based on each run (different color lines; shown in label).

easier to detect, but overall very similar. This is expected as both structures are capable of fitting the full lightcurve of GW170817 [e.g., 97]. It is clear that much shallower angular profiles would be significantly easier to detect, though an exhaustive exploration is beyond the scope of this work and challenging due to the unknown jet structure for all but one short GRB (i.e., GW170817).

Next we explore the impact of our afterglow parameter assumptions which we refer to as Case 1 and Case 2 (see Table III). While Case 1 is our default parameter setup we ex-

plore the impact of broad uniform distributions (referred to as Case 2) in the microphysical parameter ε_B and density n in Run 5 (which can most directly be compared against Run 1). In general for short GRBs the emission at X-ray, optical, and infrared wavelengths, and sometimes radio (e.g., GW170817), is most commonly between the synchrotron injection frequency ν_m and the cooling frequency ν_c such that $\nu_m < \nu < \nu_c$. In this regime the flux is positively correlated with the kinetic energy, density, and the fraction of energy in magnetic fields such that $F_\nu \propto E_{\text{kin}}^{\frac{3+p}{4}} \varepsilon_B^{\frac{1+p}{4}} n^{\frac{1}{2}}$ [83]. As such, af-

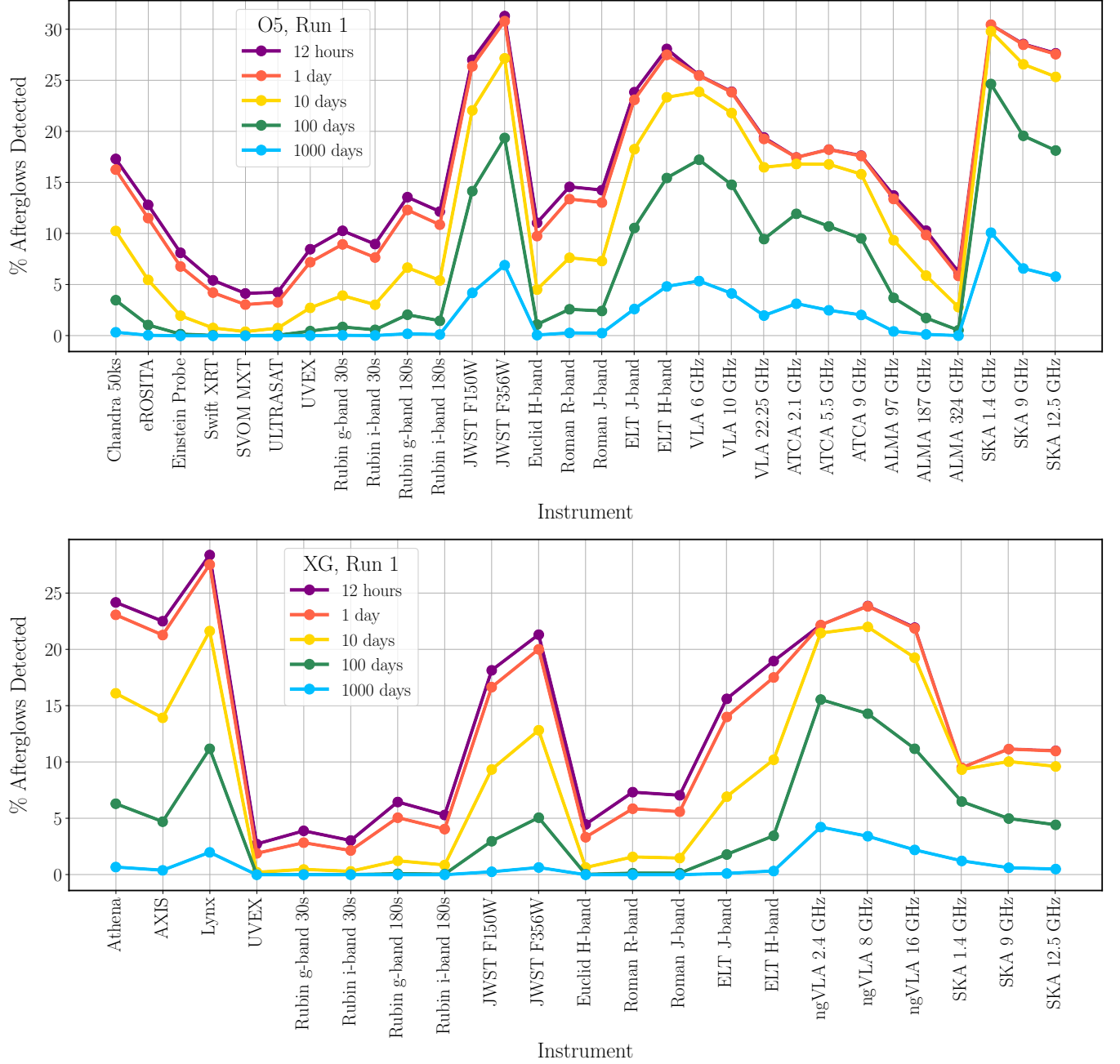


FIG. 4. Percent of afterglows detectable by each instrument for O5 (top) and XG (bottom) as a function of time after the event (observer frame). We show how many afterglows are detectable after 12 hours, 1 day, 10 days, 100 days, and 1000 days after the event. Here we consider only simulation Run 1.

terglow detection is biased towards larger values of these parameters as observed in the corner plots in Figure 7. Thus, the unknown afterglow parameters can have a significant impact on the likelihood of detecting the afterglow of a GW event.

Figure 7 clearly demonstrates this trend, which is also seen in Figure 3 where we observe that Run 5 has the highest detection fraction for all instruments. This is notably due to the allowance for larger fraction of events at higher values of ε_B and n (seen in Figure 7) which lead to brighter afterglows. The

kinetic energies are not substantially different, though Run 1 does have a tail towards lower energies [200].

Figure 3 shows that Run 5 has a particularly large increase in detectability at low frequency radio wavelengths. The large increase at radio wavelengths can be explained in two parts. First, the low frequency radio instruments are significantly more sensitive than those at higher frequencies. Secondly, the maximum flux density usually lies at radio wavelengths and is determined by flux at the injection frequency which is given

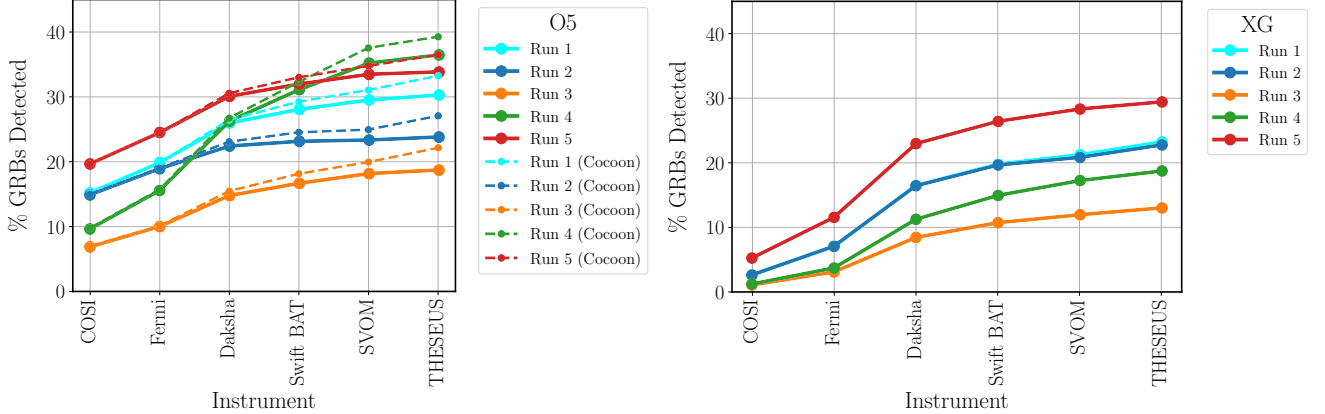


FIG. 5. Percent of prompt GRB emission detected in gamma-rays by each instrument for O5 (left) and XG (right). We show how these detections change based on each run. The addition of a quasi-isotropic cocoon (dashed lines) is only included for O5 (left).

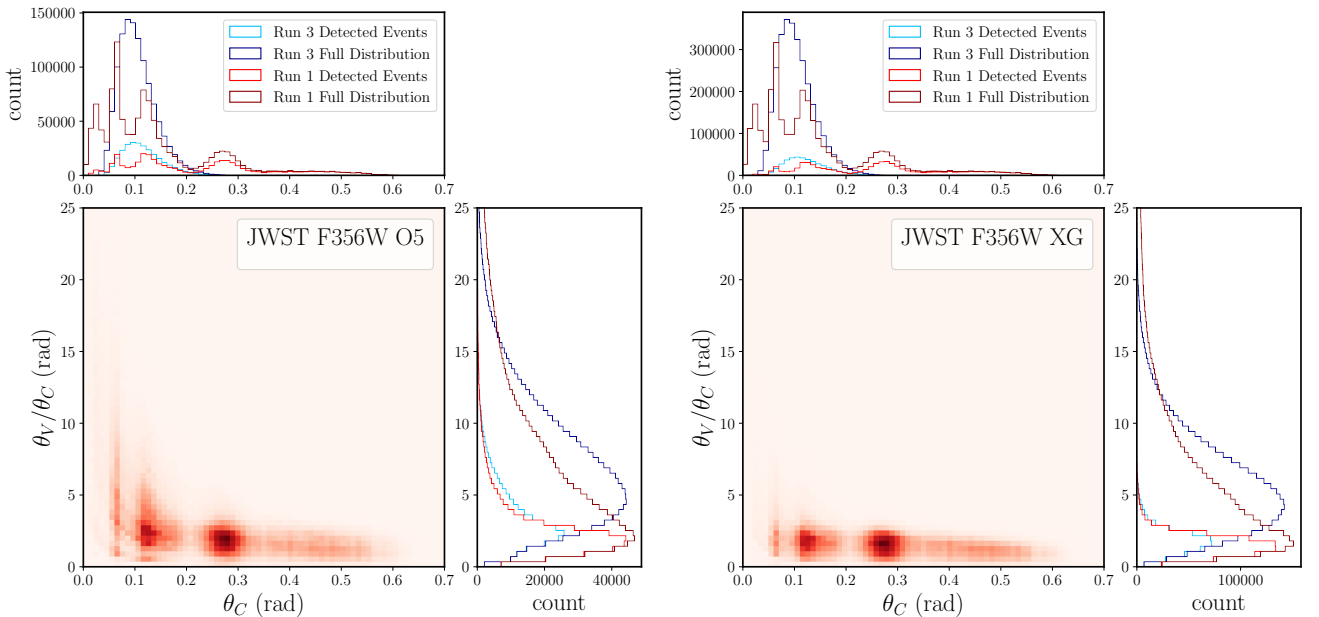


FIG. 6. Distribution of jet opening angle and jet viewing angle for *JWST/F356W* in O5 (left) and XG (right). In each panel we show the 2D distribution of the detected afterglows from Run 1, along with the corresponding 1D distributions for the two parameters, including both the distribution of all simulated afterglows and the distribution of detected ones for both Run 1 and Run 3.

by $F_{\nu_m} \propto E_{\text{kin}} \varepsilon_B^{\frac{1}{2}} n^{\frac{1}{2}}$ [83]. As this maximum flux is constant in time in a uniform density environment, and the injection frequency decreases swiftly in time $\nu_m \propto E_{\text{kin}}^{\frac{1}{2}} \varepsilon_B^{\frac{1}{2}} t^{-\frac{3}{2}}$, at late times the maximum flux will lie in the low frequency radio band, especially for events viewed off-axis such that the core emission comes into view only at later times.

B. Impact of viewing angle

As discussed in §III A, the ratio θ_v/θ_c , which we refer to as the viewing angle interchangeably with θ_v , largely dictates the detectability of an afterglow. This ratio also dictates the

lightcurve behavior such as the rising and fading slopes, the time to peak, and the flux at the peak (see also Appendix B). Figure 8 shows the behavior of the peak flux of the afterglow lightcurve (here for *JWST*) versus the viewing angle θ_v/θ_c . The inset 2D histogram displays all simulated afterglows, whereas the 1D histograms on the top and bottom present both all simulated afterglows and only those which are detected at the sensitivity of *JWST*. We see that the peak flux declines rapidly with increasing θ_v/θ_c . This is due to the rapidly decreasing kinetic energy along the line-of-sight, which dominates the peak flux for $\theta_v/\theta_c < 2$ (Appendix B). At larger angles the material along the line-of-sight has such low energy and Lorentz factor that it becomes fainter than the rising emission from the jet's core becoming de-beamed to the

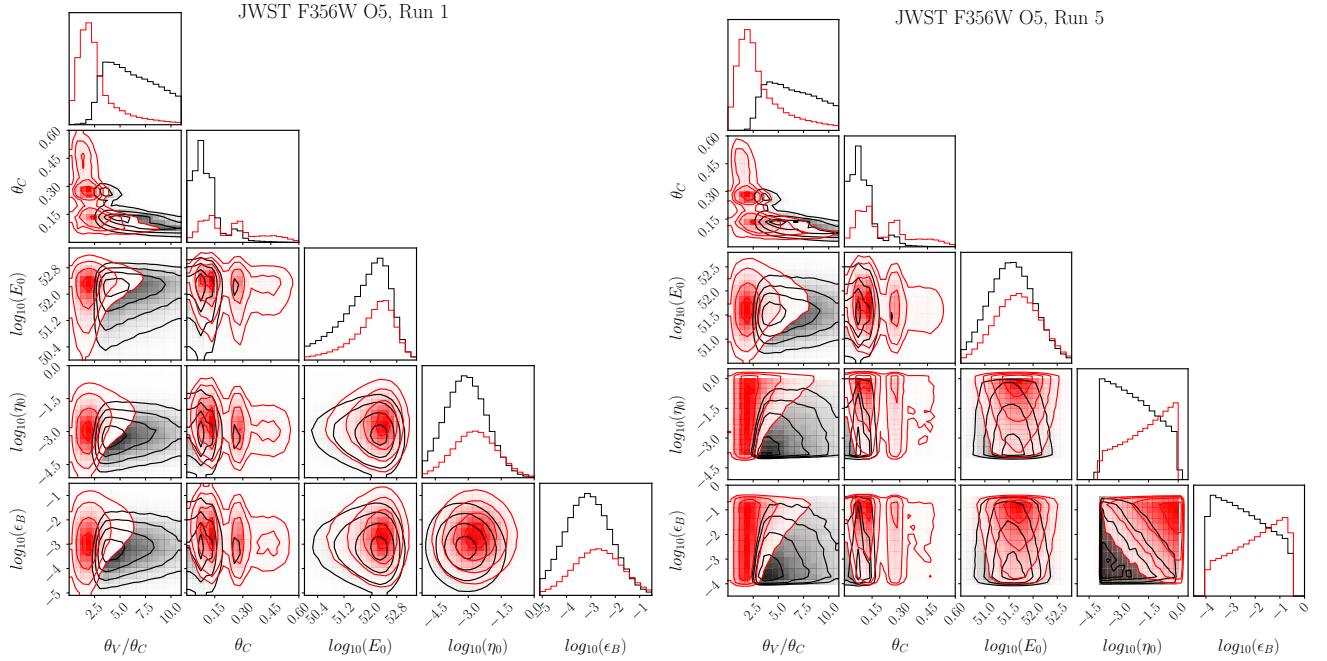


FIG. 7. Distributions of O5 afterglow parameters for Run 1 shown on the left, and Run 5 shown on the right. Distributions of the events detectable by *JWST/F356W* are shown in red, and the distributions of events that are not detectable are shown in black.

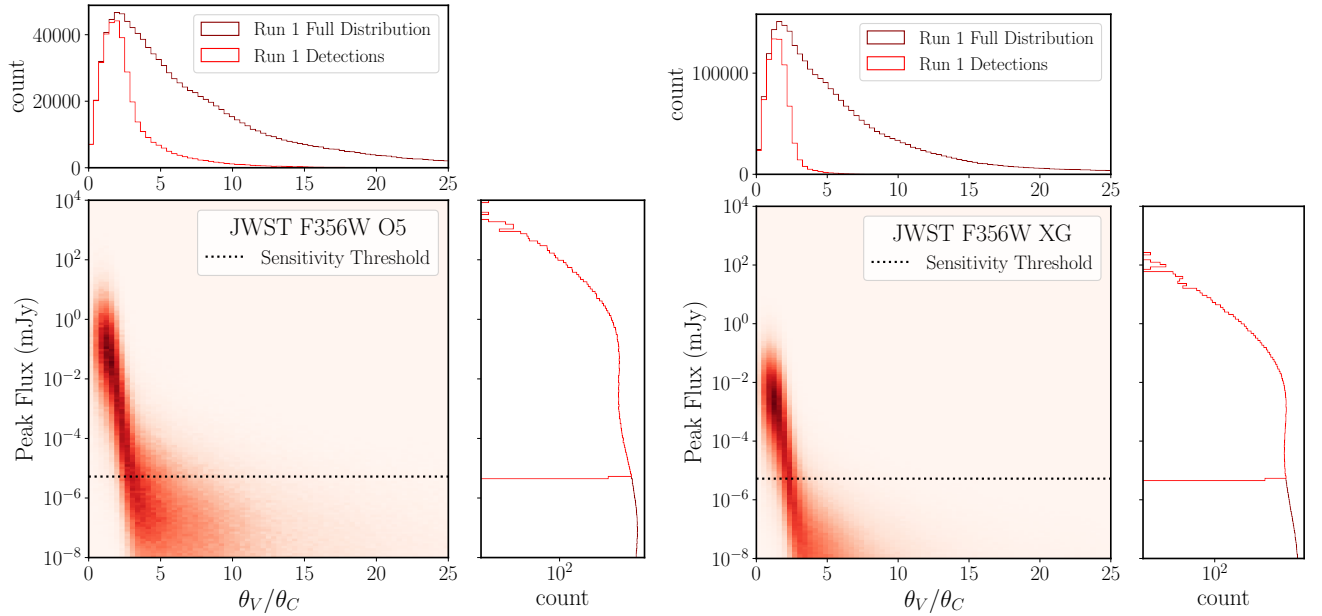


FIG. 8. Peak flux versus the ratio of viewing angle θ_v to core angle θ_c for *JWST/F356W* in O5 (left) and XG (right) for Run 1. The 2D distribution refers to all simulated afterglows, and the dotted line marks the sensitivity of the instrument; thus the portion of the 2D distribution above that line is detectable. The 1D distributions for the two parameters are shown, including both the full distribution of all simulated afterglows and the distribution of those detected.

observer. This produces a flattening in the peak flux distribution that is observed as a cloud in the 2D histogram between $\theta_v/\theta_c \approx 5 - 10$.

The lightcurve behavior is also modified. Figure 9 shows peak flux versus peak time for the O5 and XG instruments

with the largest detection fraction at near-infrared (*JWST*), radio (SKA), and X-ray (*Chandra* and *Athena*) wavelengths. Larger viewing angles θ_v/θ_c push the time of the peak to later times (see also Figure 2), similar to GW170817, which also produce lower fluxes as the shocked material has had a longer

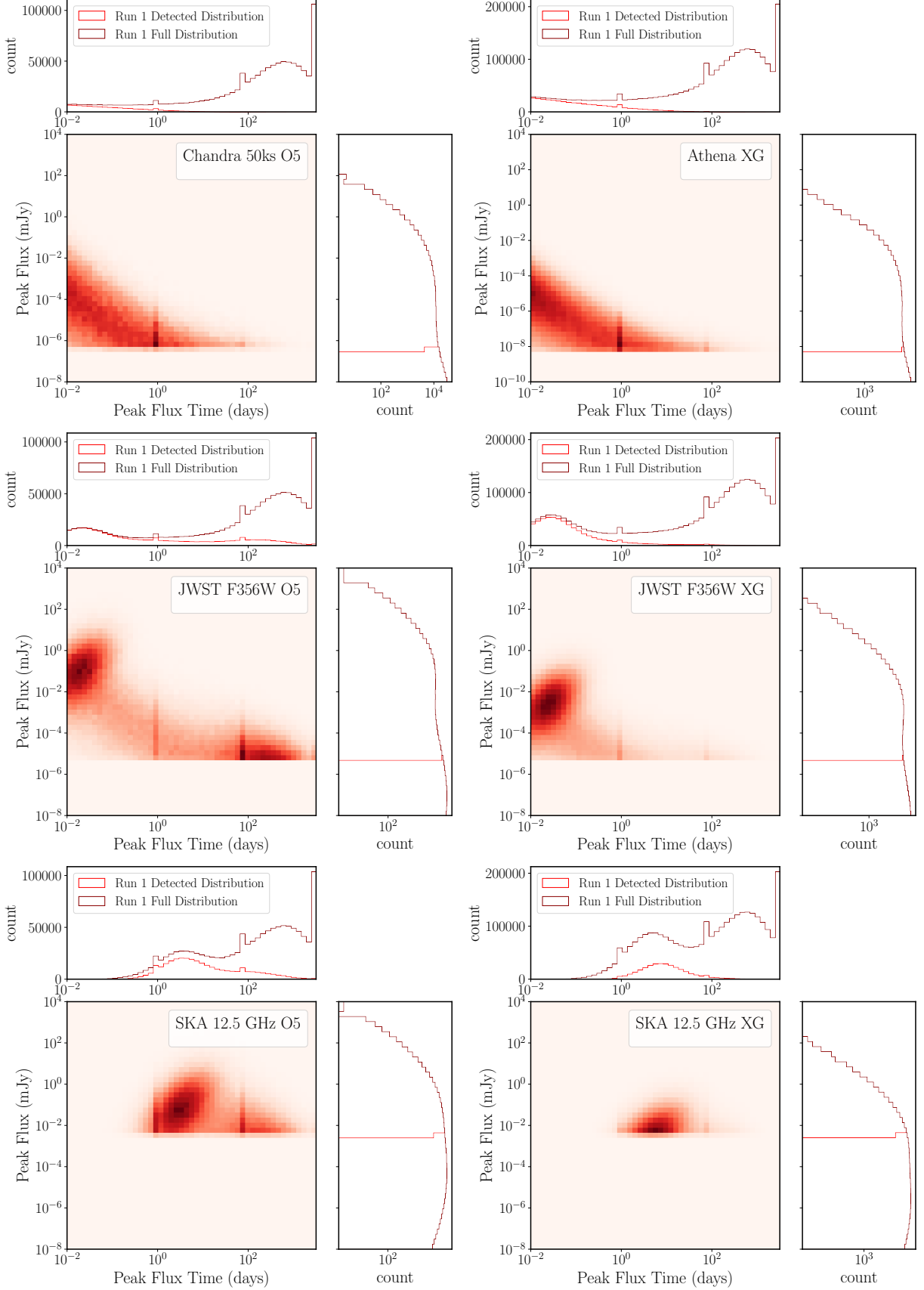


FIG. 9. Peak flux versus peak time of simulated afterglows for Run 1 at X-ray (top), near-infrared (middle), and radio (bottom) wavelengths. The left side shows O5 and right side shows XG. The 2D histograms show only detected afterglows at each wavelength. The 1D histograms for the two parameters (top and right of each figure) are projected, including both the full simulated distribution and the distribution of only the detected afterglows.

time to cool. In these figures the 2D histogram instead shows only the detectable lightcurves.

The high density region between $10^{-2} - 10^{-1}$ d in the 2D histogram for *JWST/F356W* in Figure 9 is due to ν_m passing through the band, at later times ($\sim 10 - 20$ d) ν_m shifts towards low frequency radio and produces an overdensity in the 2D histograms at the same flux levels at 12.5 GHz (Figure 9 for SKA). At later times (~ 100 d) the 12.5 GHz band lies between $\nu_m < \nu < \nu_c$ and the detectable emission is due instead to the emission from the core of the jet. In Figure 9 we see a different behavior for *Chandra* and *Athena* as the X-ray band lies above $\nu_m < 1$ keV for all times considered here.

As the viewing angle θ_v/θ_c increases, the injection frequency ν_m and the flux at the injection frequency F_{ν_m} decline rapidly due to their dependence on the line-of-sight kinetic energy. Thus for large angles ($\theta_v/\theta_c > 3$) even the *JWST/F356W* is above the injection frequency for all times considered here ($> 10^{-2}$ d). Despite the slower temporal evolution of ν_m for off-axis viewing angles [113, 250] by ~ 20 d the injection frequency is < 10 GHz for our default parameter setup (and most parameters in general) at all viewing angles. For the time of peak for far off-axis events (> 100 d) all frequencies considered in this work lie above $\nu_m < \nu$, where only the X-ray band is sometimes above the cooling frequency $\nu_c < 1$ keV.

Figures 10 (O5) and 11 (XG) show the detected fraction as a function of viewing angle and distance where each point at fixed viewing angle and distance represents a simulated GW event. For each event, 1,000 lightcurves are simulated based on the afterglow parameter assumptions (Tables III and IV) and the color of the datapoint represents the fraction of those 1,000 lightcurves that are detected by *JWST*. GW events observed closer to the axis of the jet are significantly more likely to be detected with an afterglow, though this is a function of both distance and the assumed afterglow parameters (in particular θ_c).

C. LVK O5

1. Afterglow detection

Here we discuss the afterglow detection percentage for simulated GW events during LVK O5. We focus only on our fiducial setup, referred to as Run 1 (Table III and IV). The detection percentage for each instrument is listed in Table I. This is also displayed in Figure 3 for each simulation run. For this fiducial case (Run 1), we further present the fraction of afterglows detectable after a given time (observer frame), see Figure 4.

The highest detection fractions are achieved by *JWST* in the *F356W* filter with a detection percentage of 32.4%. At radio wavelengths, SKA also has an extremely high detection percentage with 27.7% of simulated afterglows detectable at 12.5 GHz. Lastly, at X-ray wavelengths, we find that *Chandra* is capable of detecting 20% of all simulated afterglows.

JWST requires 14 d of activation time for a non-disruptive Target of Opportunity (ToO) observation, though faster responses are possible, thus we also consider the fraction of

afterglows detectable after a given time from merger (Figure 4). Of all the simulated afterglows in the *JWST/F356W* filter, 69.8% peak after 10 d. We find that *JWST/F356W* is able to detect 27% of afterglows after 10 days post-merger, and that number drops to 19% after 100 days.

At radio wavelengths, the times at which the afterglows peak are mainly concentrated at > 1 d. This is shown in Figure 9 for SKA at 12.5 GHz. SKA is capable of detecting 27.5% of all afterglows at greater than 1 day at 12.5 GHz. That number drops slightly to 25.3% at 10 days and 18.1% at 100 days. Therefore, SKA detection fractions are comparable to *JWST* over these time periods.

At X-ray wavelengths, we observe higher peak fluxes at early times (as discussed in §III B) with the peak flux decreasing as the time of the peaking (and viewing angle) increases (Figure 9). Of all simulated X-ray afterglows, 77% peak at > 1 d. *Chandra* is able to detect 16% of all simulated afterglows after 1 day, and 10.2% after 10 days. Times between 1 – 10 days fall exactly within rapid ToO timescales, and are capable of detecting a significant fraction of near on-axis events.

Because fast-turnaround ToOs on instruments like *JWST* and *Chandra* are limited, it is important to consider the advantages of using less sensitive wide-field instruments to capture afterglows at < 1 day that would otherwise not be probed by either *JWST* or *Chandra*. At UVOIR wavelengths, we consider Rubin in *g*-band with a 180 s exposure. Rubin has a detection percentage of 17.3% across all simulated afterglows with 93.6% of the detectable afterglows peaking before 1 day. This emphasizes the need for a rapid ToO response from Rubin to GW events [e.g., 60].

We perform the same checks for *Roman* and *ULTRASAT*. *Roman* (*R*-band) detects 16.7% of all afterglows that peak before 1 day, which is 92.8% of all detections. *ULTRASAT* detects 9.6% of simulated afterglows that peak within 1 day, which is 100% of all its detections. We see the same trend at X-ray frequencies as well. *Einstein Probe* has a detection percentage of 13.2%, which is 99% of all detections. While deep field instruments are still crucial for detecting afterglows at later times, these wide-field instruments are essential for the detection and localization of near on-axis events.

Based on this analysis, we conclude that radio telescopes have the best chance of detecting an afterglow counterpart to a BNS merger during LVK O5. It is important to note that all detections in this paper do not take into account constraints regarding visibility, sun positioning, and day/night observing times, all of which will realistically lower the rate of afterglow detection. Given that radio telescopes have a larger range of visibility, and are not as impacted by day/night constraints, this only improves the likelihood of detecting an afterglow in radio as compared to other wavelengths. However, it must be noted that *afterglowpy v0.8.0* does not currently include synchrotron self-absorption which could impact the lower frequency radio data considered here (e.g., SKA at 1.4 GHz).

2. Prompt gamma-ray detection

Here we quantify the detection prospects for prompt gamma-rays associated to our simulated BNS mergers. The detection percentages for each instrument (Table II) are shown in Figure 5 for each run. We show the detection percentage considering only emission from the jet, and also when adding a simple quasi-isotropic cocoon model [225] with breakout efficiency $\eta_{\text{br}} = 10^{-3}$. Our results favor the prompt emission detection of $\sim 20 - 30\%$ of BNS mergers during LVK O5 considering current instruments (e.g. *Swift*, *SVOM*).

The detections are concentrated towards small viewing angles (see Appendix C and Figure 13) where the jet’s energy is highest. As such, the detected fractions depend on the assumptions for the distribution of core opening angles, which dictates the ratio θ_v/θ_c . Only a small fraction of either distribution (RE22 or Narrow; see Table IV) are viewed within the core of their jet ($\theta_v/\theta_c < 1$) with only 1.7% for the narrow distribution of core angles and 4% for the RE22 distribution [108]. The RE22 distribution also has a significantly larger fraction within $\theta_v/\theta_c < 3$ (5) with 25% (40%) within these angles, compared to 14% (33%) for the narrow core distribution (see Figure 13). This difference favors the detection of a higher fraction of EM signals when using the RE22 distribution, due to the larger fraction of wide jets.

The gamma-ray detected events (considering *SVOM* detections for Run 1) are concentrated towards these smaller viewing angles with 50% (90%) of the distribution having $\theta_v/\theta_c < 2.1$ (3.4). This translates to $\theta_v < 0.46$ (0.94) rad for 50% (90%) of the detected population. This similar trend is also seen clearly for the afterglows in Figure 10.

The cocoon model begins to take over all detections outside of $\theta_v \gtrsim 4 - 5\theta_c$. The transition occurs when the line-of-sight gamma-ray energy $E_\gamma(\theta_v)$ of the jet drops below $\approx 10^{47}$ erg which is the approximate energy of the cocoon in our setup. The quasi-isotropic cocoon [225] is assumed to be independent of viewing angle, unlike the jet, and is detectable to a distance of ≈ 50 to 300 Mpc for *Fermi* and *SVOM*, respectively. This distance is significantly smaller than the expected BNS distances for XG detectors (Figure 11), and for this reason we do not consider the cocoon for our XG simulations. We note that for higher breakout efficiencies, e.g., $\eta_{\text{br}} = 10^{-2}$, the detected fraction at large angles ($\theta_v > \theta_w$) can be quite large, even as high as 50%.

A major caveat of the gamma-ray detections computed here is the application of a constant gamma-ray efficiency with angle, though this has been adopted in previous works on the topic [e.g., 74]. There is growing evidence that the efficiency of gamma-ray production is likely to decrease with angle [e.g., 89, 99, 251], which would lead to an even smaller fraction of off-axis detections at $\theta_v/\theta_c \gtrsim 2$. In addition, the distribution of gamma-ray energies or luminosities of cosmological short GRBs is still uncertain and other prescriptions [e.g., 218, 219] are likely to lead to different results. In particular, the luminosity distribution derived by Wanderman and Piran [218], utilized in past works [76, 99], would substantially decrease the detection rate due to its lower average gamma-ray luminosity L_γ .

3. Joint afterglow and gamma-ray detections

We have also considered the likelihood of detecting an afterglow following a gamma-ray trigger. At the base level, the detection of prompt GRB emission more often than not will reveal the presence of a relativistic outflow, and will rapidly improve the localization of the source on the sky. The rapid localization is critical to both the discovery of the afterglow and kilonova (e.g., GRB 170817A), and will allow for a quicker pointing of available facilities (e.g., VLA, *Chandra*, *JWST*).

We find joint detection⁵ fractions (considering all simulated afterglows) of $\sim 19 - 24\%$ for both currently available instruments such as *Chandra* and *JWST*, as well as future instruments such as SKA and ELT. A small fraction of total simulated afterglows are detectable without an initial GRB detection. For example, SKA has a joint GRB detection fraction of 21% for all simulated afterglows, but an additional 6% of afterglows are detectable even without a GRB trigger. This can be compared to 24% and 8% for *JWST*, respectively. *Chandra* also performs well, with a high joint detection fraction of 19%, but only 1% of simulated afterglows can be detected without a GRB trigger. This difference is mainly due to the location of the peak synchrotron flux F_{ν_m} (see §III B) which passes through the SKA and *JWST* bands, whereas X-rays frequencies do not have the same benefit for our fiducial set of parameters (or in general at later times).

We conclude that at least 6–8% of detected afterglows will lack an initial gamma-ray detection in conjunction with the GW signal (i.e., GRB 170817A and GW170817). This is a lower limit to the true fraction of detectable afterglows that will not be accompanied by gamma-rays, as we have not accounted for the instrument duty cycles or sky coverage, among other factors. These events could appear as “orphan” afterglows [109, 118] in wide-field surveys (e.g., SKA).

D. XG detectors

1. Afterglow detection

The major critical difference between O5 and XG is the distance of the detected BNS mergers. The distances of BNS mergers detectable in GWs during O5 range up to 7 Gpc (see Figure 1 for redshift or Figures 10 and 11 for luminosity distance), but are highly concentrated within 1.5 Gpc (90% CL), while the distances for the GW detectable BNS mergers in the next-generation simulations range up to 13 Gpc, and are more concentrated within 11 Gpc (90% CL). This is reflected in Figures 8 and 9 where the distribution of peak fluxes for XG afterglows is shifted to smaller values compared to O5; this is a distance dependent shift and independent of viewing angle. Therefore, the detected afterglows are concentrated

⁵ Note that here joint detection refers to both an afterglow and GRB being detected, as all simulated events already have a GW detection by construction (§II C 5).

to smaller viewing angles, as shown in Figure 11 where the majority of detections are obviously concentrated to within 14 deg (0.25 rad). The further distance of XG events means that the currently active EM telescopes we are considering in this study will not be able to pick up the fainter signals from the most distant events. As the next-generation instruments (e.g., ngVLA, *Athena*, *Lynx*) are more sensitive to fainter signals (signals from more distant events), we are still capable of detecting this distribution. However, this is one reason we see lower detection rates overall, across all telescopes, for the next-generation simulations. The detection of the afterglows of BNS mergers in this era will require rapid ToO response (e.g., *Athena*) and this should be a key goal for facilities over the next decade.

We find that the top facilities in this era at each wavelength are *Athena* and *Lynx* at X-ray wavelengths with detection percentages of 26.8% and 30.3% respectively, *JWST* at near-infrared wavelengths with a detection percentage of 24.6% in the *F356W* filter, and ngVLA at radio wavelengths with a detection percentage of 23.8% at 8 GHz.

At UVOIR wavelengths, we find that *JWST* is able to detect 20% of afterglows after 1 day and 12.8% after 10 days. At X-ray wavelengths, *Athena* has a similar detection fraction, with 23% after 1 day and 16% after 10 days. Lastly, at radio wavelengths, ngVLA (8 GHz) is capable of detecting 23.8% of all simulated afterglows after 1 day. ngVLA has no detections prior to 1 day after the GW merger. The detected fraction barely decreases out to 10 days, but only 14% are detectable past 100 d. For XG era merger events, where signals are fainter and afterglow peaks less likely to be detected than in O5, radio will be the optimal wavelength range to search in, outperforming *JWST*.

2. Prompt gamma-ray detection

The detection fraction of GRBs from simulated XG-detectable BNS is in the range $\sim 10 - 20\%$, slightly lower than the $\sim 20 - 30\%$ expected for the distances of events during LVK O5. Due to the larger distance of XG events (Figures 1 and 11) the gamma-ray detections are likewise concentrated closer to the core of the jet. In fact 50% (90%) of the detected distribution is viewed at $\theta_v/\theta_c < 1.5$ (2.4). In terms of the inclination angle this translates to $\theta_v < 0.37$ (0.7) rad. As only a small fraction of events have $\theta_v/\theta_c > 3$ (which is θ_w for Run 2) there is no large deviation between the gamma-ray detections of Run 1 and Run 2 in XG (Figure 5). In any case, the lack of far off-axis detections during XG is in agreement with inferences from cosmological short GRBs that they are not detected far off-axis at such distances [89].

3. Joint afterglow and gamma-ray detections

The fraction of joint GRB and afterglow detections during XG are quite similar to that expected during LVK O5, with the highest performing facilities (e.g., ngVLA, *Athena*, *JWST*) having a joint detection percentage of $\sim 18 - 21\%$ of

all simulated afterglows. The fraction of detectable afterglows in the absence of a GRB detection is also quite similar, around $\sim 5 - 6\%$ for ngVLA, *Athena*, and *JWST*. The similarity is likely in part due to the concentration of XG detectable BNS events towards smaller viewing angles (Figure 11). The median off-axis viewing angle for all simulated XG events is $\theta_v/\theta_c \approx 4.9$ compared to $\theta_v/\theta_c \approx 6.1$ for O5. This translates to median values of $\theta_v \approx 0.56$ rad and 0.68 rad for XG and O5, respectively. The smaller viewing angles work to offset the larger distances.

These reported joint detection fractions are when considering *THESEUS*. Other less sensitive gamma-ray facilities would allow for a larger fraction of afterglows detectable without a GRB trigger. In order to maximize the available scientific return of multimessenger observations during the XG detector period it is critical to have replacement or next-generation gamma-ray facilities in orbit.

IV. CONCLUSIONS

In this work we have simulated the gamma-ray prompt emission and the afterglows of BNS mergers detected in GWs during both LVK O5 and by next-generation detectors, such as the Cosmic Explorer and Einstein Telescope, in order to quantify the prospects for multi-messenger astronomy in the next decade. We consider a range of instruments across the electromagnetic spectrum from low frequency radio wavelengths to gamma-rays. We aim to quantify the best instruments, both current and future, for GW observations focused on the afterglow. We simulated a realistic population of BNS mergers and quantified their detectability by future GW instrumentation. The jet afterglows were simulated based on observations of cosmological short GRBs, and therefore represent realistic prospects for their detection. As expected, we find that viewing angle and jet's core half-opening opening angle have a significant impact on the detectability of the afterglow, with lower viewing angles θ_v/θ_c corresponding to increased detectability.

The best chances of detecting the jet afterglow of a BNS merger are at radio (e.g., SKA, ngVLA) or near-infrared (e.g., *JWST*) wavelengths at later times (Figures 3 and 4). This is partially due to the difficulty in localizing an afterglow (or kilonova) on rapid timescales (< 1 d) to an area small enough for the sensitive wide field instruments (e.g., *Rubin*, *Roman*, *ULTRASAT*). Instruments such as *Einstein Probe* with a 3600 deg² field of view are prime for rapid observations of the full sky localization of a GW event, especially during O5 and XG, but these instruments lack the sensitivity to detect the majority of afterglows that are likely to be produced by these GW events. Therefore, if the afterglow (or kilonova) is not rapidly localized and targeted at < 1 d the prospects improve at $\gtrsim 20$ d at radio wavelengths and ~ 100 d in the near-infrared. Over these later timescales it is easy to re-point deep field instruments, and improve their likelihood of detecting the emission from the jet, though the issue of their field of regard remains.

We find that for LVK O5 there are several telescopes that are useful for detecting the late-time afterglow of a BNS

merger. For example, on timescales of > 10 days *JWST* can detect $\sim 27\%$ of all simulated afterglows, SKA can detect $\sim 25\%$, and *Chandra* can detect $\sim 10\%$. Similar detection likelihoods are expected during the A# era (McIver et al. in prep.), which will follow the O5 run prior to the implementation of XG detectors.

The detection likelihood is lower for our Cosmic Explorer and Einstein Telescope simulations, owing to the larger distance of the detectable XG mergers, which is $\sim 10\times$ further than the median distance of the BNS mergers detectable during O5. The best instrument is the *Lynx* mission concept at X-ray wavelengths, having the highest detected fraction at 30.3% with 27.5% detected at > 1 d (Figures 3 and 4). Events viewed within < 15 deg of the jet’s axis have the highest detection fraction, which remains somewhat constant out to $z \sim 1 - 2$ (Figure 11). The ngVLA and SKA are incredibly useful at low-frequency radio wavelengths and are complementary given their locations in the Northern and Southern Hemispheres, respectively. ngVLA has an improved detection fraction over SKA after ~ 1 d, with $\sim 24\%$ as compared to SKA’s $\sim 11\%$. Finally, at UVOIR wavelengths, *JWST* is the optimal telescope, with an overall detection percentage of 24.6% and 20% after ~ 1 d.

We also explore the joint detectability of the afterglow and prompt gamma-ray emission, finding that about 20% of GW detected events may have both detections during O5 and XG. Considering the best performing instrument for gamma-ray detectability (*THESEUS* during the XG era), orphan afterglow detections with, e.g., SKA, ngVLA, and *JWST* are typically $< 10\%$ of all GW detected events. However, some simplistic assumptions such as a constant gamma ray efficiency over all angles may render our prompt gamma-ray detections optimistic. Moreover, a GRB may not be detected at the time of emission due to observability constraints, but the afterglow may still be detectable at some wavelengths at other times.

Our predictions for both afterglow and gamma-ray detection fractions are rather optimistic compared to previous studies [e.g., 73, 74]. While there are a number of differences in the methods and assumptions that go into each of the studies, a main factor in the deviation stems from *i*) our assumption that all BNS mergers launch a relativistic jet and *ii*) the assumed distribution of jet core half-opening angles θ_c . For instance, while we adopt a range of core angles given the large uncertainty in their values even from deep observations of cosmological short GRBs, past studies [e.g., 73, 74] fixed the core opening angle to the narrow jet inferred for GW170817, i.e., $\theta_c \approx 3.5$ deg [e.g., 40]. Such a narrow jet leads to a far off-axis viewing angle $\theta_v/\theta_c \approx 5 - 6$ for GW170817, causing the afterglow to peak at late times and at a significantly lower luminosity. Therefore, using such a narrow jet, not observed for the majority of the population of cosmological GRBs, inherently leads to larger off-axis viewing angles θ_v/θ_c which significantly decreases the detection likelihood. Additional differences include the parameterization of the jet’s angular structure, afterglow parameters such as n and ε_B , jet kinetic and gamma-ray energy, and assumptions for the prompt gamma-ray emission spectrum or efficiency. Each of these choice has a substantial impact on the detectability of the afterglow and

prompt emission (see §III A and III B).

In the future it may be useful to further explore afterglows as a tool to identify the EM counterpart to GW events, without the need of GRB or KN detection. We have approached this here by considering the detectability of afterglows by both wide FoV instruments and sensitive, deep instruments with small FOVs. However, identification and characterization may not be straightforward. Although orphan afterglows are rare [70, 126] and therefore the probability of chance coincidence between a GW event and an afterglow at a redshift consistent with the merger’s distance will be low, it will be useful to properly quantify the probability of association for afterglows peaking months after the GW event using statistical tools such as [252, 253] and astrophysical arguments based on multimessenger observations. Moreover, detectability of jet afterglows from binary black hole mergers should also be explored, given the possibility that these objects also launch jets when embedded in the disks of Active Galactic Nuclei (e.g., [254]). These jets can be detected as nuclear transients in coincidence with GW binary black hole mergers [255–257], and show great promise for cosmological measurements with standard sirens [258].

ACKNOWLEDGMENTS

The authors thank Alicia Rouco Escorial and Wen-fai Fong for sharing their distribution of short GRB core angles. R.K. acknowledges helpful comments from, and discussions with, Raffaella Margutti on her Undergraduate Honors Thesis at the University of California Berkeley, which served as the basis for this work. B.O. acknowledges useful discussions with Geoff Ryan and Paz Beniamini. B.O. thanks Gabriele Bruni and Alexander van der Horst for assistance with radio telescope sensitivities, and Eliza Neights and John Tomsick for assistance with gamma-ray telescope sensitivities. A.P. thanks Amanda Farah and Viviane Alfradique for help with the simulations, and Marica Branchesi and Om Salafia for useful discussion.

B.O. is supported by the McWilliams Postdoctoral Fellowship at Carnegie Mellon University. A. P. acknowledges support for this work was provided by NASA through the NASA Hubble Fellowship grant HST-HF2-51488.001-A awarded by the Space Telescope Science Institute, which is operated by Association of Universities for Research in Astronomy, Inc., for NASA, under contract NAS5-26555.

This research used resources of the National Energy Research Scientific Computing Center, a DOE Office of Science User Facility supported by the Office of Science of the U.S. Department of Energy under Contract No. DE-AC02-05CH11231 using NERSC award HEP-ERCAP0029208 and HEP-ERCAP0022871. This work used resources on the Vera Cluster at the Pittsburgh Supercomputing Center.

Appendix A: Simulated BNS merger distances and viewing angles

Here we show the distance and viewing angle of all BNS mergers detected by LVK at O5 sensitivity (Figure 10) and our XG detector setup (Figure 11). Each of the points in Figures 10 and 11 represent a single GW event for which we perform our afterglow simulations. The afterglow detection fraction at each distance and viewing angle is shown based on the colorbar.

Appendix B: Impact of Lorentz factor and jet spreading

By default `afterglowpy` [97, 171] does not include an angular profile for the bulk Lorentz factor $\Gamma(\theta)$. However, we found that this assumption, and in particular the choice of an infinite Lorentz factor (defined by default as `GammaInf`) leads to a larger fraction of detected afterglows, especially at early times. Therefore, we apply the `GammaEvenMass` flag (Equation 3) and an initial bulk Lorentz factor at the jet's core of $\Gamma_0 = 300$ [197]. This flag, and the relaxation of the default `GammaInf` setting, is only accurate within `afterglowpy` when lateral jet spreading is neglected. We find that our afterglow detectability inferences are not significantly impacted by lateral spreading, which has the largest effect after the afterglow peak (see also the comparison in [259]). As such we do not believe that our inferences for the afterglow detection percentages would significantly change if spreading were included in our calculations.

The detected fraction of events depends most strongly on the peak flux of the afterglow. Here we discuss the analytic expectations for the peak afterglow flux and how different assumptions within `afterglowpy` match these expectations. The angular Lorentz factor profile $\Gamma(\theta)$ modifies the time of the lightcurve peak for smaller viewing angles $\theta_v/\theta_c \lesssim 2$. For these smaller angles the time of the afterglow peak and the peak flux can be computed by using the line-of-sight energy and Lorentz factor (see also [89] for a discussion). As we adopt the same angular profile for energy and Lorentz factor (Equation 3) this can be easily derived. The (on-axis) time of deceleration is given by $t_{\text{dec},0} \propto (E_{\text{kin},0}/n)^{1/3} \Gamma_0^{-8/3}$ for a uniform density environment [196, 197, 260–264]. Using the same scalings in energy and Lorentz factor, the deceleration of line of sight material produces an afterglow peak at:

$$t_{\text{dec}}(\theta_v) = t_{\text{dec},0} E_{\text{kin}}(\theta)^{-7/3}. \quad (\text{B1})$$

A similar scaling can be derived for the peak flux due to deceleration:

$$F_{\text{dec}}(\theta_v) = F_{\text{dec},0} E_{\text{kin}}(\theta)^{17/5}. \quad (\text{B2})$$

For a GJ this can be written as:

$$t_{\text{dec}}(\theta_v) = t_{\text{dec},0} \exp\left(-\frac{1}{2} \frac{\theta_v^2}{\theta_c^2}\right)^{-7/3}, \quad (\text{B3})$$

$$F_{\text{dec}}(\theta_v) = F_{\text{dec},0} \exp\left(-\frac{1}{2} \frac{\theta_v^2}{\theta_c^2}\right)^{17/5}. \quad (\text{B4})$$

These equations hold for smaller viewing angles $\theta_v/\theta_c \lesssim 2$ and $\theta_v \lesssim \theta_w$ for a GJ and $\theta_v/\theta_c \lesssim 3$ for a PLJ, whereas for larger viewing angles the time of the afterglow peak begins to be dictated by the jet's core becoming de-beamed to the observer [see, e.g., 89, 113, 250, for a discussion].

For larger viewing angles and no lateral jet spreading the lightcurve will peak when the jet's core becomes de-beamed to the observer which occurs when $\Gamma \approx \theta_v^{-1}$, such that the peak time t_p is [89, 109, 113]

$$t_p \propto t_j \left(\frac{\Delta\theta}{\theta_c}\right)^{8/3}, \quad (\text{B5})$$

where t_j is the on-axis time of the jet break [212–214] and $\Delta\theta = \theta_v - \theta_c$. The far off-axis scaling for the peak flux F_p is independent of jet spreading and provided by [109, 215]

$$F_p \propto F_j \left(\frac{\Delta\theta}{\theta_c}\right)^{-2p}, \quad (\text{B6})$$

where F_j is the flux at on-axis jet break time. As the peak flux dictates detectability and the fact the dependence is not modified by jet spreading we are confident the impact of our assumptions are negligible. These equations hold for a tophat jet, but are also accurate for `afterglowpy` at large angles or for $\theta_v \gtrsim \theta_w$.

As an example we compute lightcurves for a GJ over 200 log-spaced viewing angles between $\theta_v/\theta_c = \{0, 9\}$ for a core half-opening angle $\theta_c = 0.1$ rad and a truncation angle $\theta_w = 0.5$ rad.

We compute the peak time and flux of these lightcurves for both the default `GammaInf` setting and for `GammaEvenMass` with an initial core Lorentz factor $\Gamma_0 = 300$. The lightcurves are computed at an observer frame frequency of 1 keV between 10^{-4} and 1500 d (observer frame). The results are displayed in Figure 12. We verified these scaling relations also hold for a PLJ.

We see good agreement between the analytic scalings described above and the `afterglowpy` lightcurves for `GammaEvenMass`. There is a natural transition regime between the analytic expectations that is due to the assumed value of $\theta_w = 5\theta_c$. For viewing angles $\theta_v \gtrsim \theta_w$ the tophat jet scalings exactly match the lightcurve behavior. For smaller values of θ_w these equations will apply for smaller angles from the core.

It is worth pointing out that for the `GammaInf` assumption that the peak time is always the first value in the lightcurve grid when $\theta_v < \theta_w$. Hence the purple line showing a steep vertical rise from our smallest time value to the tophat expectation at precisely $\theta_w = 5\theta_c$.

If we consider detectability only for times greater than 1 day after the merger then these issues no longer greatly impact detectability and the peak flux is very similar for both Lorentz factor assumptions. However, for times less than 1 day, using `GammaInf` can lead to higher inferred peak fluxes by a factor of up to $1,000\times$ for a GJ (and more for a PLJ) and thus significantly increase the fraction of detected afterglows. This deviation would be more significant if earlier timescales

($< 10^{-4}$ d) are considered as for Gamma Inf the flux is always higher at early times (unless $\theta_v > \theta_w$).

Another mechanism to consider is potential variations to the initial Lorentz factor of the jet's core. We adopted a canonical value of $\Gamma_0 = 300$ which is the median value inferred for long GRBs in a uniform environment by Ghirlanda *et al.* [197]. It is reasonable to expect a range of Lorentz factors for short GRBs, and we comment that using a smaller Lorentz factor, e.g., $\Gamma_0 = 100$, leads to a later peak time ($t_{\text{dec},0} \propto \Gamma_0^{-8/3}$) and therefore a lower peak flux. For the parameters considered here (Figure 12) this variation in Lorentz factor leads to a higher peak flux by a factor of $\lesssim 10$ (a factor of ~ 3 for $\theta_v/\theta_c = 2$) and no variation for times > 1 day.

We further note that these comparisons apply only to frequencies above the synchrotron injection frequency ν_m , typically the optical and X-ray bands. For radio wavelengths, which are likely below ν_m (especially at early times), the peak time and flux of the afterglow do not depend at all on deceleration of line-of-sight material and instead occur either when ν_m passes through the observed band or when the jet break $t_j(\theta_v)$ occurs. As such, the radio afterglow detectability is not impacted by any of these assumptions for the initial Lorentz factor, Lorentz factor angular structure, or the jet truncation

angle. We verified this using `afterglowpy` with a similar methodology to that outlined above for Figure 12.

Appendix C: Impact of viewing angle on prompt gamma-ray detection

While Figure 5 shows the fraction of simulated events detected in gamma-rays, it does not include information related to the viewing angle. Therefore, in Figure 13 we show the distribution of viewing angles θ_v/θ_c of events detected in gamma-rays versus the total simulated population for both the RE22 distribution [108] of core angles (left panel) and the narrow Gaussian distribution of core angles (right panel). In both panels we have adopted a GJ with truncation angle $\theta_w = 5\theta_c$, and we observe that the steep drop in detections occurs before this truncation angle. All detections at angles larger than $\theta_v > \theta_w$ (dashed lines) are due to emission from the quasi-isotropic cocoon [225]. Due to the low assumed breakout efficiency $\eta_{\text{br}} = 10^{-3}$ the cocoon has a limited impact on detectability (see also Figure 5). However higher values, e.g., $\eta_{\text{br}} = 10^{-2}$, lead to a significant fraction of detected events at large angles.

-
- [1] LIGO Scientific Collaboration, Advanced LIGO, [Classical and Quantum Gravity](#) **32**, 074001 (2015), [arXiv:1411.4547 \[gr-qc\]](#).
 - [2] F. Acernese, M. Agathos, K. Agatsuma, D. Aisa, N. Allemandou, A. Allocca, J. Amarni, P. Astone, G. Balestri, G. Ballardin, F. Barone, J.-P. Baronick, M. Barsuglia, A. Basti, F. Basti, T. S. Bauer, V. Bavigadda, M. Bejger, M. G. Beker, C. Belczynski, D. Bersanetti, A. Bertolini, M. Bitossi, M. A. Bizouard, S. Bloemen, M. Blom, M. Boer, G. Bogaert, D. Bondi, F. Bondu, L. Bonelli, R. Bonnand, V. Boschi, L. Bosi, T. Bouedo, C. Bradaschia, M. Branchesi, T. Briant, A. Brillet, V. Brisson, T. Bulik, H. J. Bulten, D. Buskulic, C. Buy, G. Cagnoli, E. Calloni, C. Campegni, B. Canuel, F. Carbognani, F. Cavalier, R. Cavalieri, G. Celli, E. Cesarini, E. Chassande-Mottin, A. Chincarini, A. Chiummo, S. Chua, F. Cleva, E. Coccia, P.-F. Cohadon, A. Colla, M. Colombini, A. Conte, J.-P. Coulon, E. Cuoco, A. Dalmaz, S. D'Antonio, V. Dattilo, M. Davier, R. Day, G. Debreczeni, J. Degallaix, S. Deléglise, W. D. Pozzo, H. Dereli, R. D. Rosa, L. D. Fiore, A. D. Lieto, A. D. Virgilio, M. Doets, V. Dolique, M. Drago, M. Ducrot, G. Endrőczi, V. Fafone, S. Farinon, I. Ferrante, F. Ferrini, F. Fidecaro, I. Fiori, R. Flaminio, J.-D. Fournier, S. Franco, S. Frasca, F. Frasconi, L. Gammaiton, F. Garufi, M. Gaspard, A. Gatto, G. Gemme, B. Gendre, E. Genin, A. Gennai, S. Ghosh, L. Giacobone, A. Giazotto, R. Gouaty, M. Granata, G. Greco, P. Groot, G. M. Guidi, J. Harms, A. Heidmann, H. Heitmann, P. Hello, G. Hemming, E. Hennes, D. Hofman, P. Jaradowski, R. J. G. Jonker, M. Kasprzack, F. Kéfélian, I. Kowalska, M. Kraan, A. Królak, A. Kutynia, C. Lazzaro, M. Leonardi, N. Leroy, N. Letendre, T. G. F. Li, B. Lieunard, M. Lorenzini, V. Lorette, G. Losurdo, C. Magazzù, E. Majorana, I. Maksimovic, V. Malvezzi, N. Man, V. Mangano, M. Mantovani, F. Marchesoni, F. Marion, J. Marque, F. Martelli, L. Martellini, A. Masserot, D. Meacher, J. Meidam, F. Mezzani, C. Michel, L. Milano, Y. Minenkov, A. Moggi, M. Mohan, M. Montani, N. Morganado, B. Mours, F. Mul, M. F. Nagy, I. Nardeccchia, L. Naticchioni, G. Nelemans, I. Neri, M. Neri, F. Nocera, E. Pacaud, C. Palomba, F. Paoletti, A. Paoli, A. Pasqualetti, R. Passaquieti, D. Passuello, M. Perciballi, S. Petit, M. Pichot, F. Piergiovanni, G. Pillant, A. Piluso, L. Pinard, R. Poggiani, M. Priyatjelj, G. A. Prodi, M. Punturo, P. Puppo, D. S. Rabeling, I. Rácz, P. Rapagnani, M. Razzano, V. Re, T. Regimbau, F. Ricci, F. Robinet, A. Rocchi, L. Rolland, R. Romano, D. Rosińska, P. Ruggi, E. Saracco, B. Sassolas, F. Schimmel, D. Sentenac, V. Sequino, S. Shah, K. Siellez, N. Straniero, B. Swinkels, M. Tacca, M. Tonelli, F. Travasso, M. Turconi, G. Vajente, N. van Bakel, M. van Beuzekom, J. F. J. van den Brand, C. V. D. Broeck, M. V. van der Sluys, J. van Heijningen, M. Vasúth, G. Vedovato, J. Veitch, D. Verkindt, F. Ventrano, A. Viceré, J.-Y. Vinet, G. Visser, H. Vocca, R. Ward, M. Was, L.-W. Wei, M. Yvert, A. Z. Žny, and J.-P. Zendri, Advanced virgo: a second-generation interferometric gravitational wave detector, [Classical and Quantum Gravity](#) **32**, 024001 (2014).
 - [3] T. Akutsu *et al.* (KAGRA), Overview of KAGRA: Detector design and construction history, [PTEP](#) **2021**, 05A101 (2021), [arXiv:2005.05574 \[physics.ins-det\]](#).
 - [4] B. P. Abbott, R. Abbott, T. Abbott, F. Acernese, K. Ackley, C. Adams, T. Adams, P. Addesso, R. X. Adhikari, V. B. Adya, *et al.*, Gw170817: observation of gravitational waves from a binary neutron star inspiral, [Physical review letters](#) **119**, 161101 (2017).
 - [5] A. Goldstein, P. Veres, E. Burns, M. S. Briggs, R. Hamburg, D. Kocevski, C. A. Wilson-Hodge, R. D. Preece, S. Poolakkil, O. J. Roberts, C. M. Hui, V. Connaughton, J. Racusin, A. von Kienlin, T. Dal Canton, N. Christensen, T. Littenberg, K. Siellez, L. Blackburn, J. Broida, E. Bissaldi,

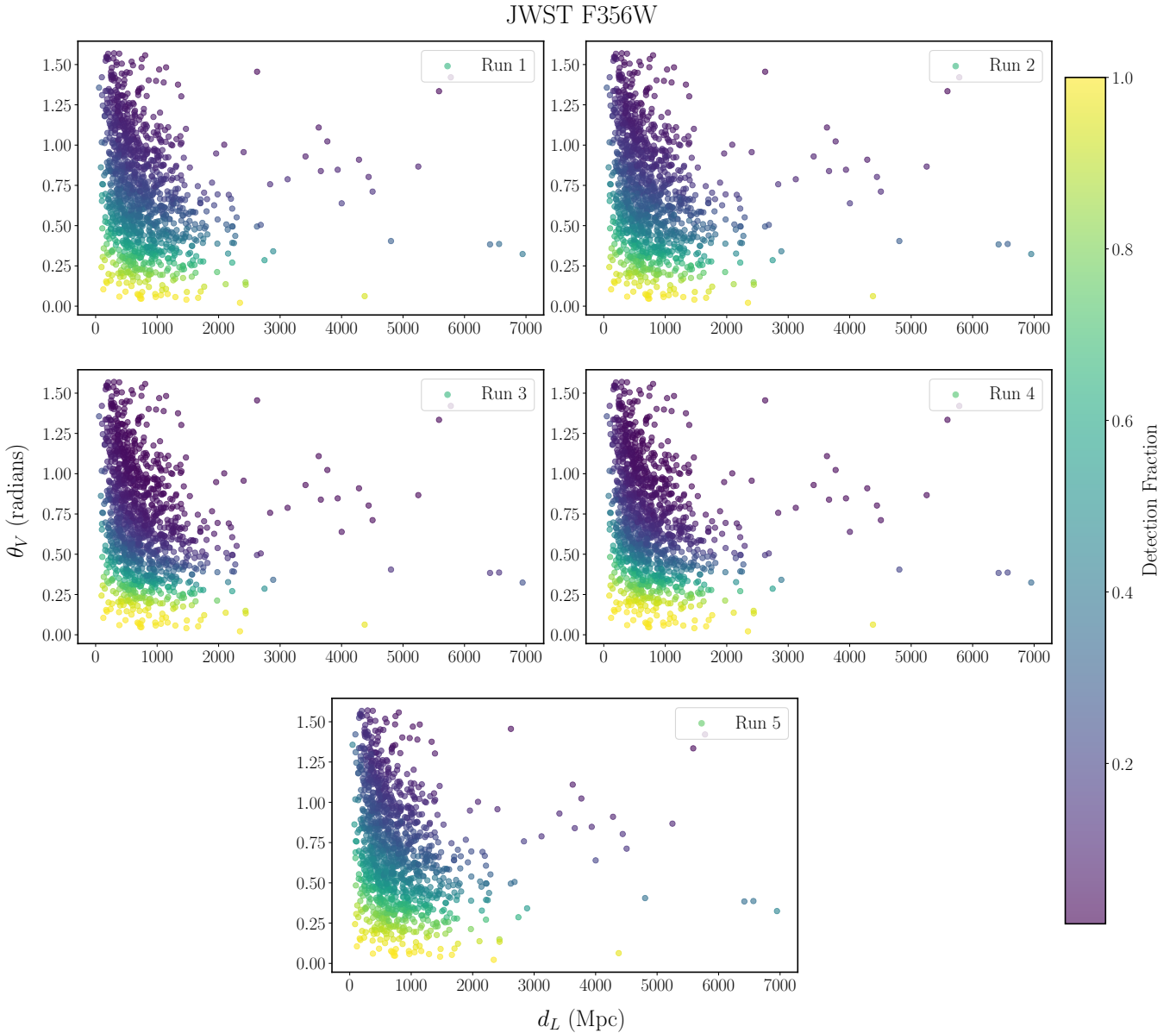


FIG. 10. The distance and viewing angle of all simulated BNS merger detected in GWs during LVK O5 for all five simulation runs. The colorbar shows the fraction of the 1,000 simulated afterglows which are detected by *JWST* in the *F356W* filter for each of the simulated mergers.

- W. H. Cleveland, M. H. Gibby, M. M. Giles, R. M. Kippen, S. McBreen, J. McEnery, C. A. Meegan, W. S. Paciesas, and M. Stanbro, An Ordinary Short Gamma-Ray Burst with Extraordinary Implications: Fermi-GBM Detection of GRB 170817A, *The Astrophysical Journal Letters* **848**, L14 (2017), [arXiv:1710.05446 \[astro-ph.HE\]](https://arxiv.org/abs/1710.05446).
- [6] V. Savchenko, C. Ferrigno, E. Kuulkers, A. Bazzano, E. Bozzo, S. Brandt, J. Chenevez, T. J. L. Courvoisier, R. Diehl, A. Domingo, L. Hanlon, E. Jourdain, A. von Kienlin, P. Laurent, F. Lebrun, A. Lutovinov, A. Martin-Carrillo, S. Mereghetti, L. Natalucci, J. Rodi, J. P. Roques, R. Sunyaev, and P. Ubertini, INTEGRAL Detection of the First Prompt Gamma-Ray Signal Coincident with the Gravitational-wave Event GW170817, *The Astrophysical Journal Letters* **848**,

- L15 (2017), [arXiv:1710.05449 \[astro-ph.HE\]](https://arxiv.org/abs/1710.05449).
 [7] I. Andreoni, K. Ackley, J. Cooke, A. Acharyya, J. R. Allison, G. E. Anderson, M. C. B. Ashley, D. Baade, M. Bailes, K. Bannister, A. Beardsley, M. S. Bessell, F. Bian, P. A. Bland, M. Boer, T. Booler, A. Brandeker, I. S. Brown, D. A. H. Buckley, S. W. Chang, D. M. Coward, S. Crawford, H. Crisp, B. Crosse, A. Cucchiara, M. Cupák, J. S. de Gois, A. Deller, H. A. R. Devillepoix, D. Dobie, E. Elmer, D. Emrich, W. Farah, T. J. Farrell, T. Franzen, B. M. Gaensler, D. K. Galloway, B. Gendre, T. Giblin, A. Goobar, J. Green, P. J. Hancock, B. A. D. Hartig, E. J. Howell, L. Horsley, A. Hotan, R. M. Howie, L. Hu, Y. Hu, C. W. James, S. Johnston, M. Johnston-Hollitt, D. L. Kaplan, M. Kasliwal, E. F. Keane, D. Kenney, A. Klotz, R. Lau, R. Laugier, E. Lenc,

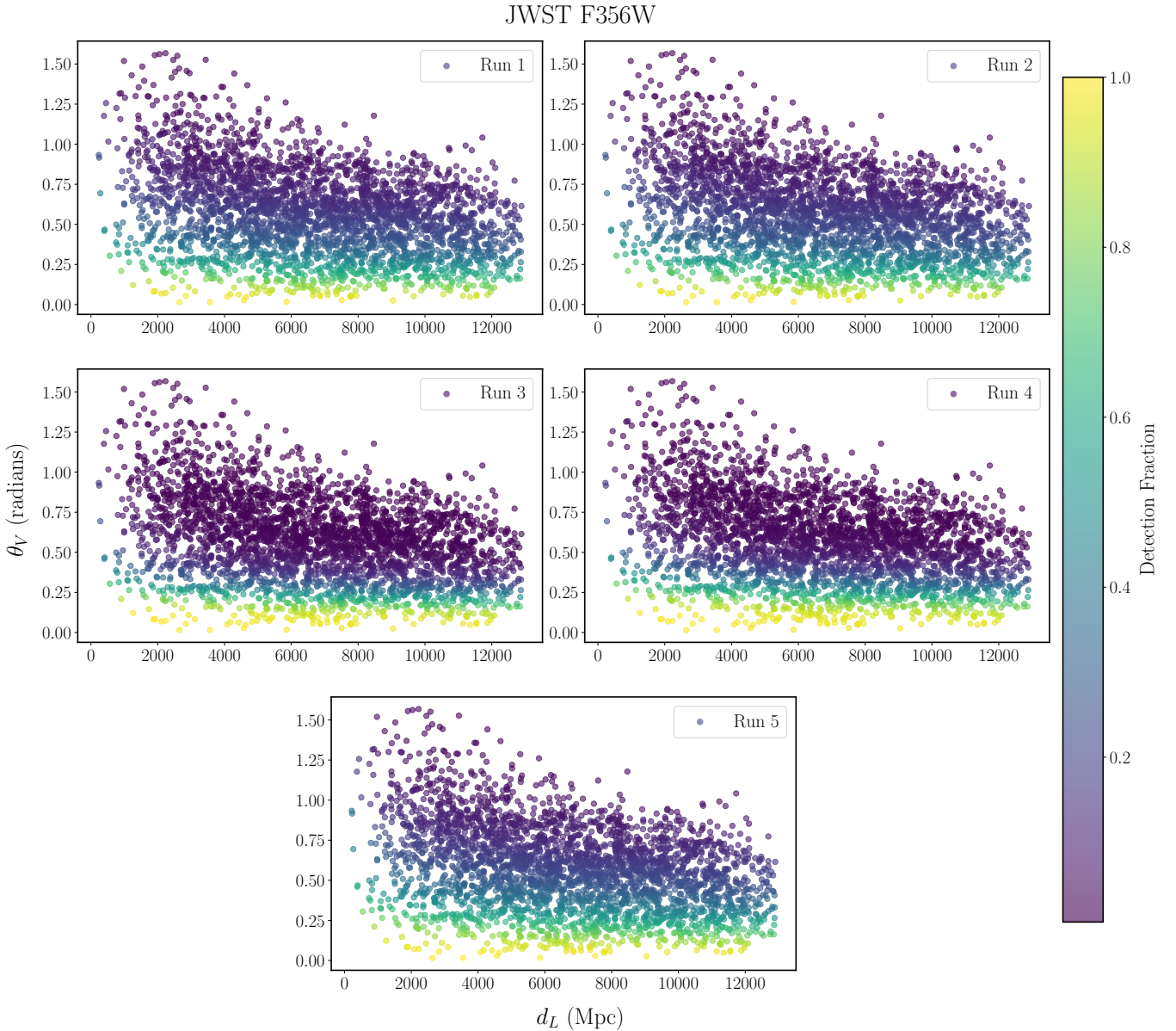


FIG. 11. Same as Figure 10 for BNS mergers detectable by our XG detector setup.

X. Li, E. Liang, C. Lidman, L. C. Luvaal, C. Lynch, B. Ma, D. Macpherson, J. Mao, D. E. McClelland, C. McCully, A. Möller, M. F. Morales, D. Morris, T. Murphy, K. Noy-sena, C. A. Onken, N. B. Orange, S. Osłowski, D. Pallot, J. Paxman, S. B. Potter, T. Pritchard, W. Raja, R. Ridden-Harper, E. Romero-Colmenero, E. M. Sadler, E. K. Sansom, R. A. Scalzo, B. P. Schmidt, S. M. Scott, N. Seghouani, Z. Shang, R. M. Shannon, L. Shao, M. M. Shara, R. Sharp, M. Sokolowski, J. Sollerman, J. Staff, K. Steele, T. Sun, N. B. Suntzeff, C. Tao, S. Tingay, M. C. Towner, P. Thierry, C. Trott, B. E. Tucker, P. Väistänen, V. V. Krishnan, M. Walker, L. Wang, X. Wang, R. Wayth, M. Whiting, A. Williams, T. Williams, C. Wolf, C. Wu, X. Wu, J. Yang, X. Yuan, H. Zhang, J. Zhou, and H. Zovaro, Follow Up of GW170817 and Its Electromagnetic Counterpart by Australian-Led Observing Programmes, *Publ. Astron. Soc. Australia* **34**, e069 (2017), [arXiv:1710.05846 \[astro-ph.HE\]](https://arxiv.org/abs/1710.05846).

- [8] I. Arcavi, G. Hosseinzadeh, D. A. Howell, C. McCully, D. Poznanski, D. Kasen, J. Barnes, M. Zaltzman, S. Vasylyev, D. Maoz, and S. Valenti, Optical emission from a kilonova following a gravitational-wave-detected neutron-star merger, *Nature (London)* **551**, 64 (2017), [arXiv:1710.05843 \[astro-ph.HE\]](https://arxiv.org/abs/1710.05843).
- [9] R. Chornock, E. Berger, D. Kasen, P. S. Cowperthwaite, M. Nicholl, V. A. Villar, K. D. Alexander, P. K. Blanchard, T. Eftekhari, W. Fong, R. Margutti, P. K. G. Williams, J. Annis, D. Brout, D. A. Brown, H. Y. Chen, M. R. Drout, B. Farr, R. J. Foley, J. A. Frieman, C. L. Fryer, K. Herner, D. E. Holz, R. Kessler, T. Matheson, B. D. Metzger, E. Quataert, A. Rest, M. Sako, D. M. Scolnic, N. Smith, and M. Soares-Santos, The Electromagnetic Counterpart of the Binary Neutron Star Merger LIGO/Virgo GW170817. IV. Detection of

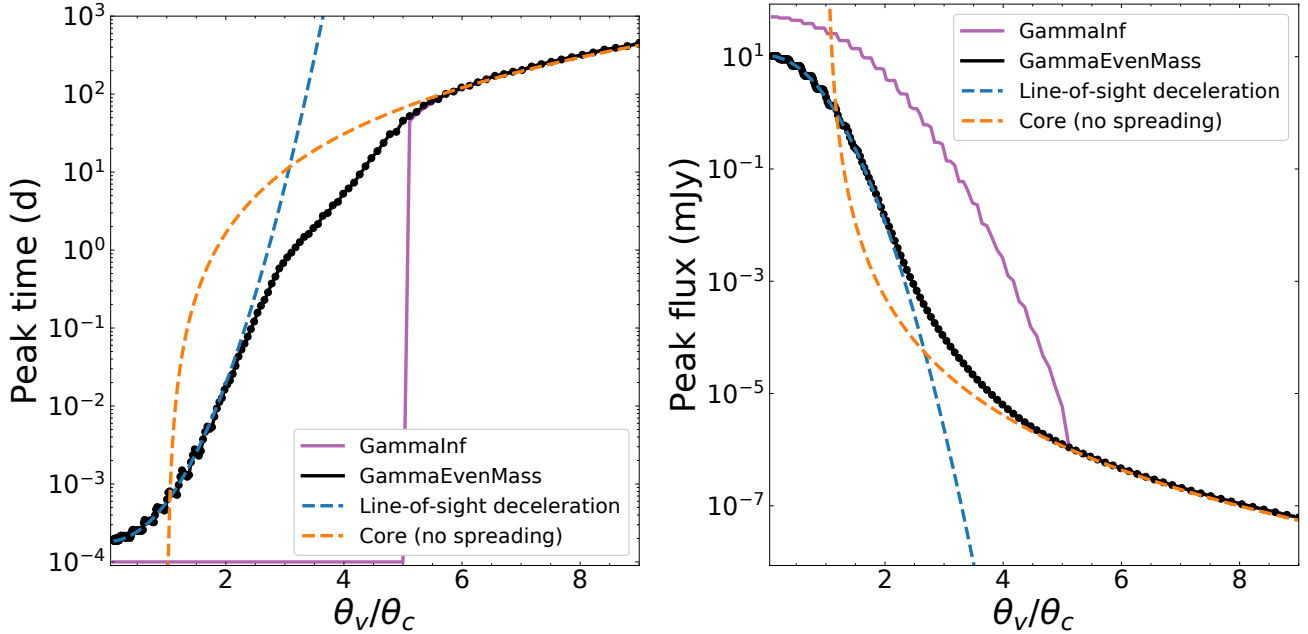


FIG. 12. Peak time t_p and flux F_p versus viewing angle θ_v/θ_c using `afterglowpy`. We show the results for a GJ for both the default setting (GammaInf) and an angular Lorentz factor profile (GammaEvenMass). The peak time and flux match the expected analytic scalings. The afterglow parameters are: $\Gamma_0 = 300$, $E_{\text{kin},0} = 10^{52}$ erg, $n = 10^{-2}$ cm $^{-3}$, $\varepsilon_e = 10^{-1}$, $\varepsilon_B = 10^{-2}$, $p = 2.2$, $\theta_c = 0.1$ rad, and $\theta_w = 0.5$ rad computed at a distance of 150 Mpc at $\nu = 1$ keV.

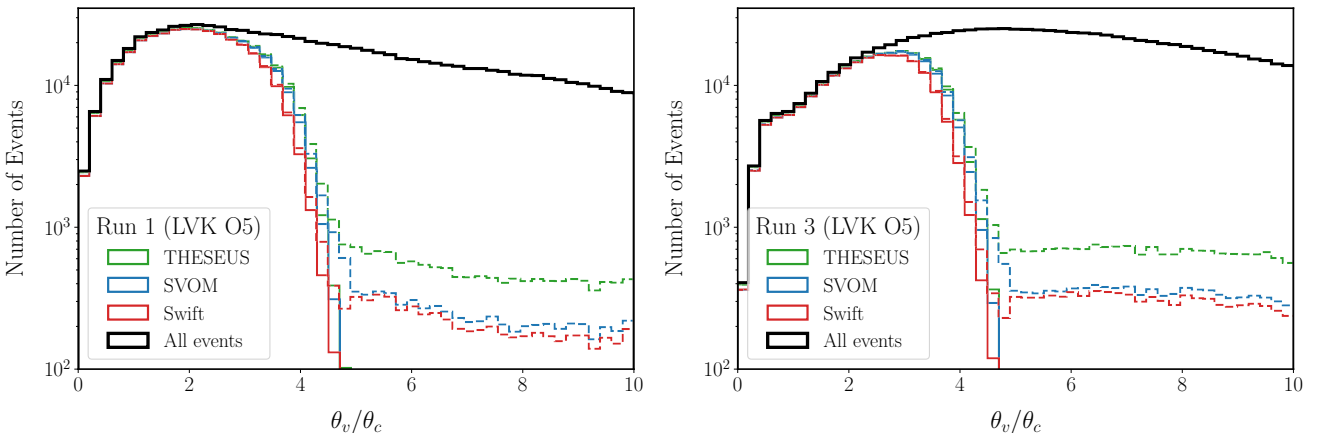


FIG. 13. Distribution of viewing angles for events detected in gamma-rays. Solid lines represent the GJ model, whereas dashed lines are for the GJ model with the addition of a quasi-isotropic cocoon.

Near-infrared Signatures of r-process Nucleosynthesis with Gemini-South, [The Astrophysical Journal Letters 848, L19 \(2017\)](#), arXiv:1710.05454 [astro-ph.HE].

- [10] D. A. Coulter, R. J. Foley, C. D. Kilpatrick, M. R. Drout, A. L. Piro, B. J. Shappee, M. R. Siebert, J. D. Simon, N. Ulloa, D. Kasen, B. F. Madore, A. Murguia-Berthier, Y. C. Pan, J. X. Prochaska, E. Ramirez-Ruiz, A. Rest, and C. Rojas-Bravo, Swope Supernova Survey 2017a (SSS17a), the optical counterpart to a gravitational wave source, [Science 358, 1556 \(2017\)](#), arXiv:1710.05452 [astro-ph.HE].
- [11] S. Covino, K. Wiersema, Y. Z. Fan, K. Toma, A. B. Higgins, A. Melandri, P. D'Avanzo, C. G. Mundell, E. Palazzi, N. R. Tanvir, M. G. Bernardini, M. Branchesi, E. Brocato, S. Campana, S. di Serego Alighieri, D. Götz, J. P. U. Fynbo, W. Gao,

A. Gomboc, B. Gompertz, J. Greiner, J. Hjorth, Z. P. Jin, L. Kaper, S. Klose, S. Kobayashi, D. Kopac, C. Kouveliotou, A. J. Levan, J. Mao, D. Malesani, E. Pian, A. Rossi, R. Salvaterra, R. L. C. Starling, I. Steele, G. Tagliaferri, E. Troja, A. J. van der Horst, and R. A. M. J. Wijers, The unpolarized macronova associated with the gravitational wave event GW 170817, [Nature Astronomy 1, 791 \(2017\)](#), arXiv:1710.05849 [astro-ph.HE].

- [12] P. S. Cowperthwaite, E. Berger, V. A. Villar, B. D. Metzger, M. Nicholl, R. Chornock, P. K. Blanchard, W. Fong, R. Margutti, M. Soares-Santos, K. D. Alexander, S. Allam, J. Annis, D. Brout, D. A. Brown, R. E. Butler, H. Y. Chen, H. T. Diehl, Z. Doctor, M. R. Drout, T. Eftekhari, B. Farr, D. A. Finley, R. J. Foley, J. A. Frieman, C. L. Fryer, J. García-

- Bellido, M. S. S. Gill, J. Guillochon, K. Herner, D. E. Holz, D. Kasen, R. Kessler, J. Marriner, T. Matheson, J. Neilsen, E. H., E. Quataert, A. Palmese, A. Rest, M. Sako, D. M. Scolnic, N. Smith, D. L. Tucker, P. K. G. Williams, E. Balbinot, J. L. Carlin, E. R. Cook, F. Durret, T. S. Li, P. A. A. Lopes, A. C. C. Lourenço, J. L. Marshall, G. E. Medina, J. Muir, R. R. Muñoz, M. Sauseda, D. J. Schlegel, L. F. Secco, A. K. Vivas, W. Wester, A. Zenteno, Y. Zhang, T. M. C. Abbott, M. Banerji, K. Bechtol, A. Benoit-Lévy, E. Bertin, E. Buckley-Geer, D. L. Burke, D. Capozzi, A. Carnero Rosell, M. Carrasco Kind, F. J. Castander, M. Crocce, C. E. Cunha, C. B. D’Andrea, L. N. da Costa, C. Davis, D. L. DePoy, S. Desai, J. P. Dietrich, A. Drlica-Wagner, T. F. Eifler, A. E. Evrard, E. Fernand ez, B. Flaugher, P. Fosalba, E. Gaztanaga, D. W. Gerdes, T. Giannantonio, D. A. Goldstein, D. Gruen, R. A. Gruendl, G. Gutierrez, K. Honscheid, B. Jain, D. J. James, T. Jeltema, M. W. G. Johnson, M. D. Johnson, S. Kent, E. Krause, R. Kron, K. Kuehn, N. Nuropatkin, O. Lahav, M. Lima, H. Lin, M. A. G. Maia, M. March, P. Martini, R. G. McMahon, F. Menanteau, C. J. Miller, R. Miquel, J. J. Mohr, E. Neilsen, R. C. Nichol, R. L. C. Ogando, A. A. Plazas, N. Roe, A. K. Romer, A. Roodman, E. S. Rykoff, E. Sanchez, V. Scarpine, R. Schindler, M. Schubnell, I. Sevilla-Noarbe, M. Smith, R. C. Smith, F. Sobreira, E. Suchyta, M. E. C. Swanson, G. Tarle, D. Thomas, R. C. Thomas, M. A. Troxel, V. Vikram, A. R. Walker, R. H. Wechsler, J. Weller, B. Yanny, and J. Zuntz, The Electromagnetic Counterpart of the Binary Neutron Star Merger LIGO/Virgo GW170817. II. UV, Optical, and Near-infrared Light Curves and Comparison to Kilonova Models, *The Astrophysical Journal Letters* **848**, L17 (2017), [arXiv:1710.05840 \[astro-ph.HE\]](#).
- [13] M. R. Drout, A. L. Piro, B. J. Shappee, C. D. Kilpatrick, J. D. Simon, C. Contreras, D. A. Coulter, R. J. Foley, M. R. Siebert, N. Morrell, K. Boutsia, F. Di Mille, T. W. S. Holoi, D. Kasen, J. A. Kollmeier, B. F. Madore, A. J. Monson, A. Murguia-Berthier, Y. C. Pan, J. X. Prochaska, E. Ramirez-Ruiz, A. Rest, C. Adams, K. Alatalo, E. Bañados, J. Baumgarten, T. C. Beers, R. A. Bernstein, T. Bitsakis, A. Campillay, T. T. Hansen, C. R. Higgs, A. P. Ji, G. Maravelias, J. L. Marshall, C. Moni Bidin, J. L. Prieto, K. C. Rasmussen, C. Rojas-Bravo, A. L. Strom, N. Ulloa, J. Vargas-González, Z. Wan, and D. D. Whitten, Light curves of the neutron star merger GW170817/SSS17a: Implications for r-process nucleosynthesis, *Science* **358**, 1570 (2017), [arXiv:1710.05443 \[astro-ph.HE\]](#).
- [14] P. A. Evans, S. B. Cenko, J. A. Kennea, S. W. K. Emery, N. P. M. Kuin, O. Korobkin, R. T. Wollaeger, C. L. Fryer, K. K. Madsen, F. A. Harrison, Y. Xu, E. Nakar, K. Hotokezaka, A. Lien, S. Campana, S. R. Oates, E. Troja, A. A. Breeveld, F. E. Marshall, S. D. Barthelmy, A. P. Beardmore, D. N. Burrows, G. Cusumano, A. D’Aì, P. D’Avanzo, V. D’Elia, M. de Pasquale, W. P. Even, C. J. Fontes, K. Forster, J. Garcia, P. Giommi, B. Grefenstette, C. Gronwall, D. H. Hartmann, M. Heida, A. L. Hungerford, M. M. Kasliwal, H. A. Krimm, A. J. Levan, D. Malesani, A. Melandri, H. Miyasaka, J. A. Nousek, P. T. O’Brien, J. P. Osborne, C. Pagani, K. L. Page, D. M. Palmer, M. Perri, S. Pike, J. L. Racusin, S. Rosswog, M. H. Siegel, T. Sakamoto, B. Sbarufatti, G. Tagliaferri, N. R. Tanvir, and A. Tohuvavohu, Swift and NuSTAR observations of GW170817: Detection of a blue kilonova, *Science* **358**, 1565 (2017), [arXiv:1710.05437 \[astro-ph.HE\]](#).
- [15] M. M. Kasliwal, E. Nakar, L. P. Singer, D. L. Kaplan, D. O. Cook, A. Van Sistine, R. M. Lau, C. Fremling, O. Gottlieb, J. E. Jencson, S. M. Adams, U. Feindt, K. Hotokezaka, S. Ghosh, D. A. Perley, P. C. Yu, T. Piran, J. R. Allison, G. C. Anupama, A. Balasubramanian, K. W. Bannister, J. Bally, J. Barnes, S. Barway, E. Bellm, V. Bhalerao, D. Bhattacharya, N. Blagorodnova, J. S. Bloom, P. R. Brady, C. Cannella, D. Chatterjee, S. B. Cenko, B. E. Cobb, C. Copperwheat, A. Corsi, K. De, D. Dobie, S. W. K. Emery, P. A. Evans, O. D. Fox, D. A. Frail, C. Frohmaier, A. Goobar, G. Hallinan, F. Harrison, G. Helou, T. Hinderer, A. Y. Q. Ho, A. Horesh, W. H. Ip, R. Itoh, D. Kasen, H. Kim, N. P. M. Kuin, T. Kupfer, C. Lynch, K. Madsen, P. A. Mazzali, A. A. Miller, K. Mooley, T. Murphy, C. C. Ngeow, D. Nichols, S. Nissanke, P. Nugent, E. O. Ofek, H. Qi, R. M. Quimby, S. Rosswog, F. Rusu, E. M. Sadler, P. Schmidt, J. Sollerman, I. Steele, A. R. Williamson, Y. Xu, L. Yan, Y. Yatsu, C. Zhang, and W. Zhao, Illuminating gravitational waves: A concordant picture of photons from a neutron star merger, *Science* **358**, 1559 (2017), [arXiv:1710.05436 \[astro-ph.HE\]](#).
- [16] V. M. Lipunov, E. Gorbovskoy, V. G. Kornilov, N. . Tyurina, P. Balanutsa, A. Kuznetsov, D. Vlasenko, D. Kuvshinov, I. Gorbunov, D. A. H. Buckley, A. V. Krylov, R. Podesta, C. Lopez, F. Podesta, H. Levato, C. Saffe, C. Mallamachi, S. Potter, N. M. Budnev, O. Gress, Y. Ishmuhametova, V. Vladimirov, D. Zimnukhov, V. Yurkov, Y. Sergienko, A. Gabovich, R. Rebolo, M. Serra-Ricart, G. Israelyan, V. Chazov, X. Wang, A. Tlatov, and M. I. Panchenko, MASTER Optical Detection of the First LIGO/Virgo Neutron Star Binary Merger GW170817, *The Astrophysical Journal Letters* **850**, L1 (2017), [arXiv:1710.05461 \[astro-ph.HE\]](#).
- [17] M. Nicholl, E. Berger, D. Kasen, B. D. Metzger, J. Elias, C. Briceño, K. D. Alexander, P. K. Blanchard, R. Chornock, P. S. Cowperthwaite, T. Eftekhari, W. Fong, R. Margutti, V. A. Villar, P. K. G. Williams, W. Brown, J. Annis, A. Bahramian, D. Brout, D. A. Brown, H. Y. Chen, J. C. Clemens, E. Dennihy, B. Dunlap, D. E. Holz, E. Marchesini, F. Massaro, N. Moskowitz, I. Pelisoli, A. Rest, F. Ricci, M. Sako, M. Soares-Santos, and J. Strader, The Electromagnetic Counterpart of the Binary Neutron Star Merger LIGO/Virgo GW170817. III. Optical and UV Spectra of a Blue Kilonova from Fast Polar Ejecta, *The Astrophysical Journal Letters* **848**, L18 (2017), [arXiv:1710.05456 \[astro-ph.HE\]](#).
- [18] E. Pian, P. D’Avanzo, S. Benetti, M. Branchesi, E. Brocato, S. Campana, E. Cappellaro, S. Covino, V. D’Elia, J. P. U. Fynbo, F. Getman, G. Ghirlanda, G. Ghisellini, A. Grado, G. Greco, J. Hjorth, C. Kouveliotou, A. Levan, L. Limatola, D. Malesani, P. A. Mazzali, A. Melandri, P. Møller, L. Nicastro, E. Palazzi, S. Piranomonte, A. Rossi, O. S. Salafia, J. Selsing, G. Stratta, M. Tanaka, N. R. Tanvir, L. Tomasella, D. Watson, S. Yang, L. Amati, L. A. Antonelli, S. Ascenzi, M. G. Bernardini, M. Boér, F. Bufano, A. Bulgarelli, M. Capaccioli, P. Casella, A. J. Castro-Tirado, E. Chassande-Mottin, R. Ciolfi, C. M. Copperwheat, M. Dadina, G. De Cesare, A. di Paola, Y. Z. Fan, B. Gendre, G. Giuffrida, A. Giunta, L. K. Hunt, G. L. Israel, Z. P. Jin, M. M. Kasliwal, S. Klose, M. Lisi, F. Longo, E. Maiorano, M. Mapelli, N. Masetti, L. Nava, B. Patricelli, D. Perley, A. Pescalli, T. Piran, A. Possenti, L. Pulone, M. Razzano, R. Salvaterra, P. Schipani, M. Spera, A. Stamerla, L. Stella, G. Tagliaferri, V. Testa, E. Troja, M. Turatto, S. D. Vergani, and D. Vergani, Spectroscopic identification of r-process nucleosynthesis in a double neutron-star merger, *Nature (London)* **551**, 67 (2017), [arXiv:1710.05858 \[astro-ph.HE\]](#).
- [19] B. J. Shappee, J. D. Simon, M. R. Drout, A. L. Piro, N. Morrell, J. L. Prieto, D. Kasen, T. W. S. Holoi, J. A. Kollmeier, D. D. Kelson, D. A. Coulter, R. J. Foley, C. D. Kilpatrick,

- M. R. Siebert, B. F. Madore, A. Murgia-Berthier, Y. C. Pan, J. X. Prochaska, E. Ramirez-Ruiz, A. Rest, C. Adams, K. Alatalo, E. Bañados, J. Baughman, R. A. Bernstein, T. Bitsakis, K. Boutsia, J. R. Bravo, F. Di Mille, C. R. Higgs, A. P. Ji, G. Maravelias, J. L. Marshall, V. M. Placco, G. Prieto, and Z. Wan, Early spectra of the gravitational wave source GW170817: Evolution of a neutron star merger, *Science* **358**, 1574 (2017), [arXiv:1710.05432 \[astro-ph.HE\]](#).
- [20] S. J. Smartt, T. W. Chen, A. Jerkstrand, M. Coughlin, E. Kankare, S. A. Sim, M. Fraser, C. Inserra, K. Maguire, K. C. Chambers, M. E. Huber, T. Krühler, G. Leloudas, M. Magee, L. J. Shingles, K. W. Smith, D. R. Young, J. Tonry, R. Kotak, A. Gal-Yam, J. D. Lyman, D. S. Homan, C. Agliozzo, J. P. Anderson, C. R. Angus, C. Ashall, C. Barbarino, F. E. Bauer, M. Berton, M. T. Botticella, M. Bulla, J. Bulger, G. Cannizzaro, Z. Cano, R. Cartier, A. Cikota, P. Clark, A. De Cia, M. Della Valle, L. Denneau, M. Dennefeld, L. Dessart, G. Dimitriadis, N. Elias-Rosa, R. E. Firth, H. Flewelling, A. Flörs, A. Franckowiak, C. Frohmaier, L. Galbany, S. González-Gaitán, J. Greiner, M. Gromadzki, A. N. Guelbenzu, C. P. Gutiérrez, A. Hamanowicz, L. Hanlon, J. Harmanen, K. E. Heintz, A. Heinze, M. S. Hernandez, S. T. Hodgkin, I. M. Hook, L. Izzo, P. A. James, P. G. Jonker, W. E. Kerzendorf, S. Klose, Z. Kostrzewa-Rutkowska, M. Kowalski, M. Kromer, H. Kuncarayakti, A. Lawrence, T. B. Lowe, E. A. Magnier, I. Manulis, A. Martin-Carrillo, S. Mattila, O. McBrien, A. Müller, J. Nordin, D. O'Neill, F. Onori, J. T. Palmerio, A. Pastorello, F. Patat, G. Pignata, P. Podsiadlowski, M. L. Pumo, S. J. Prentice, A. Rau, A. Razza, A. Rest, T. Reynolds, R. Roy, A. J. Ruiter, K. A. Rybicki, L. Salmon, P. Schady, A. S. B. Schultz, T. Schweyer, I. R. Seitenzahl, M. Smith, J. Sollerman, B. Stalder, C. W. Stubbs, M. Sullivan, H. Szegedi, F. Taddia, S. Taubenberger, G. Terreran, B. van Soelen, J. Vos, R. J. Wainscoat, N. A. Walton, C. Waters, H. Weiland, M. Willman, P. Wiseman, D. E. Wright, Ł. Wyrykowski, and O. Yaron, A kilonova as the electromagnetic counterpart to a gravitational-wave source, *Nature (London)* **551**, 75 (2017), [arXiv:1710.05841 \[astro-ph.HE\]](#).
- [21] M. Soares-Santos, D. E. Holz, J. Annis, R. Chornock, K. Herner, E. Berger, D. Brout, H. Y. Chen, R. Kessler, M. Sako, S. Allam, D. L. Tucker, R. E. Butler, A. Palmese, Z. Doctor, H. T. Diehl, J. Frieman, B. Yanny, H. Lin, D. Scolnic, P. Cowperthwaite, E. Neilsen, J. Marriner, N. Kuropatkin, W. G. Hartley, F. Paz-Chinchón, K. D. Alexander, E. Balbinot, P. Blanchard, D. A. Brown, J. L. Carlin, C. Conselice, E. R. Cook, A. Drlica-Wagner, M. R. Drout, F. Durret, T. Eftekhar, B. Farr, D. A. Finley, R. J. Foley, W. Fong, C. L. Fryer, J. García-Bellido, M. S. S. Gill, R. A. Gruendl, C. Hanna, D. Kasen, T. S. Li, P. A. A. Lopes, A. C. C. Lourenço, R. Margutti, J. L. Marshall, T. Matheson, G. E. Medina, B. D. Metzger, R. R. Muñoz, J. Muir, M. Nicholl, E. Quataert, A. Rest, M. Sauseda, D. J. Schlegel, L. F. Secco, F. Sobreira, A. Stebbins, V. A. Villar, K. Vivas, A. R. Walker, W. Wester, P. K. G. Williams, A. Zenteno, Y. Zhang, T. M. C. Abbott, F. B. Abdalla, M. Banerji, K. Bechtol, A. Benoit-Lévy, E. Bertin, D. Brooks, E. Buckley-Geer, D. L. Burke, A. Carnero Rosell, M. Carrasco Kind, J. Carretero, F. J. Castander, M. Crocce, C. E. Cunha, C. B. D'Andrea, L. N. da Costa, C. Davis, S. Desai, J. P. Dietrich, P. Doel, T. F. Eifler, E. Fernández, B. Flaugher, P. Fosalba, E. Gaztanaga, D. W. Gerdes, T. Giannantonio, D. A. Goldstein, D. Gruen, J. Gschwend, G. Gutierrez, K. Honscheid, B. Jain, D. J. James, T. Jeltema, M. W. G. Johnson, M. D. Johnson, S. Kent, E. Krause, R. Kron, K. Kuehn, S. Kuhlmann, O. Lahav, M. Lima, M. A. G. Maia, M. March, R. G. McMahon, F. Menanteau, R. Miquel, J. J. Mohr, R. C. Nichol, B. Nord, R. L. C. Ogando, D. Petravick, A. A. Plazas, A. K. Romer, A. Roodman, E. S. Rykoff, E. Sanchez, V. Scarpine, M. Schubnell, I. Sevilla-Noarbe, M. Smith, R. C. Smith, E. Suchyta, M. E. C. Swanson, G. Tarle, D. Thomas, R. C. Thomas, M. A. Troxel, V. Vikram, R. H. Wechsler, J. Weller, Dark Energy Survey, and Dark Energy Camera GW-EM Collaboration, The Electromagnetic Counterpart of the Binary Neutron Star Merger LIGO/Virgo GW170817. I. Discovery of the Optical Counterpart Using the Dark Energy Camera, *The Astrophysical Journal Letters* **848**, L16 (2017), [arXiv:1710.05459 \[astro-ph.HE\]](#).
- [22] N. R. Tanvir, A. J. Levan, C. González-Fernández, O. Korobkin, I. Mandel, S. Rosswog, J. Hjorth, P. D'Avanzo, A. S. Fruchter, C. L. Fryer, T. Kangas, B. Milvang-Jensen, S. Rosetti, D. Steeghs, R. T. Wollaeger, Z. Cano, C. M. Copperwheat, S. Covino, V. D'Elia, A. de Ugarte Postigo, P. A. Evans, W. P. Even, S. Fairhurst, R. Figuera Jaimes, C. J. Fontes, Y. I. Fujii, J. P. U. Fynbo, B. P. Gompertz, J. Greiner, G. Hodosan, M. J. Irwin, P. Jakobsson, U. G. Jørgensen, D. A. Kann, J. D. Lyman, D. Malesani, R. G. McMahon, A. Melandri, P. T. O'Brien, J. P. Osborne, E. Palazzi, D. A. Perley, E. Pian, S. Piranomonte, M. Rabus, E. Rol, A. Rowlinson, S. Schulze, P. Sutton, C. C. Thöne, K. Ulaczyk, D. Watson, K. Wiersema, and R. A. M. J. Wijers, The Emergence of a Lanthanide-rich Kilonova Following the Merger of Two Neutron Stars, *The Astrophysical Journal Letters* **848**, L27 (2017), [arXiv:1710.05455 \[astro-ph.HE\]](#).
- [23] Y. Utsumi, M. Tanaka, N. Tominaga, M. Yoshida, S. Barway, T. Nagayama, T. Zenko, K. Aoki, T. Fujiyoshi, H. Furusawa, K. S. Kawabata, S. Koshida, C.-H. Lee, T. Morokuma, K. Motohara, F. Nakata, R. Ohsawa, K. Ohta, H. Okita, A. Tajitsu, I. Tanaka, T. Terai, N. Yasuda, F. Abe, Y. Asakura, I. A. Bond, S. Miyazaki, T. Sumi, P. J. Tristram, S. Honda, R. Itoh, Y. Itoh, M. Kawabata, K. Morihana, H. Nagashima, T. Nakaoka, T. Ohshima, J. Takahashi, M. Takayama, W. Aoki, S. Baar, M. Doi, F. Finet, N. Kanda, N. Kawai, J. H. Kim, D. Kuroda, W. Liu, K. Matsubayashi, K. L. Murata, H. Nagai, T. Saito, Y. Saito, S. Sako, Y. Sekiguchi, Y. Tamura, M. Tanaka, M. Uemura, and M. S. Yamaguchi, J-GEM observations of an electromagnetic counterpart to the neutron star merger GW170817, *PASJ* **69**, 101 (2017), [arXiv:1710.05848 \[astro-ph.HE\]](#).
- [24] S. Valenti, D. J. Sand, S. Yang, E. Cappellaro, L. Tartaglia, A. Corsi, S. W. Jha, D. E. Reichart, J. Haislip, and V. Kouprianov, The Discovery of the Electromagnetic Counterpart of GW170817: Kilonova AT 2017gfo/DLT17ck, *The Astrophysical Journal Letters* **848**, L24 (2017), [arXiv:1710.05854 \[astro-ph.HE\]](#).
- [25] R. Margutti, E. Berger, W. Fong, C. Guidorzi, K. D. Alexander, B. D. Metzger, P. K. Blanchard, P. S. Cowperthwaite, R. Chornock, T. Eftekhar, M. Nicholl, V. A. Villar, P. K. G. Williams, J. Annis, D. A. Brown, H. Chen, Z. Doctor, J. A. Frieman, D. E. Holz, M. Sako, and M. Soares-Santos, The Electromagnetic Counterpart of the Binary Neutron Star Merger LIGO/Virgo GW170817. V. Rising X-Ray Emission from an Off-axis Jet, *The Astrophysical Journal Letters* **848**, L20 (2017), [arXiv:1710.05431 \[astro-ph.HE\]](#).
- [26] E. Troja, L. Piro, H. van Eerten, R. T. Wollaeger, M. Im, O. D. Fox, N. R. Butler, S. B. Cenko, T. Sakamoto, C. L. Fryer, R. Ricci, A. Lien, R. E. Ryan, O. Korobkin, S. K. Lee, J. M. Burgess, W. H. Lee, A. M. Watson, C. Choi, S. Covino, P. D'Avanzo, C. J. Fontes, J. B. González, H. G. Khan-drika, J. Kim, S. L. Kim, C. U. Lee, H. M. Lee, A. Kutyrev,

- G. Lim, R. Sánchez-Ramírez, S. Veilleux, M. H. Wieringa, and Y. Yoon, The X-ray counterpart to the gravitational-wave event GW170817, *Nature (London)* **551**, 71 (2017), [arXiv:1710.05433 \[astro-ph.HE\]](#).
- [27] G. Hallinan, A. Corsi, K. P. Mooley, K. Hotokezaka, E. Nakar, M. M. Kasliwal, D. L. Kaplan, D. A. Frail, S. T. Myers, T. Murphy, K. De, D. Dobie, J. R. Allison, K. W. Bannister, V. Bhalerao, P. Chandra, T. E. Clarke, S. Giacintucci, A. Y. Q. Ho, A. Horesh, N. E. Cassim, S. R. Kulkarni, E. Lenc, F. J. Lockman, C. Lynch, D. Nichols, S. Nissanke, N. Palliyaguru, W. M. Peters, T. Piran, J. Rana, E. M. Sadler, and L. P. Singer, A radio counterpart to a neutron star merger, *Science* **358**, 1579 (2017), [arXiv:1710.05435 \[astro-ph.HE\]](#).
- [28] K. D. Alexander, E. Berger, W. Fong, P. K. G. Williams, C. Guidorzi, R. Margutti, B. D. Metzger, J. Annis, P. K. Blanchard, D. Brout, D. A. Brown, H. Y. Chen, R. Chornock, P. S. Cowperthwaite, M. Drout, T. Eftekhari, J. Frieman, D. E. Holz, M. Nicholl, A. Rest, M. Sako, M. Soares-Santos, and V. A. Villar, The Electromagnetic Counterpart of the Binary Neutron Star Merger LIGO/Virgo GW170817. VI. Radio Constraints on a Relativistic Jet and Predictions for Late-time Emission from the Kilonova Ejecta, *The Astrophysical Journal Letters* **848**, L21 (2017), [arXiv:1710.05457 \[astro-ph.HE\]](#).
- [29] D. Haggard, M. Nynka, J. J. Ruan, V. Kalogera, S. B. Cenko, P. Evans, and J. A. Kennea, A Deep Chandra X-Ray Study of Neutron Star Coalescence GW170817, *The Astrophysical Journal Letters* **848**, L25 (2017), [arXiv:1710.05852 \[astro-ph.HE\]](#).
- [30] G. P. Lamb and S. Kobayashi, Electromagnetic counterparts to structured jets from gravitational wave detected mergers, *MNRAS* **472**, 4953 (2017), [arXiv:1706.03000 \[astro-ph.HE\]](#).
- [31] D. Lazzati, R. Perna, B. J. Morsony, D. Lopez-Camara, M. Cantiello, R. Ciolfi, B. Giacomazzo, and J. C. Workman, Late Time Afterglow Observations Reveal a Collimated Relativistic Jet in the Ejecta of the Binary Neutron Star Merger GW170817, *Phys. Rev. Lett.* **120**, 241103 (2018), [arXiv:1712.03237 \[astro-ph.HE\]](#).
- [32] L. Resmi, S. Schulze, C. H. Ishwara-Chandra, K. Misra, J. Buchner, M. De Pasquale, R. Sánchez-Ramírez, S. Klose, S. Kim, N. R. Tanvir, and P. T. O'Brien, Low-frequency View of GW170817/GRB 170817A with the Giant Metrewave Radio Telescope, *Astrophys. J.* **867**, 57 (2018), [arXiv:1803.02768 \[astro-ph.HE\]](#).
- [33] K. P. Mooley, A. T. Deller, O. Gottlieb, E. Nakar, G. Hallinan, S. Bourke, D. A. Frail, A. Horesh, A. Corsi, and K. Hotokezaka, Superluminal motion of a relativistic jet in the neutron-star merger GW170817, *Nature (London)* **561**, 355 (2018), [arXiv:1806.09693 \[astro-ph.HE\]](#).
- [34] P. D'Avanzo, S. Campana, O. S. Salafia, G. Ghirlanda, G. Ghisellini, A. Melandri, M. G. Bernardini, M. Branchesi, E. Chassande-Mottin, S. Covino, V. D'Elia, L. Nava, R. Salvaterra, G. Tagliaferri, and S. D. Vergani, The evolution of the X-ray afterglow emission of GW 170817/ GRB 170817A in XMM-Newton observations, *Astronomy & Astrophysics* **613**, L1 (2018), [arXiv:1801.06164 \[astro-ph.HE\]](#).
- [35] K. D. Alexander, R. Margutti, P. K. Blanchard, W. Fong, E. Berger, A. Hajela, T. Eftekhari, R. Chornock, P. S. Cowperthwaite, D. Giannios, C. Guidorzi, A. Kathirgamaraju, A. MacFadyen, B. D. Metzger, M. Nicholl, L. Sironi, V. A. Villar, P. K. G. Williams, X. Xie, and J. Zrake, A Decline in the X-Ray through Radio Emission from GW170817 Continues to Support an Off-axis Structured Jet, *Astrophys. J.* **863**, L18 (2018), [arXiv:1805.02870 \[astro-ph.HE\]](#).
- [36] X. Xie, J. Zrake, and A. MacFadyen, Numerical Simulations of the Jet Dynamics and Synchrotron Radiation of Binary Neutron Star Merger Event GW170817/GRB 170817A, *Astrophys. J.* **863**, 58 (2018), [arXiv:1804.09345 \[astro-ph.HE\]](#).
- [37] M. Nynka, J. J. Ruan, D. Haggard, and P. A. Evans, Fading of the X-Ray Afterglow of Neutron Star Merger GW170817/GRB 170817A at 260 Days, *The Astrophysical Journal Letters* **862**, L19 (2018), [arXiv:1805.04093 \[astro-ph.HE\]](#).
- [38] R. Margutti, K. D. Alexander, X. Xie, L. Sironi, B. D. Metzger, A. Kathirgamaraju, W. Fong, P. K. Blanchard, E. Berger, A. MacFadyen, D. Giannios, C. Guidorzi, A. Hajela, R. Chornock, P. S. Cowperthwaite, T. Eftekhari, M. Nicholl, V. A. Villar, P. K. G. Williams, and J. Zrake, The Binary Neutron Star Event LIGO/Virgo GW170817 160 Days after Merger: Synchrotron Emission across the Electromagnetic Spectrum, *The Astrophysical Journal Letters* **856**, L18 (2018), [arXiv:1801.03531 \[astro-ph.HE\]](#).
- [39] R. Gill and J. Granot, Afterglow imaging and polarization of misaligned structured GRB jets and cocoons: breaking the degeneracy in GRB 170817A, *MNRAS* **478**, 4128 (2018), [arXiv:1803.05892 \[astro-ph.HE\]](#).
- [40] G. Ghirlanda, O. S. Salafia, Z. Paragi, M. Giroletti, J. Yang, B. Marcote, J. Blanchard, I. Agudo, T. An, M. G. Bernardini, R. Beswick, M. Branchesi, S. Campana, C. Casadio, E. Chassande-Mottin, M. Colpi, S. Covino, P. D'Avanzo, V. D'Elia, S. Frey, M. Gawronski, G. Ghisellini, L. I. Gurvits, P. G. Jonker, H. J. van Langevelde, A. Melandri, J. Moldon, L. Nava, A. Perego, M. A. Perez-Torres, C. Reynolds, R. Salvaterra, G. Tagliaferri, T. Venturi, S. D. Vergani, and M. Zhang, Compact radio emission indicates a structured jet was produced by a binary neutron star merger, *Science* **363**, 968 (2019), [arXiv:1808.00469 \[astro-ph.HE\]](#).
- [41] E. Nakar, The electromagnetic counterparts of compact binary mergers, *Physics Reports* **886**, 1 (2020).
- [42] R. Margutti and R. Chornock, First multimessenger observations of a neutron star merger, *Annual Review of Astronomy and Astrophysics* **59**, 155 (2021).
- [43] B. F. Schutz, Determining the hubble constant from gravitational wave observations, *Nature* **323**, 310 (1986).
- [44] B. P. Abbott, R. Abbott, T. D. Abbott, F. Acernese, K. Ackley, C. Adams, T. Adams, P. Addesso, R. X. Adhikari, V. B. Adya, and et al., A gravitational-wave standard siren measurement of the Hubble constant, *Nature (London)* **551**, 85 (2017), [arXiv:1710.05835](#).
- [45] H.-Y. Chen, M. Fishbach, and D. E. Holz, A two per cent Hubble constant measurement from standard sirens within five years, *Nature (London)* **562**, 545 (2018), [arXiv:1712.06531 \[astro-ph.CO\]](#).
- [46] S. M. Feeney, H. V. Peiris, A. R. Williamson, S. M. Nissanke, D. J. Mortlock, J. Alsing, and D. Scolnic, Prospects for Resolving the Hubble Constant Tension with Standard Sirens, *Phys. Rev. Lett.* **122**, 061105 (2019), [arXiv:1802.03404 \[astro-ph.CO\]](#).
- [47] K. Hotokezaka, E. Nakar, O. Gottlieb, S. Nissanke, K. Madsuda, G. Hallinan, K. P. Mooley, and A. T. Deller, A Hubble constant measurement from superluminal motion of the jet in GW170817, *Nature Astronomy* **3**, 940 (2019), [arXiv:1806.10596 \[astro-ph.CO\]](#).
- [48] T. Dietrich, M. W. Coughlin, P. T. H. Pang, M. Bulla, J. Heinzel, L. Issa, I. Tews, and S. Antier, Multimessenger constraints on the neutron-star equation of state and the Hubble constant, *Science* **370**, 1450 (2020), [arXiv:2002.11355 \[astro-ph.HE\]](#).

- [49] R. Abbott *et al.* (LIGO Scientific, Virgo, KAGRA), Constraints on the Cosmic Expansion History from GWTC-3, *Astrophys. J.* **949**, 76 (2023), arXiv:2111.03604 [astro-ph.CO].
- [50] A. Palmese, C. R. Bom, S. Mucesh, and W. G. Hartley, A standard siren measurement of the hubble constant using gravitational-wave events from the first three ligo/virgo observing runs and the desi legacy survey, *The Astrophysical Journal* **943**, 56 (2023).
- [51] A. Palmese, R. Kaur, A. Hajela, R. Margutti, A. McDowell, and A. MacFadyen, Standard siren measurement of the hubble constant using gw170817 and the latest observations of the electromagnetic counterpart afterglow, *Physical Review D* **109**, 063508 (2024).
- [52] P. Petrov, L. P. Singer, M. W. Coughlin, V. Kumar, M. Almualla, S. Anand, M. Bulla, T. Dietrich, F. Foucart, and N. Guessoum, Data-driven Expectations for Electromagnetic Counterpart Searches Based on LIGO/Virgo Public Alerts, *Astrophys. J.* **924**, 54 (2022), arXiv:2108.07277 [astro-ph.HE].
- [53] R. W. Kiendrebeogo, A. M. Farah, E. M. Foley, A. Gray, N. Kunert, A. Puecher, A. Toivonen, R. O. VandenBerg, S. Anand, T. Ahumada, V. Karambelkar, M. W. Coughlin, T. Dietrich, S. Z. Kam, P. T. H. Pang, L. P. Singer, and N. Sravan, Updated observing scenarios and multimessenger implications for the international gravitational-wave networks o4 and o5, *The Astrophysical Journal* **958**, 158 (2023).
- [54] Z. Doctor, R. Kessler, H. Y. Chen, B. Farr, D. A. Finley, R. J. Foley, D. A. Goldstein, D. E. Holz, A. G. Kim, E. Morganson, M. Sako, D. Scolnic, M. Smith, M. Soares-Santos, H. Spinka, T. M. C. Abbott, F. B. Abdalla, S. Allam, J. Annis, K. Bechtol, A. Benoit-Lévy, E. Bertin, D. Brooks, E. Buckley-Geer, D. L. Burke, A. Carnero Rosell, M. Carrasco Kind, J. Carretero, C. E. Cunha, C. B. D’Andrea, L. N. da Costa, D. L. DePoy, S. Desai, H. T. Diehl, A. Drlica-Wagner, T. F. Eifler, J. Frieman, J. García-Bellido, E. Gaztanaga, D. W. Gerdes, R. A. Gruendl, J. Gschwend, G. Gutierrez, D. J. James, E. Krause, K. Kuehn, N. Kuropatkin, O. Lahav, T. S. Li, M. Lima, M. A. G. Maia, M. March, J. L. Marshall, F. Menanteau, R. Miquel, E. Neilsen, R. C. Nichol, B. Nord, A. A. Plazas, A. K. Romer, E. Sanchez, V. Scarpine, M. Schubnell, I. Sevilla-Noarbe, R. C. Smith, F. Sobreira, E. Suchyta, M. E. C. Swanson, G. Tarle, A. R. Walker, W. Wester, and DES Collaboration, A Search for Kilonovae in the Dark Energy Survey, *Astrophys. J.* **837**, 57 (2017), arXiv:1611.08052 [astro-ph.HE].
- [55] I. Andreoni, S. Anand, F. B. Bianco, S. B. Cenko, P. S. Cowperthwaite, M. W. Coughlin, M. Drout, V. Z. Golkhou, D. L. Kaplan, K. P. Mooley, T. A. Pritchard, L. P. Singer, S. Webb, w. s. o. t. LSST Transient, and Variable Stars Collaboration, A Strategy for LSST to Unveil a Population of Kilonovae without Gravitational-wave Triggers, *PASP* **131**, 068004 (2019), arXiv:1812.03161 [astro-ph.IM].
- [56] F. B. Bianco, M. R. Drout, M. L. Graham, T. A. Pritchard, R. Biswas, G. Narayan, I. Andreoni, P. S. Cowperthwaite, T. Ribeiro, W. S. o. t. LSST Transient, and Variable Stars Collaboration, Presto-Color: A Photometric Survey Cadence for Explosive Physics and Fast Transients, *PASP* **131**, 068002 (2019), arXiv:1812.03146 [astro-ph.IM].
- [57] M. Almualla, S. Anand, M. W. Coughlin, T. Dietrich, N. Guessoum, A. Sagués Carracedo, T. Ahumada, I. Andreoni, S. Antier, E. C. Bellm, M. Bulla, and L. P. Singer, Optimizing serendipitous detections of kilonovae: cadence and filter selection, *MNRAS* **504**, 2822 (2021), arXiv:2011.10421 [astro-ph.HE].
- [58] O. R. McBrien, S. J. Smartt, M. E. Huber, A. Rest, K. C. Chambers, C. Barbieri, M. Bulla, S. Jha, M. Gromadzki, S. Srivastav, K. W. Smith, D. R. Young, S. McLaughlin, C. Inserra, M. Nicholl, M. Fraser, K. Maguire, T. W. Chen, T. Wevers, J. P. Anderson, T. E. Müller-Bravo, F. Olivares E., E. Kankare, A. Gal-Yam, and C. Waters, PS15cey and PS17cke: prospective candidates from the Pan-STARRS Search for kilonovae, *MNRAS* **500**, 4213 (2021), arXiv:2006.10442 [astro-ph.HE].
- [59] E. A. Chase, B. O’Connor, C. L. Fryer, E. Troja, O. Korobkin, R. T. Wollaeger, M. Ristic, C. J. Fontes, A. L. Hungerford, and A. M. Herring, Kilonova Detectability with Wide-field Instruments, *Astrophys. J.* **927**, 163 (2022), arXiv:2105.12268 [astro-ph.HE].
- [60] I. Andreoni, R. Margutti, O. S. Salafia, B. Parazin, V. A. Villar, M. W. Coughlin, P. Yoachim, K. Mortensen, D. Brethauer, S. J. Smartt, M. M. Kasliwal, K. D. Alexander, S. Anand, E. Berger, M. G. Bernardini, F. B. Bianco, P. K. Blanchard, J. S. Bloom, E. Brocato, M. Bulla, R. Cartier, S. B. Cenko, R. Chornock, C. M. Copperwheat, A. Corsi, F. D’Ammando, P. D’Avanzo, L. É. Hélène Datrier, R. J. Foley, G. Ghirlanda, A. Goobar, J. Grindlay, A. Hajela, D. E. Holz, V. Karambelkar, E. C. Kool, G. P. Lamb, T. Laskar, A. Levan, K. Maguire, M. May, A. Melandri, D. Milisavljevic, A. A. Miller, M. Nicholl, S. M. Nissanke, A. Palmese, S. Piranomonte, A. Rest, A. Sagués-Carracedo, K. Siellez, L. P. Singer, M. Smith, D. Steeghs, and N. Tanvir, Target-of-opportunity Observations of Gravitational-wave Events with Vera C. Rubin Observatory, *ApJS* **260**, 18 (2022), arXiv:2111.01945 [astro-ph.HE].
- [61] I. Andreoni, M. W. Coughlin, M. Almualla, E. C. Bellm, F. B. Bianco, M. Bulla, A. Cucchiara, T. Dietrich, A. Goobar, E. C. Kool, X. Li, F. Ragosta, A. Sagués-Carracedo, and L. P. Singer, Optimizing Cadences with Realistic Light-curve Filtering for Serendipitous Kilonova Discovery with Vera Rubin Observatory, *ApJS* **258**, 5 (2022), arXiv:2106.06820 [astro-ph.HE].
- [62] I. Andreoni, M. W. Coughlin, A. W. Criswell, M. Bulla, A. Toivonen, L. P. Singer, A. Palmese, E. Burns, S. Gezari, M. M. Kasliwal, R. W. Kiendrebeogo, A. Mahabal, T. J. Moriya, A. Rest, D. Scolnic, R. A. Simcoe, J. Soon, R. Stein, and T. Travouillon, Enabling kilonova science with Nancy Grace Roman Space Telescope, *Astroparticle Physics* **155**, 102904 (2024), arXiv:2307.09511 [astro-ph.HE].
- [63] C. R. Bom, J. Annis, A. Garcia, A. Palmese, N. Sherman, M. Soares-Santos, L. Santana-Silva, R. Morgan, K. Bechtol, T. Davis, H. T. Diehl, S. S. Allam, T. G. Bachmann, B. M. O. Fraga, J. García-Bellido, M. S. S. Gill, K. Herner, C. D. Kilpatrick, M. Makler, F. Olivares E., M. E. S. Pereira, J. Pineda, A. Santos, D. L. Tucker, M. P. Wiesner, M. Aguena, O. Alves, D. Bacon, P. H. Bernardinelli, E. Bertin, S. Bocquet, D. Brooks, M. Carrasco Kind, J. Carretero, C. Conselice, M. Costanzi, L. N. da Costa, J. De Vicente, S. Desai, P. Doel, S. Everett, I. Ferrero, J. Frieman, M. Gatti, D. W. Gerdes, D. Gruen, R. A. Gruendl, G. Gutierrez, S. R. Hinton, D. L. Hollowood, K. Honscheid, D. J. James, K. Kuehn, N. Kuropatkin, P. Melchior, J. Mena-Fernández, F. Menanteau, A. Pieres, A. A. Plazas Malagón, M. Raveri, M. Rodriguez-Monroy, E. Sanchez, B. Santiago, I. Sevilla-Noarbe, M. Smith, E. Suchyta, M. E. C. Swanson, G. Tarle, C. To, and N. Weaverdyck, Designing an Optimal Kilonova Search Using DECam for Gravitational-wave Events, *Astrophys. J.* **960**, 122 (2024), arXiv:2302.04878 [astro-ph.HE].

- [64] F. Ragosta, T. Ahumada, S. Piranomonte, I. Andreoni, A. Melandri, A. Colombo, and M. W. Coughlin, Kilonova Parameter Estimation with LSST at Vera C. Rubin Observatory, *Astrophys. J.* **966**, 214 (2024), arXiv:2403.14016 [astro-ph.HE].
- [65] K. Kunnumkai, A. Palmese, M. Bulla, T. Dietrich, A. M. Farah, and P. T. H. Pang, Kilonova emission from GW230529 and mass gap neutron star-black hole mergers, arXiv e-prints , arXiv:2409.10651 (2024), arXiv:2409.10651 [astro-ph.HE].
- [66] K. Kunnumkai, A. Palmese, *et al.*, in prep. (2024).
- [67] O. S. Salafia, M. Colpi, M. Branchesi, E. Chassande-Mottin, G. Ghirlanda, G. Ghisellini, and S. D. Vergani, Where and When: Optimal Scheduling of the Electromagnetic Follow-up of Gravitational-wave Events Based on Counterpart Light-curve Models, *Astrophys. J.* **846**, 62 (2017), arXiv:1704.05851 [astro-ph.HE].
- [68] A. Corsi, N. M. Lloyd-Ronning, D. Carbone, D. A. Frail, D. Lazzati, E. J. Murphy, R. O’Shaughnessy, B. J. Owen, D. J. Sand, W.-F. Fong, K. Spekkens, and A. Seymour, Astro2020 Science White Paper: Radio Counterparts of Compact Object Mergers in the Era of Gravitational-Wave Astronomy, arXiv e-prints , arXiv:1903.10589 (2019), arXiv:1903.10589 [astro-ph.IM].
- [69] R. Duque, P. Beniamini, F. Daigne, and R. Mochkovitch, Probing binary neutron star mergers in dense environments using afterglow counterparts, *Astronomy & Astrophysics* **639**, A15 (2020), arXiv:1911.03302 [astro-ph.HE].
- [70] A. Y. Q. Ho, D. A. Perley, P. Beniamini, S. B. Cenko, S. R. Kulkarni, I. Andreoni, L. P. Singer, K. De, M. M. Kasliwal, C. Fremling, E. C. Bellm, R. Dekany, A. Delacroix, D. A. Duev, D. A. Goldstein, V. Z. Golkhou, A. Goobar, M. J. Graham, D. Hale, T. Kupfer, R. R. Laher, F. J. Masci, A. A. Miller, J. D. Neill, R. Riddle, B. Rusholme, D. L. Shupe, R. Smith, J. Sollerman, and J. van Roestel, ZTF20aaajnksq (AT 2020blt): A Fast Optical Transient at $z \approx 2.9$ with No Detected Gamma-Ray Burst Counterpart, *Astrophys. J.* **905**, 98 (2020), arXiv:2006.10761 [astro-ph.HE].
- [71] J. Yu, H. Song, S. Ai, H. Gao, F. Wang, Y. Wang, Y. Lu, W. Fang, and W. Zhao, Multimessenger Detection Rates and Distributions of Binary Neutron Star Mergers and Their Cosmological Implications, *Astrophys. J.* **916**, 54 (2021), arXiv:2104.12374 [astro-ph.HE].
- [72] O. M. Boersma and J. van Leeuwen, Investigating the detection rates and inference of gravitational-wave and radio emission from black hole neutron star mergers, *Astronomy & Astrophysics* **664**, A160 (2022), arXiv:2202.02181 [astro-ph.HE].
- [73] A. Colombo, O. S. Salafia, F. Gabrielli, G. Ghirlanda, B. Giacomazzo, A. Perego, and M. Colpi, Multi-messenger Observations of Binary Neutron Star Mergers in the O4 Run, *Astrophys. J.* **937**, 79 (2022), arXiv:2204.07592 [astro-ph.HE].
- [74] S. Ronchini, M. Branchesi, G. Oganesyan, B. Banerjee, U. Dupletsas, G. Ghirlanda, J. Harms, M. Mapelli, and F. Santoliquido, Perspectives for multimessenger astronomy with the next generation of gravitational-wave detectors and high-energy satellites, *Astronomy & Astrophysics* **665**, A97 (2022), arXiv:2204.01746 [astro-ph.HE].
- [75] J. G. Ducoin, B. Desoubrie, F. Daigne, and N. Leroy, Optimization of the SVOM satellite strategy for the rapid follow-up of gravitational wave events, *MNRAS* **524**, 4000 (2023), arXiv:2210.12120 [astro-ph.IM].
- [76] S. Bhattacharjee, S. Banerjee, V. Bhalerao, P. Beniamini, S. Bose, K. Hotokezaka, A. Pai, M. Saleem, and G. Waratkar, Joint gravitational wave-short GRB detection of binary neutron star mergers with existing and future facilities, *MNRAS* **528**, 4255 (2024), arXiv:2401.13636 [astro-ph.HE].
- [77] B. J. Morsonyi, R. De Los Santos, R. Hernandez, J. Bustamante, B. Yassuiae, G. Astorga, J. Parra, and J. C. Workman, The afterglow of GW170817 from every angle: prospects for detecting the afterglows of binary neutron star mergers, *MNRAS* **533**, 510 (2024), arXiv:2306.00076 [astro-ph.HE].
- [78] C. Pellouin and F. Daigne, The Very High Energy Afterglow of Structured Jets: GW 170817 and Prospects for Future Detections, arXiv e-prints , arXiv:2406.08254 (2024), arXiv:2406.08254 [astro-ph.HE].
- [79] T. Mondal, S. Chakraborty, L. Resmi, and D. Bose, Follow-up of Neutron Star Mergers with CTA and Prospects for Joint Detection with Gravitational-Wave Detectors, arXiv e-prints , arXiv:2409.07916 (2024), arXiv:2409.07916 [astro-ph.HE].
- [80] P. Mészáros and M. J. Rees, Optical and Long-Wavelength Afterglow from Gamma-Ray Bursts, *Astrophys. J.* **476**, 232 (1997), arXiv:astro-ph/9606043 [astro-ph].
- [81] R. Sari, T. Piran, and R. Narayan, Spectra and Light Curves of Gamma-Ray Burst Afterglows, *The Astrophysical Journal Letters* **497**, L17 (1998), arXiv:astro-ph/9712005 [astro-ph].
- [82] R. A. M. J. Wijers and T. J. Galama, Physical Parameters of GRB 970508 and GRB 971214 from Their Afterglow Synchrotron Emission, *Astrophys. J.* **523**, 177 (1999), arXiv:astro-ph/9805341 [astro-ph].
- [83] J. Granot and R. Sari, The Shape of Spectral Breaks in Gamma-Ray Burst Afterglows, *Astrophys. J.* **568**, 820 (2002), arXiv:astro-ph/0108027 [astro-ph].
- [84] E. Costa, F. Frontera, J. Heise, M. Feroci, J. in’t Zand, F. Fiore, M. N. Cinti, D. Dal Fiume, L. Nicastro, M. Orlan-dini, E. Palazzi, M. Rapisarda, G. Zavattini, R. Jager, A. Parmar, A. Owens, S. Molendi, G. Cusumano, M. C. Maccarone, S. Giarrusso, A. Coletta, L. A. Antonelli, P. Giommi, J. M. Muller, L. Piro, and R. C. Butler, Discovery of an X-ray afterglow associated with the γ -ray burst of 28 February 1997, *Nature (London)* **387**, 783 (1997), arXiv:astro-ph/9706065 [astro-ph].
- [85] J. van Paradijs, P. J. Groot, T. Galama, C. Kouveliotou, R. G. Strom, J. Telting, R. G. M. Rutten, G. J. Fishman, C. A. Meegan, M. Pettini, N. Tanvir, J. Bloom, H. Pedersen, H. U. Nørsgaard-Nielsen, M. Linden-Vørnle, J. Melnick, G. Van der Steene, M. Bremer, R. Naber, J. Heise, J. in’t Zand, E. Costa, M. Feroci, L. Piro, F. Frontera, G. Zavattini, L. Nicastro, E. Palazzi, K. Bennett, L. Hanlon, and A. Parmar, Transient optical emission from the error box of the γ -ray burst of 28 February 1997, *Nature (London)* **386**, 686 (1997).
- [86] J. van Paradijs, C. Kouveliotou, and R. A. M. J. Wijers, Gamma-Ray Burst Afterglows, *ARA&A* **38**, 379 (2000).
- [87] D. A. Frail, S. R. Kulkarni, L. Nicastro, M. Feroci, and G. B. Taylor, The radio afterglow from the γ -ray burst of 8 May 1997, *Nature (London)* **389**, 261 (1997).
- [88] T. Matsumoto, E. Nakar, and T. Piran, Generalized compactness limit from an arbitrary viewing angle, *MNRAS* **486**, 1563 (2019), arXiv:1903.06712 [astro-ph.HE].
- [89] B. O’Connor, P. Beniamini, and R. Gill, X-ray afterglow limits on the viewing angles of short gamma-ray bursts, *MNRAS* **533**, 1629 (2024), arXiv:2406.05297 [astro-ph.HE].
- [90] K. P. Mooley, J. Anderson, and W. Lu, Optical superluminal motion measurement in the neutron-star merger GW170817, *Nature (London)* **610**, 273 (2022), arXiv:2210.06568 [astro-ph.HE].
- [91] G. Ghirlanda and R. Salvaterra, The Cosmic History of Long Gamma-Ray Bursts, *Astrophys. J.* **932**, 10 (2022).
- [92] J. J. Fernández, S. Kobayashi, and G. P. Lamb, Lateral spreading effects on VLBI radio images of neutron star merger jets,

- [MNRAS](#) **509**, 395 (2022).
- [93] S. Makhathini, K. P. Mooley, M. Brightman, K. Hotokezaka, A. J. Nayana, H. T. Intema, D. Dobie, E. Lenc, D. A. Perley, C. Fremling, J. Moldòn, D. Lazzati, D. L. Kaplan, A. Balasubramanian, I. S. Brown, D. Carbone, P. Chandra, A. Corsi, F. Camilo, A. Deller, D. A. Frail, T. Murphy, E. J. Murphy, E. Nakar, O. Smirnov, R. J. Beswick, R. Fender, G. Hallinan, I. Heywood, M. Kasliwal, B. Lee, W. Lu, J. Rana, S. Perkins, S. V. White, G. I. G. Józsa, B. Hugo, and P. Kamphuis, The Panchromatic Afterglow of GW170817: The Full Uniform Data Set, Modeling, Comparison with Previous Results, and Implications, [Astrophys. J.](#) **922**, 154 (2021), [arXiv:2006.02382 \[astro-ph.HE\]](#).
- [94] A. Hajela, R. Margutti, J. S. Bright, K. D. Alexander, B. D. Metzger, V. Nedora, A. Kathirgamaraju, B. Margalit, D. Radice, C. Guidorzi, E. Berger, A. MacFadyen, D. Giannios, R. Chornock, I. Heywood, L. Sironi, O. Gottlieb, D. Coppejans, T. Laskar, Y. Cendes, R. B. Duran, T. Eftekhar, W. Fong, A. McDowell, M. Nicholl, X. Xie, J. Zrake, S. Bernuzzi, F. S. Broekgaarden, C. D. Kilpatrick, G. Terreran, V. A. Villar, P. K. Blanchard, S. Gomez, G. Hosseinzadeh, D. J. Matthews, and J. C. Rastinejad, Evidence for X-Ray Emission in Excess to the Jet-afterglow Decay 3.5 yr after the Binary Neutron Star Merger GW 170817: A New Emission Component, [The Astrophysical Journal Letters](#) **927**, L17 (2022), [arXiv:2104.02070 \[astro-ph.HE\]](#).
- [95] A. Balasubramanian, A. Corsi, K. P. Mooley, K. Hotokezaka, D. L. Kaplan, D. A. Frail, G. Hallinan, D. Lazzati, and E. J. Murphy, GW170817 4.5 Yr After Merger: Dynamical Ejecta Afterglow Constraints, [Astrophys. J.](#) **938**, 12 (2022), [arXiv:2205.14788 \[astro-ph.HE\]](#).
- [96] T. Govreen-Segal and E. Nakar, The Structure and Evolution of Relativistic Jetted Blast Waves, [arXiv e-prints](#) , [arXiv:2311.09297](#) (2023), [arXiv:2311.09297 \[astro-ph.HE\]](#).
- [97] G. Ryan, H. van Eerten, E. Troja, L. Piro, B. O'Connor, and R. Ricci, Modelling of Long-Term Afterglow Counterparts to Gravitational Wave Events: The Full View of GRB 170817A, [arXiv e-prints](#) , [arXiv:2310.02328](#) (2023), [arXiv:2310.02328 \[astro-ph.HE\]](#).
- [98] A. McDowell and A. MacFadyen, Revisiting the Parameter Space of Binary Neutron Star Merger Event GW170817, [Astrophys. J.](#) **945**, 135 (2023), [arXiv:2302.11394 \[astro-ph.HE\]](#).
- [99] P. Beniamini and E. Nakar, Observational constraints on the structure of gamma-ray burst jets, [MNRAS](#) **482**, 5430 (2019), [arXiv:1808.07493 \[astro-ph.HE\]](#).
- [100] A. Farah, R. Essick, Z. Doctor, M. Fishbach, and D. E. Holz, Counting on Short Gamma-Ray Bursts: Gravitational-wave Constraints of Jet Geometry, [Astrophys. J.](#) **895**, 108 (2020), [arXiv:1912.04906 \[astro-ph.HE\]](#).
- [101] S. Biscoveanu, E. Thrane, and S. Vitale, Constraining Short Gamma-Ray Burst Jet Properties with Gravitational Waves and Gamma-Rays, [Astrophys. J.](#) **893**, 38 (2020), [arXiv:1911.01379 \[astro-ph.HE\]](#).
- [102] F. Hayes, I. S. Heng, J. Veitch, and D. Williams, Comparing Short Gamma-Ray Burst Jet Structure Models, [Astrophys. J.](#) **891**, 124 (2020), [arXiv:1911.04190 \[astro-ph.HE\]](#).
- [103] N. Sarin, P. D. Lasky, F. H. Vivanco, S. P. Stevenson, D. Chatopadhyay, R. Smith, and E. Thrane, Linking the rates of neutron star binaries and short gamma-ray bursts, [Phys. Rev. D](#) **105**, 083004 (2022), [arXiv:2201.08491 \[astro-ph.HE\]](#).
- [104] F. Hayes, I. S. Heng, G. Lamb, E.-T. Lin, J. Veitch, and M. J. Williams, Unpacking Merger Jets: A Bayesian Analysis of GW170817, GW190425 and Electromagnetic Observations of Short Gamma-Ray Bursts, [Astrophys. J.](#) **954**, 92 (2023), [arXiv:2305.06275 \[astro-ph.HE\]](#).
- [105] B. S. Sathyaprakash and B. F. Schutz, Physics, Astrophysics and Cosmology with Gravitational Waves, [Living Reviews in Relativity](#) **12**, 2 (2009), [arXiv:0903.0338 \[gr-qc\]](#).
- [106] B. F. Schutz, Networks of gravitational wave detectors and three figures of merit, [Classical and Quantum Gravity](#) **28**, 125023 (2011), [arXiv:1102.5421 \[astro-ph.IM\]](#).
- [107] W. Fong, E. Berger, R. Margutti, and B. A. Zauderer, A Decade of Short-duration Gamma-Ray Burst Broadband Afterglows: Energetics, Circumburst Densities, and Jet Opening Angles, [Astrophys. J.](#) **815**, 102 (2015), [arXiv:1509.02922 \[astro-ph.HE\]](#).
- [108] A. Rouco Escorial, W.-f. Fong, E. Berger, T. Laskar, R. Margutti, G. Schroeder, J. C. Rastinejad, D. Cornish, S. Popp, M. Lally, A. E. Nugent, K. Paterson, B. D. Metzger, R. Chornock, K. Alexander, Y. Cendes, and T. Eftekhar, The Jet Opening Angle and Event Rate Distributions of Short Gamma-ray Bursts from Late-time X-ray Afterglows, [arXiv e-prints](#) , [arXiv:2210.05695](#) (2022), [arXiv:2210.05695 \[astro-ph.HE\]](#).
- [109] E. Nakar, T. Piran, and J. Granot, The Detectability of Orphan Afterglows, [Astrophys. J.](#) **579**, 699 (2002), [arXiv:astro-ph/0204203 \[astro-ph\]](#).
- [110] E. Rossi, D. Lazzati, and M. J. Rees, Afterglow light curves, viewing angle and the jet structure of γ -ray bursts, [MNRAS](#) **332**, 945 (2002), [arXiv:astro-ph/0112083 \[astro-ph\]](#).
- [111] A. Panaitescu and P. Kumar, The Effect of Angular Structure of Gamma-Ray Burst Outflows on the Afterglow Emission, [Astrophys. J.](#) **592**, 390 (2003), [arXiv:astro-ph/0301032 \[astro-ph\]](#).
- [112] H. van Eerten, W. Zhang, and A. MacFadyen, Off-axis Gamma-ray Burst Afterglow Modeling Based on a Two-dimensional Axisymmetric Hydrodynamics Simulation, [Astrophys. J.](#) **722**, 235 (2010), [arXiv:1006.5125 \[astro-ph.HE\]](#).
- [113] P. Beniamini, J. Granot, and R. Gill, Afterglow light curves from misaligned structured jets, [MNRAS](#) **493**, 3521 (2020), [arXiv:2001.02239 \[astro-ph.HE\]](#).
- [114] Y. F. Huang, Z. G. Dai, and T. Lu, Failed gamma-ray bursts and orphan afterglows, [MNRAS](#) **332**, 735 (2002), [arXiv:astro-ph/0112469 \[astro-ph\]](#).
- [115] N. Dalal, K. Griest, and J. Puet, The Difficulty in Using Orphan Afterglows to Measure Gamma-Ray Burst Beaming, [Astrophys. J.](#) **564**, 209 (2002), [arXiv:astro-ph/0103436 \[astro-ph\]](#).
- [116] T. Totani and A. Panaitescu, Orphan Afterglows of Collimated Gamma-Ray Bursts: Rate Predictions and Prospects for Detection, [Astrophys. J.](#) **576**, 120 (2002), [arXiv:astro-ph/0204258 \[astro-ph\]](#).
- [117] A. Levinson, E. O. Ofek, E. Waxman, and A. Gal-Yam, Orphan Gamma-Ray Burst Radio Afterglows: Candidates and Constraints on Beaming, [Astrophys. J.](#) **576**, 923 (2002), [arXiv:astro-ph/0203262 \[astro-ph\]](#).
- [118] J. E. Rhoads, Dirty Fireballs and Orphan Afterglows: A Tale of Two Transients, [Astrophys. J.](#) **591**, 1097 (2003), [arXiv:astro-ph/0301011 \[astro-ph\]](#).
- [119] T. Piran, E. Nakar, and S. Rosswog, The electromagnetic signals of compact binary mergers, [MNRAS](#) **430**, 2121 (2013), [arXiv:1204.6242 \[astro-ph.HE\]](#).
- [120] S. B. Cenko, S. R. Kulkarni, A. Horesh, A. Corsi, D. B. Fox, J. Carpenter, D. A. Frail, P. E. Nugent, D. A. Perley, D. Gruber, A. Gal-Yam, P. J. Groot, G. Hallinan, E. O. Ofek, A. Rau, C. L. MacLeod, A. A. Miller, J. S. Bloom, A. V. Filippenko, M. M. Kasliwal, N. M. Law, A. N. Morgan, D. Polishook, D. Poznanski, R. M. Quimby, B. Sesar, K. J. Shen, J. M. Silverman,

- and A. Sternberg, Discovery of a Cosmological, Relativistic Outburst via its Rapidly Fading Optical Emission, *Astrophys. J.* **769**, 130 (2013), arXiv:1304.4236 [astro-ph.CO].
- [121] C. J. Law, B. M. Gaensler, B. D. Metzger, E. O. Ofek, and L. Sironi, Discovery of the Luminous, Decades-long, Extragalactic Radio Transient FIRST J141918.9+394036, *The Astrophysical Journal Letters* **866**, L22 (2018), arXiv:1808.08964 [astro-ph.HE].
- [122] I. Andreoni, M. W. Coughlin, E. C. Kool, M. M. Kasliwal, H. Kumar, V. Bhalerao, A. S. Carracedo, A. Y. Q. Ho, P. T. H. Pang, D. Saraogi, K. Sharma, V. Shenoy, E. Burns, T. Ahumada, S. Anand, L. P. Singer, D. A. Perley, K. De, U. C. Fremling, E. C. Bellm, M. Bulla, A. Crellin-Quick, T. Dietrich, A. Drake, D. A. Duev, A. Goobar, M. J. Graham, D. L. Kaplan, S. R. Kulkarni, R. R. Laher, A. A. Mahabal, D. L. Shupe, J. Sollerman, R. Walters, and Y. Yao, Fast-transient Searches in Real Time with ZTFReST: Identification of Three Optically Discovered Gamma-Ray Burst Afterglows and New Constraints on the Kilonova Rate, *Astrophys. J.* **918**, 63 (2021), arXiv:2104.06352 [astro-ph.HE].
- [123] N. Sarin, R. Hamburg, E. Burns, G. Ashton, P. D. Lasky, and G. P. Lamb, Low-efficiency long gamma-ray bursts: a case study with AT2020blt, *MNRAS* **512**, 1391 (2022), arXiv:2106.01556 [astro-ph.HE].
- [124] R. Gupta, A. Kumar, S. B. Pandey, A. J. Castro-Tirado, A. Ghosh, Y. D. Dimple, Hu, E. Fernández-García, M. D. Caballero-García, M. Á. Castro-Tirado, R. P. Hedrosa, I. Hermelo, I. Vico, K. Misra, B. Kumar, A. Aryan, and S. N. Tiwari, Revealing nature of GRB 210205A, ZTF21aaeyldq (AT2021any) and follow-up observations with the 4Kx4K CCD imager + 3.6m DOT, *Journal of Astrophysics and Astronomy* **43**, 11 (2022), arXiv:2111.11795 [astro-ph.HE].
- [125] D. A. Perley, A. Y. Q. Ho, M. Fausnaugh, G. P. Lamb, M. M. Kasliwal, T. Ahumada, S. Anand, I. Andreoni, E. Bellm, V. Bhalerao, B. Bolin, T. G. Brink, E. Burns, S. B. Cenko, A. Corsi, A. V. Filippenko, D. Frederiks, A. Goldstein, R. Hamburg, R. Jayaraman, P. G. Jonker, E. C. Kool, S. Kulkarni, H. Kumar, R. Laher, A. Levan, A. Lysenko, R. A. Perley, G. R. Ricker, R. Riddle, A. Ridnaiia, B. Rusholme, R. Smith, D. Svinkin, M. Ulanov, G. Waratkar, and Y. Yao, AT2019pim: A Luminous Orphan Afterglow from a Moderately Relativistic Outflow, arXiv e-prints , arXiv:2401.16470 (2024), arXiv:2401.16470 [astro-ph.HE].
- [126] J. Freeburn, J. Cooke, A. Möller, D. Dobie, J. Zhang, O. Sharhan Salafia, K. Siellez, K. Auchettl, S. Goode, T. M. C. Abbott, I. Andreoni, R. Allen, N. Van Bemmel, and S. Webb, A Fast-cadence Search for Gamma-Ray Burst Orphan Afterglows with the Deeper, Wider, Faster Programme, arXiv e-prints , arXiv:2405.11949 (2024), arXiv:2405.11949 [astro-ph.HE].
- [127] H.-Y. Chen, S. Vitale, and R. Narayan, Viewing Angle of Binary Neutron Star Mergers, *Physical Review X* **9**, 031028 (2019), arXiv:1807.05226 [astro-ph.HE].
- [128] D. Reitze, R. X. Adhikari, S. Ballmer, B. Barish, L. Barsotti, G. Billingsley, D. A. Brown, Y. Chen, D. Coyne, R. Eisenstein, et al., Cosmic explorer: the us contribution to gravitational-wave astronomy beyond ligo, arXiv preprint arXiv:1907.04833 (2019).
- [129] M. Maggiore, C. Van Den Broeck, N. Bartolo, E. Belgacem, D. Bertacca, M. A. Bizouard, M. Branchesi, S. Clesse, S. Foffa, J. García-Bellido, et al., Science case for the einstein telescope, *Journal of Cosmology and Astroparticle Physics* **2020** (03), 050.
- [130] N. Aghanim, Y. Akrami, M. Ashdown, J. Aumont, C. Baccigalupi, M. Ballardini, A. J. Banday, R. Barreiro, N. Bartolo, S. Basak, et al., Planck 2018 results-vi. cosmological parameters, *Astronomy & Astrophysics* **641**, A6 (2020).
- [131] L. P. Singer and L. R. Price, Rapid bayesian position reconstruction for gravitational-wave transients, *Physical Review D* **93**, 024013 (2016).
- [132] LIGO Scientific Collaboration, Virgo Collaboration, and KAGRA Collaboration, *LVK Algorithm Library - LALSuite*, Free software (GPL) (2018).
- [133] R. Abbott, T. Abbott, F. Acernese, K. Ackley, C. Adams, N. Adhikari, R. Adhikari, V. Adya, C. Affeldt, D. Agarwal, et al., Population of merging compact binaries inferred using gravitational waves through gwtc-3, *Physical Review X* **13**, 011048 (2023).
- [134] M. Fishbach, R. Essick, and D. E. Holz, Does matter matter? using the mass distribution to distinguish neutron stars and black holes, *The Astrophysical Journal Letters* **899**, L8 (2020).
- [135] A. Farah, M. Fishbach, R. Essick, D. E. Holz, and S. Galaudage, Bridging the gap: Categorizing gravitational-wave events at the transition between neutron stars and black holes, *The Astrophysical Journal* **931**, 108 (2022).
- [136] P. Madau and M. Dickinson, Cosmic Star-Formation History, *ARA&A* **52**, 415 (2014), arXiv:1403.0007 [astro-ph.CO].
- [137] V. Srivastava, D. Davis, K. Kuns, P. Landry, S. Ballmer, M. Evans, E. D. Hall, J. Read, and B. S. Sathyaprakash, Science-driven tunable design of cosmic explorer detectors, *The Astrophysical Journal* **931**, 22 (2022).
- [138] S. Hild, M. Abernathy, F. Acernese, P. Amaro-Seoane, N. Andersson, K. Arun, F. Barone, B. Barr, M. Barsuglia, M. Beker, N. Beveridge, S. Birindelli, S. Bose, L. Bosi, S. Braccini, C. Bradaschia, T. Bulik, E. Calloni, G. Cella, E. Chassande Mottin, S. Chelkowski, A. Chincarini, J. Clark, E. Coccia, C. Colacino, J. Colas, A. Cumming, L. Cunningham, E. Cuoco, S. Danilishin, K. Danzmann, R. De Salvo, T. Dent, R. De Rosa, L. Di Fiore, A. Di Virgilio, M. Doets, V. Fafone, P. Falferi, R. Flaminio, J. Franc, F. Frasconi, A. Freise, D. Friedrich, P. Fulda, J. Gair, G. Gemme, E. Genin, A. Gennai, A. Giazotto, K. Glampedakis, C. Gräf, M. Granata, H. Grote, G. Guidi, A. Gurkovsky, G. Hammond, M. Hannam, J. Harms, D. Heinert, M. Hendry, I. Heng, E. Hennes, J. Hough, S. Husa, S. Huttner, G. Jones, F. Khalili, K. Kokeyama, K. Kokkotas, B. Krishnan, T. G. F. Li, M. Lorenzini, H. Lück, E. Majorana, I. Mandel, V. Mandic, M. Mantovani, I. Martin, C. Michel, Y. Minenkov, N. Moggado, S. Mosca, B. Mours, H. Müller-Ebhardt, P. Murray, R. Nawrot, J. Nelson, R. Oshaughnessy, C. D. Ott, C. Palomba, A. Paoli, G. Parguez, A. Pasqualetti, R. Pasqualetti, D. Passuello, L. Pinard, W. Plastino, R. Poggiani, P. Popolizio, M. Prato, M. Punturo, P. Puppo, D. Rabelling, P. Rapagnani, J. Read, T. Regimbau, H. Rehbein, S. Reid, F. Ricci, F. Richard, A. Rocchi, S. Rowan, A. Rüdiger, L. Santamaría, B. Sassolas, B. Sathyaprakash, R. Schnabel, C. Schwarz, P. Seidel, A. Sintes, K. Somiya, F. Speirits, K. Strain, S. Strigin, P. Sutton, S. Tarabrin, A. Thüring, J. van den Brand, M. van Veggel, C. van den Broeck, A. Vecchio, J. Veitch, F. Vetrano, A. Vicere, S. Vyatchanin, B. Willke, G. Woan, and K. Yamamoto, Sensitivity studies for third-generation gravitational wave observatories, *Classical and Quantum Gravity* **28**, 094013 (2011), arXiv:1012.0908 [gr-qc].
- [139] M. C. Weisskopf, H. D. Tananbaum, L. P. Van Speybroeck, and S. L. O'Dell, Chandra x-ray observatory (cxo): overview, X-ray optics, instruments, and missions iii **4012**, 2 (2000).

- [140] P. Predehl, R. Andritschke, V. Arefiev, V. Babyshkin, O. Batanov, W. Becker, H. Böhringer, A. Bogomolov, T. Boller, K. Borm, *et al.*, The erosita x-ray telescope on srg, *Astronomy & Astrophysics* **647**, A1 (2021).
- [141] J. Zhang, L. Qi, Y. Yang, J. Wang, Y. Liu, W. Cui, D. Zhao, S. Jia, T. Li, T. Chen, *et al.*, Estimate of the background and sensitivity of the follow-up x-ray telescope onboard einstein probe, *Astroparticle Physics* **137**, 102668 (2022).
- [142] W. Yuan, C. Zhang, Y. Chen, and Z. Ling, The einstein probe mission, in *Handbook of X-ray and Gamma-ray Astrophysics* (Springer, 2022) pp. 1–30.
- [143] P. A. Evans, K. L. Page, J. P. Osborne, A. P. Beardmore, R. Willingale, D. N. Burrows, J. A. Kennea, M. Perri, M. Capalbi, G. Tagliaferri, and S. B. Cenko, 2SXPS: An Improved and Expanded Swift X-Ray Telescope Point-source Catalog, *ApJS* **247**, 54 (2020), arXiv:1911.11710 [astro-ph.IM].
- [144] B. Schneider, N. Renault-Tinacci, D. Götz, A. Meuris, P. Ferrando, V. Burwitz, E. Doumayrou, T. Lavanant, N. Meidinger, and K. Mercier, Spectral performance of the Microchannel X-ray Telescope on board the SVOM mission, *Experimental Astronomy* **56**, 77 (2023), arXiv:2212.09863 [astro-ph.IM].
- [145] L. Piro, M. Ahlers, A. Coleiro, M. Colpi, E. Wilhelmi, M. Guainazzi, P. Jonker, P. M. Namara, D. Nichols, P. O'Brien, *et al.*, Multi-messenger-athena synergy white paper, arXiv preprint arXiv:2110.15677 (2021).
- [146] K. Nandra, D. Barret, X. Barcons, A. Fabian, J.-W. d. Herder, L. Piro, M. Watson, C. Adami, J. Aird, J. M. Afonso, *et al.*, The hot and energetic universe: A white paper presenting the science theme motivating the athena+ mission, arXiv preprint arXiv:1306.2307 (2013).
- [147] R. F. Mushotzky, J. Aird, A. J. Barger, N. Cappelluti, G. Chartas, L. Corrales, R. Eufrasio, A. C. Fabian, A. D. Falcone, E. Gallo, *et al.*, The advanced x-ray imaging satellite, arXiv preprint arXiv:1903.04083 (2019).
- [148] J. A. Gaskin, D. A. Swartz, A. Vikhlinin, F. Özel, K. E. Gelmis, J. W. Arenberg, S. R. Bandler, M. W. Bautz, M. M. Civitani, A. Dominguez, *et al.*, Lynx x-ray observatory: an overview, *Journal of Astronomical Telescopes, Instruments, and Systems* **5**, 021001 (2019).
- [149] Y. Shvartzvald, E. Waxman, A. Gal-Yam, E. Ofek, S. Ben-Ami, D. Berge, M. Kowalski, R. Bühlert, S. Worm, J. Rhoads, *et al.*, Ultrasat: A wide-field time-domain uv space telescope, arXiv preprint arXiv:2304.14482 (2023).
- [150] S. Kulkarni, F. A. Harrison, B. W. Grefenstette, H. P. Earnshaw, I. Andreoni, D. A. Berg, J. S. Bloom, S. B. Cenko, R. Chornock, J. L. Christiansen, *et al.*, Science with the ultraviolet explorer (uvex), arXiv preprint arXiv:2111.15608 (2021).
- [151] Ž. Ivezić, S. M. Kahn, J. A. Tyson, B. Abel, E. Acosta, R. Allsman, D. Alonso, Y. AlSayyad, S. F. Anderson, J. Andrew, *et al.*, Lsst: from science drivers to reference design and anticipated data products, *The Astrophysical Journal* **873**, 111 (2019).
- [152] R. Laureijs, J. Amiaux, S. Arduini, J.-L. Augueres, J. Brinchmann, R. Cole, M. Cropper, C. Dabin, L. Duvet, A. Ealet, *et al.*, Euclid definition study report, arXiv preprint arXiv:1110.3193 (2011).
- [153] D. Spergel, N. Gehrels, J. Breckinridge, M. Donahue, A. Dressler, B. S. Gaudi, T. Greene, O. Guyon, C. Hirata, J. Kalirai, N. J. Kasdin, W. Moos, S. Perlmutter, M. Postman, B. Rauscher, J. Rhodes, Y. Wang, D. Weinberg, J. Centrella, W. Traub, C. Baltay, J. Colbert, D. Bennett, A. Kiessling, B. Macintosh, J. Merten, M. Mortonson, M. Penny, E. Rozo, D. Savransky, K. Stapelfeldt, Y. Zu, C. Baker, E. Cheng, D. Content, J. Dooley, M. Foote, R. Goullioud, K. Grady, C. Jackson, J. Kruk, M. Levine, M. Melton, C. Peddie, J. Ruffa, and S. Shaklan, Wide-Field InfraRed Survey Telescope-Astrophysics Focused Telescope Assets WFIRST-AFTA Final Report, arXiv e-prints , arXiv:1305.5422 (2013), arXiv:1305.5422 [astro-ph.IM].
- [154] D. Spergel, N. Gehrels, C. Baltay, D. Bennett, J. Breckinridge, M. Donahue, A. Dressler, B. S. Gaudi, T. Greene, O. Guyon, C. Hirata, J. Kalirai, N. J. Kasdin, B. Macintosh, W. Moos, S. Perlmutter, M. Postman, B. Rauscher, J. Rhodes, Y. Wang, D. Weinberg, D. Benford, M. Hudson, W. S. Jeong, Y. Mellier, W. Traub, T. Yamada, P. Capak, J. Colbert, D. Masters, M. Penny, D. Savransky, D. Stern, N. Zimmerman, R. Barry, L. Bartusek, K. Carpenter, E. Cheng, D. Content, F. Dekens, R. Demers, K. Grady, C. Jackson, G. Kuan, J. Kruk, M. Melton, B. Nemati, B. Parvin, I. Poberezhskiy, C. Peddie, J. Ruffa, J. K. Wallace, A. Whipple, E. Wollack, and F. Zhao, Wide-Field Infrared Survey Telescope-Astrophysics Focused Telescope Assets WFIRST-AFTA 2015 Report, arXiv e-prints , arXiv:1503.03757 (2015), arXiv:1503.03757 [astro-ph.IM].
- [155] J. Rigby, M. Perrin, M. McElwain, R. Kimble, S. Friedman, M. Lallo, R. Doyon, L. Feinberg, P. Ferruit, A. Glasse, *et al.*, The science performance of jwst as characterized in commissioning, *Publications of the Astronomical Society of the Pacific* **135**, 048001 (2023).
- [156] R. Davies, V. Hörmann, S. Rabien, E. Sturm, J. Alves, Y. Clénet, J. Kotilainen, F. Lang-Bardl, H. Nicklas, J. U. Pott, E. Tolstoy, B. Vulcani, and MICADO Consortium, MICADO: The Multi-Adaptive Optics Camera for Deep Observations, *The Messenger* **182**, 17 (2021), arXiv:2103.11631 [astro-ph.IM].
- [157] A. Wootten and A. R. Thompson, The atacama large millimeter/submillimeter array, *Proceedings of the IEEE* **97**, 1463 (2009).
- [158] W. E. Wilson, R. H. Ferris, P. Axtens, A. Brown, E. Davis, G. Hampson, M. Leach, P. Roberts, S. Saunders, B. S. Koribalski, *et al.*, The australia telescope compact array broad-band backend: description and first results, *Monthly Notices of the Royal Astronomical Society* **416**, 832 (2011).
- [159] J. J. Condon, W. Cotton, E. Greisen, Q. Yin, R. A. Perley, G. Taylor, and J. Broderick, The nrao vla sky survey, *The Astronomical Journal* **115**, 1693 (1998).
- [160] R. Braun, A. Bonaldi, T. Bourke, E. Keane, and J. Wagg, Anticipated ska1 science performance, in *SKA-TEL-SKO-0000818* (2017).
- [161] P. E. Dewdney, P. J. Hall, R. T. Schilizzi, and T. J. L. Lazio, The square kilometre array, *Proceedings of the IEEE* **97**, 1482 (2009).
- [162] B. Butler, W. Grammer, R. Selina, E. J. Murphy, and C. Carilli, The sensitivity of the next generation very large array (ngvla), in *American Astronomical Society Meeting Abstracts# 231*, Vol. 231 (2018) pp. 342–09.
- [163] B. Butler, W. Grammer, R. Selina, E. Murphy, and C. Carilli, *ngVLA Sensitivity*, Tech. Rep. (ngVLA Memo 21, 2019).
- [164] A. Lien, T. Sakamoto, N. Gehrels, D. M. Palmer, S. D. Barthelmy, C. Graziani, and J. K. Cannizzo, Probing the cosmic gamma-ray burst rate with trigger simulations of the swift burst alert telescope, *The Astrophysical Journal* **783**, 24 (2014).
- [165] A. von Kienlin, C. A. Meegan, W. S. Paciesas, P. N. Bhat, E. Bissaldi, M. S. Briggs, E. Burns, W. H. Cleveland, M. H. Gibby, M. M. Giles, A. Goldstein, R. Hamburg, C. M. Hui, D. Kocevski, B. Mailyan, C. Malacaria, S. Poolakkil, R. D.

- Preece, O. J. Roberts, P. Veres, and C. A. Wilson-Hodge, The Fourth Fermi-GBM Gamma-Ray Burst Catalog: A Decade of Data, *Astrophys. J.* **893**, 46 (2020), arXiv:2002.11460 [astro-ph.HE].
- [166] B. Arcier, *Detection of high-energy transients with SVOM-ECLAIRs*, Ph.D. thesis, IRAP, University of Toulouse (2022).
- [167] V. Bhalerao, D. Sawant, A. Pai, S. Tendulkar, S. Vadawale, D. Bhattacharya, V. Rana, H. K. L. Adalja, G. C. Anupama, S. Bala, S. Banerjee, J. Basu, H. Belatikar, P. Beniamini, M. Bhaganagare, A. Bhaskar, S. Bhattacharjee, S. Bose, B. Cenko, M. Vijay Chanda, G. Dewangan, V. Dixit, A. Dutta, P. Gawade, A. Ghodgaonkar, S. Kumar Goyal, S. Gunasekaran, M. Hemanth, K. Hotokezaka, S. Iyyani, P. J. Guruprasad, M. Kasliwal, J. G. Koyande, S. Kulkarni, A. Kutty, T. Ladiya, S. Mahapatra, D. Marla, S. Mate, A. Mehla, N. P. S. Mithun, S. More, R. Mote, D. Mukherjee, S. Narang, S. Narendranath, A. Nema, S. Nimbalkar, S. Nissankhe, S. Palit, J. Patel, A. Patel, B. Paul, P. Pradeep, P. Ramachandran, K. Roy, B. S. B. Saiguhan, J. Saji, M. Saleem, D. Saraogi, P. Sastry, M. Shanmugam, P. Sharma, A. Shetye, N. Singh, S. Singh, A. Singhal, S. Sreekumar, S. Sridhar, R. Srinivasan, S. Tallur, N. K. Tiwari, A. Lakshmi Vadladi, C. S. Vaishnava, S. Vishwakarma, and G. Waratkar, Science with the Daksha high energy transients mission, *Experimental Astronomy* **57**, 23 (2024), arXiv:2211.12052 [astro-ph.HE].
- [168] V. Bhalerao, S. Vadawale, S. Tendulkar, D. Bhattacharya, V. Rana, H. K. L. Adalja, H. Belatikar, M. Bhaganagare, G. Dewangan, A. Ghodgaonkar, S. Kumar Goyal, S. Gunasekaran, G. P. J. J. G. Koyande, S. Kulkarni, A. Kutty, T. Ladiya, S. Mahapatra, D. Marla, S. Mate, N. P. S. Mithun, R. Mote, S. Narang, A. Nema, S. Nimbalkar, A. Pai, S. Palit, A. Patel, J. Patel, P. Pradeep, P. Ramachandran, B. S. Bharath Saiguhan, D. Saraogi, D. Sawant, M. Shanmugam, P. Sharma, A. Shetye, N. Singh, S. Singh, A. Singhal, S. Sreekumar, S. Sridhar, R. Srinivasan, S. Tallur, N. K. Tiwari, A. Lakshmi Vadladi, C. S. Vaishnava, S. Vishwakarma, and G. Waratkar, Daksha: on alert for high energy transients, *Experimental Astronomy* **57**, 24 (2024), arXiv:2211.12055 [astro-ph.IM].
- [169] L. Amati, P. O'Brien, D. Götz, E. Bozzo, C. Tenzer, F. Frontera, G. Ghirlanda, C. Labanti, J. P. Osborne, G. Stratta, N. Tanvir, R. Willingale, P. Attina, R. Campana, A. J. Castro-Tirado, C. Contini, F. Fuschino, A. Gomboc, R. Hudec, P. Orleanski, E. Renotte, T. Rodic, Z. Bagoly, A. Blain, P. Callanan, S. Covino, A. Ferrara, E. Le Floch, M. Marisaldi, S. Mereghetti, P. Rosati, A. Vacchi, P. D'Avanzo, P. Giommi, S. Piranomonte, L. Piro, V. Reglero, A. Rossi, A. Santangelo, R. Salvaterra, G. Tagliaferri, S. Vergani, S. Vinciguerra, M. Briggs, E. Campolongo, R. Ciolfi, V. Connaughton, B. Cordier, B. Morelli, M. Orlandini, C. Adam, A. Argan, J. L. Atteia, N. Auricchio, L. Balazs, G. Baldazzi, S. Basa, R. Basak, P. Bellutti, M. G. Bernardini, G. Bertuccio, J. Braga, M. Branchesi, S. Brandt, E. Brocato, C. Budtz-Jorgensen, A. Bulgarelli, L. Burderi, J. Camp, S. Capozziello, J. Caruana, P. Casella, B. Cenko, P. Chardonnet, B. Ciardi, S. Colafrancesco, M. G. Dainotti, V. D'Elia, D. De Martino, M. De Pasquale, E. Del Monte, M. Della Valle, A. Drago, Y. Evangelista, M. Feroci, F. Finelli, M. Fiorini, J. Fynbo, A. Gal-Yam, B. Gendre, G. Ghisellini, A. Grado, C. Guidorzi, M. Hafizi, L. Hanlon, J. Hjorth, L. Izzo, L. Kiss, P. Kumar, I. Kuvvetli, M. Lavagna, T. Li, F. Longo, M. Lyutikov, U. Maio, E. Maiorano, P. Malcovati, D. Malesani, R. Margutti, A. Martin-Carrillo, N. Masetti, S. McBreen, R. Mignani, G. Morgante, C. Mundell, H. U. Nargaard-Nielsen, L. Nicastro, E. Palazzi, S. Paltani, F. Panessa, G. Pareschi, A. Pe'er, A. V. Pe-nacchioni, E. Pian, E. Piedipalumbo, T. Piran, G. Rauw, M. Razzano, A. Read, L. Rezzolla, P. Romano, R. Ruffini, S. Savaglio, V. Sguera, P. Schady, W. Skidmore, L. Song, E. Stanway, R. Starling, M. Topinka, E. Troja, M. van Putten, E. Vanzella, S. Vercellone, C. Wilson-Hodge, D. Yonetoku, G. Zampa, N. Zampa, B. Zhang, B. B. Zhang, S. Zhang, S. N. Zhang, A. Antonelli, F. Bianco, S. Boci, M. Boer, M. T. Botticella, O. Boulade, C. Butler, S. Campana, F. Capitanio, A. Celotti, Y. Chen, M. Colpi, A. Comastri, J. G. Cuby, M. Dadina, A. De Luca, Y. W. Dong, S. Etteri, P. Gandhi, E. Geza, J. Greiner, S. Guiriec, J. Harms, M. Hernanz, A. Hornstrup, I. Hutchinson, G. Israel, P. Jonker, Y. Kaneko, N. Kawai, K. Wiersema, S. Korpela, V. Lebrun, F. Lu, A. MacFadyen, G. Malaguti, L. Maraschi, A. Melandri, M. Modjaz, D. Morris, N. Omodei, A. Paizis, P. Páta, V. Petrosian, A. Rachevski, J. Rhoads, F. Ryde, L. Sabau-Graziati, N. Shigehiro, M. Sims, J. Soomin, D. Szécsi, Y. Urata, M. Uslenghi, L. Valenziano, G. Vianello, S. Vojtech, D. Watson, and J. Zicha, The THESEUS space mission concept: science case, design and expected performances, *Advances in Space Research* **62**, 191 (2018), arXiv:1710.04638 [astro-ph.IM].
- [170] L. Amati, P. T. O'Brien, D. Götz, E. Bozzo, A. Santangelo, N. Tanvir, F. Frontera, S. Mereghetti, J. P. Osborne, A. Blain, S. Basa, M. Branchesi, L. Burderi, M. Caballero-García, A. J. Castro-Tirado, L. Christensen, R. Ciolfi, A. De Rosa, V. Doroshenko, A. Ferrara, G. Ghirlanda, L. Hanlon, P. Heddermann, I. Hutchinson, C. Labanti, E. Le Floch, H. Lerman, S. Paltani, V. Reglero, L. Rezzolla, P. Rosati, R. Salvaterra, G. Stratta, C. Tenzer, and Theseus Consortium, The THESEUS space mission: science goals, requirements and mission concept, *Experimental Astronomy* **52**, 183 (2021), arXiv:2104.09531 [astro-ph.IM].
- [171] G. Ryan, H. van Eerten, L. Piro, and E. Troja, Gamma-Ray Burst Afterglows in the Multimessenger Era: Numerical Models and Closure Relations, *Astrophys. J.* **896**, 166 (2020), arXiv:1909.11691 [astro-ph.HE].
- [172] N. Gehrels, G. Chincarini, P. Giommi, K. O. Mason, J. A. Nousek, A. A. Wells, N. E. White, S. D. Barthelmy, D. N. Burrows, L. R. Cominsky, K. C. Hurley, F. E. Marshall, P. Mészáros, P. W. A. Roming, L. Angelini, L. M. Barbier, T. Belloni, S. Campana, P. A. Caraveo, M. M. Chester, O. Citterio, T. L. Cline, M. S. Cropper, J. R. Cummings, A. J. Dean, E. D. Feigelson, E. E. Fenimore, D. A. Frail, A. S. Fruchter, G. P. Garnire, K. Gendreau, G. Ghisellini, J. Greiner, J. E. Hill, S. D. Hunsberger, H. A. Krimm, S. R. Kulkarni, P. Kumar, F. Lebrun, N. M. Lloyd-Ronning, C. B. Markwardt, B. J. Mattson, R. F. Mushotzky, J. P. Norris, J. Osborne, B. Paczynski, D. M. Palmer, H. S. Park, A. M. Parsons, J. Paul, M. J. Rees, C. S. Reynolds, J. E. Rhoads, T. P. Sasseen, B. E. Schaefer, A. T. Short, A. P. Smale, I. A. Smith, L. Stella, G. Tagliaferri, T. Takahashi, M. Tashiro, L. K. Townsley, J. Tueller, M. J. L. Turner, M. Vietri, W. Voges, M. J. Ward, R. Willingale, F. M. Zerbi, and W. W. Zhang, The Swift Gamma-Ray Burst Mission, *Astrophys. J.* **611**, 1005 (2004), arXiv:astro-ph/0405233 [astro-ph].
- [173] D. N. Burrows, J. E. Hill, J. A. Nousek, J. A. Kennea, A. Wells, J. P. Osborne, A. F. Abbey, A. Beardmore, K. Mukerjee, A. D. T. Short, G. Chincarini, S. Campana, O. Citterio, A. Moretti, C. Pagani, G. Tagliaferri, P. Giommi, M. Capalbi, F. Tamburelli, L. Angelini, G. Cusumano, H. W. Bräuning, W. Burkert, and G. D. Hartner, The Swift X-Ray Telescope, *Space Sci. Rev.* **120**, 165 (2005), arXiv:astro-ph/0508071 [astro-ph].

- [174] J. Paul, J. Wei, S. Basa, and S.-N. Zhang, The Chinese-French SVOM mission for gamma-ray burst studies, *Comptes Rendus Physique* **12**, 298 (2011), arXiv:1104.0606 [astro-ph.HE].
- [175] B. Cordier, J. Wei, J. L. Atteia, S. Basa, A. Claret, F. Daigne, J. Deng, Y. Dong, O. Godet, A. Goldwurm, D. Götz, X. Han, A. Klotz, C. Lachaud, J. Osborne, Y. Qiu, S. Schanne, B. Wu, J. Wang, C. Wu, L. Xin, B. Zhang, and S. N. Zhang, The SVOM gamma-ray burst mission, arXiv e-prints , arXiv:1512.03323 (2015), arXiv:1512.03323 [astro-ph.IM].
- [176] Euclid Collaboration, Euclid. I. Overview of the Euclid mission, arXiv e-prints , arXiv:2405.13491 (2024), arXiv:2405.13491 [astro-ph.CO].
- [177] G. Mosby Jr, B. J. Rauscher, C. Bennett, E. S. Cheng, S. Cheung, A. Cillis, D. Content, D. Cottingham, R. Foltz, J. Gygax, *et al.*, Properties and characteristics of the nancy grace roman space telescope h4rg-10 detectors, *Journal of Astronomical Telescopes, Instruments, and Systems* **6**, 046001 (2020).
- [178] C. Macculi, A. Argan, M. D’Andrea, S. Lotti, G. Minervini, L. Piro, L. Ferrari Barusso, C. Boragno, E. Celasco, G. Gallucci, F. Gatti, D. Grossi, M. Rigano, F. Chiarello, G. Torrioli, M. Fiorini, M. Uslenghi, D. Brienza, E. Cavazzuti, S. Puccetti, A. Volpe, and P. Bastia, The Cryogenic Anticoincidence Detector for the NewAthena X-IFU Instrument: A Program Overview, *Condensed Matter* **8**, 108 (2023).
- [179] S. D. Barthelmy, L. M. Barbier, J. R. Cummings, E. E. Fenimore, N. Gehrels, D. Hullinger, H. A. Krimm, C. B. Markwardt, D. M. Palmer, A. Parsons, G. Sato, M. Suzuki, T. Takahashi, M. Tashiro, and J. Tueller, The Burst Alert Telescope (BAT) on the SWIFT Midex Mission, *Space Sci. Rev.* **120**, 143 (2005), arXiv:astro-ph/0507410 [astro-ph].
- [180] C. Meegan, G. Lichti, P. N. Bhat, E. Bissaldi, M. S. Briggs, V. Connaughton, R. Diehl, G. Fishman, J. Greiner, A. S. Hoover, A. J. van der Horst, A. von Kienlin, R. M. Kippen, C. Kouveliotou, S. McBreen, W. S. Paciesas, R. Preece, H. Steinle, M. S. Wallace, R. B. Wilson, and C. Wilson-Hodge, The Fermi Gamma-ray Burst Monitor, *Astrophys. J.* **702**, 791 (2009), arXiv:0908.0450 [astro-ph.IM].
- [181] M. Llamas Lanza, O. Godet, B. Arcier, M. Yassine, J. L. Atteia, and L. Bouchet, High-z gamma-ray burst detection by SVOM/ECLAIRS: Impact of instrumental biases on the bursts’ measured properties, *Astronomy & Astrophysics* **685**, A163 (2024), arXiv:2403.03266 [astro-ph.HE].
- [182] J. Tomsick, A. Zoglauer, C. Sleator, H. Lazar, J. Beechert, S. Boggs, J. Roberts, T. Siegert, A. Lowell, E. Wulf, E. Grove, B. Philips, T. Brandt, A. Smale, C. Kierans, E. Burns, D. Hartmann, M. Leising, M. Ajello, C. Fryer, M. Amman, H.-K. Chang, P. Jean, and P. von Ballmoos, The Compton Spectrometer and Imager, in *Bulletin of the American Astronomical Society*, Vol. 51 (2019) p. 98, arXiv:1908.04334 [astro-ph.IM].
- [183] J. A. Tomsick, S. E. Boggs, A. Zoglauer, D. Hartmann, M. Ajello, E. Burns, C. Fryer, C. Karwin, C. Kierans, A. Lowell, J. Malzac, J. Roberts, P. Saint-Hilaire, A. Shih, T. Siegert, C. Sleator, T. Takahashi, F. Tavecchio, E. Wulf, J. Beechert, H. Gulick, A. Joens, H. Lazar, E. Neights, J. C. Martinez Oliveros, S. Matsumoto, T. Melia, H. Yoneda, M. Amman, D. Bal, P. von Ballmoos, H. Bates, M. Böttcher, A. Bulgarelli, E. Cavazzuti, H.-K. Chang, C. Chen, C.-Y. Chu, A. Ciabattoni, L. Costamante, L. Dreyer, V. Fioretto, F. Fenu, S. Gallego, G. Ghirlanda, E. Grove, C.-Y. Huang, P. Jean, N. Khatiya, J. Knöldseder, M. Krause, M. Leising, T. R. Lewis, J. P. Lommel, L. Marcotulli, I. Martinez-Castellanos, S. Mittal, M. Negro, S. Al Nussirat, K. Nakazawa, U. Oberlack, D. Palmore, G. Panebianco, N. Parmiggiani, T. Parrotan, S. N. Pike, F. Rogers, H. Schutte, Y. Sheng, A. P. Smale, J. Smith, A. Trigg, T. Venters, Y. Watanabe, and H. Zhang, The Compton Spectrometer and Imager, arXiv e-prints , arXiv:2308.12362 (2023), arXiv:2308.12362 [astro-ph.HE].
- [184] H. C. Gulick, E. Neights, S. Al Nussirat, C. Tianyi Chen, K. Ching, C. Dove, A. Joens, C. Kierans, H. Liu, I. Martinez, R. Mician, S. Nagasawa, S. Nandyala, I. Schmidtke, D. Shah, A. Zoglauer, K. Nakazawa, T. Takahashi, J.-C. Martinez Oliveros, and J. A. Tomsick, Across the soft gamma-ray regime: utilizing simultaneous detections in the Compton Spectrometer and Imager (COSI) and the Background and Transient Observer (BTO) to understand astrophysical transients, arXiv e-prints , arXiv:2407.07155 (2024), arXiv:2407.07155 [astro-ph.HE].
- [185] R. Sari and A. A. Esin, On the Synchrotron Self-Compton Emission from Relativistic Shocks and Its Implications for Gamma-Ray Burst Afterglows, *Astrophys. J.* **548**, 787 (2001), arXiv:astro-ph/0005253 [astro-ph].
- [186] Y.-C. Zou, Y.-Z. Fan, and T. Piran, The possible high-energy emission from GRB 080319B and origins of the GeV emission of GRBs 080514B, 080916C and 081024B, *MNRAS* **396**, 1163 (2009), arXiv:0811.2997 [astro-ph].
- [187] P. Beniamini, L. Nava, R. B. Duran, and T. Piran, Energies of GRB blast waves and prompt efficiencies as implied by modelling of X-ray and GeV afterglows, *MNRAS* **454**, 1073 (2015), arXiv:1504.04833 [astro-ph.HE].
- [188] T. E. Jacobich, P. Beniamini, and A. J. van der Horst, Modelling synchrotron self-Compton and Klein-Nishina effects in gamma-ray burst afterglows, *MNRAS* **504**, 528 (2021), arXiv:2007.04418 [astro-ph.HE].
- [189] G. A. McCarthy and T. Laskar, Klein-Nishina Corrections to the Spectra and Light Curves of Gamma-ray Burst Afterglows, arXiv e-prints , arXiv:2405.11309 (2024), arXiv:2405.11309 [astro-ph.HE].
- [190] B. O’Connor, P. Beniamini, and C. Kouveliotou, Constraints on the circumburst environments of short gamma-ray bursts, *MNRAS* **495**, 4782 (2020), arXiv:2004.00031 [astro-ph.HE].
- [191] M. A. Aloy, H. T. Janka, and E. Müller, Relativistic outflows from remnants of compact object mergers and their viability for short gamma-ray bursts, *Astronomy & Astrophysics* **436**, 273 (2005), arXiv:astro-ph/0408291 [astro-ph].
- [192] E. Troja, H. van Eerten, B. Zhang, G. Ryan, L. Piro, R. Ricci, B. O’Connor, M. H. Wieringa, S. B. Cenko, and T. Sakamoto, A thousand days after the merger: Continued X-ray emission from GW170817, *MNRAS* **498**, 5643 (2020), arXiv:2006.01150 [astro-ph.HE].
- [193] E. Troja, C. L. Fryer, B. O’Connor, G. Ryan, S. Dichiara, A. Kumar, N. Ito, R. Gupta, R. T. Wollaeger, J. P. Norris, N. Kawai, N. R. Butler, A. Aryan, K. Misra, R. Hosokawa, K. L. Murata, M. Niwano, S. B. Pandey, A. Kutyrev, H. J. van Eerten, E. A. Chase, Y. D. Hu, M. D. Caballero-Garcia, and A. J. Castro-Tirado, A nearby long gamma-ray burst from a merger of compact objects, *Nature (London)* **612**, 228 (2022), arXiv:2209.03363 [astro-ph.HE].
- [194] E.-W. Liang, S.-X. Yi, J. Zhang, H.-J. Lü, B.-B. Zhang, and B. Zhang, Constraining Gamma-ray Burst Initial Lorentz Factor with the Afterglow Onset Feature and Discovery of a Tight Γ_0 -E γ_{iso} Correlation, *Astrophys. J.* **725**, 2209 (2010), arXiv:0912.4800 [astro-ph.HE].
- [195] J. Lü, Y.-C. Zou, W.-H. Lei, B. Zhang, Q. Wu, D.-X. Wang, E.-W. Liang, and H.-J. Lü, Lorentz-factor-Isotropic-luminosity/Energy Correlations of Gamma-Ray Bursts and Their Interpretation, *Astrophys. J.* **751**, 49 (2012), arXiv:1109.3757 [astro-ph.HE].

- [196] G. Ghirlanda, G. Ghisellini, L. Nava, R. Salvaterra, G. Tagliaferri, S. Campana, S. Covino, P. D’Avanzo, D. Fugazza, A. Melandri, and S. D. Vergani, The impact of selection biases on the E_{peak} - L_{ISO} correlation of gamma-ray bursts, *MNRAS* **422**, 2553 (2012), arXiv:1203.0003 [astro-ph.HE].
- [197] G. Ghirlanda, F. Nappo, G. Ghisellini, A. Melandri, G. Marcarini, L. Nava, O. S. Salafia, S. Campana, and R. Salvaterra, Bulk Lorentz factors of gamma-ray bursts, *Astronomy & Astrophysics* **609**, A112 (2018), arXiv:1711.06257 [astro-ph.HE].
- [198] M. Müller, S. Mukherjee, and G. Ryan, Be careful in multi-messenger inference of the Hubble constant: A path forward for robust inference, *arXiv e-prints*, arXiv:2406.11965 (2024), arXiv:2406.11965 [astro-ph.CO].
- [199] P. Beniamini, M. Petropoulou, R. Barniol Duran, and D. Giannios, A lesson from GW170817: most neutron star mergers result in tightly collimated successful GRB jets, *MNRAS* **483**, 840 (2019), arXiv:1808.04831 [astro-ph.HE].
- [200] G. Ghirlanda, O. S. Salafia, A. Pescalli, G. Ghisellini, R. Salvaterra, E. Chassande-Mottin, M. Colpi, F. Nappo, P. D’Avanzo, A. Melandri, M. G. Bernardini, M. Branchesi, S. Campana, R. Ciolfi, S. Covino, D. Götz, S. D. Vergani, M. Zennaro, and G. Tagliaferri, Short gamma-ray bursts at the dawn of the gravitational wave era, *Astronomy & Astrophysics* **594**, A84 (2016), arXiv:1607.07875 [astro-ph.HE].
- [201] S. Mandhai, G. P. Lamb, N. R. Tanvir, J. Bray, C. J. Nixon, R. A. J. Eyles-Ferris, A. J. Levan, and B. P. Gompertz, Exploring compact binary merger host galaxies and environments with zELDA, *MNRAS* **514**, 2716 (2022), arXiv:2109.09714 [astro-ph.HE].
- [202] W. Fong, E. Berger, R. Chornock, R. Margutti, A. J. Levan, N. R. Tanvir, R. L. Tunnicliffe, I. Czekala, D. B. Fox, D. A. Perley, S. B. Cenko, B. A. Zauderer, T. Laskar, S. E. Persson, A. J. Monson, D. D. Kelson, C. Birk, D. Murphy, M. Servillat, and G. Anglada, Demographics of the Galaxies Hosting Short-duration Gamma-Ray Bursts, *Astrophys. J.* **769**, 56 (2013), arXiv:1302.3221 [astro-ph.HE].
- [203] W.-f. Fong, A. E. Nugent, Y. Dong, E. Berger, K. Paterson, R. Chornock, A. Levan, P. Blanchard, K. D. Alexander, J. Andrews, B. E. Cobb, A. Cucchiara, D. Fox, C. L. Fryer, A. C. Gordon, C. D. Kilpatrick, R. Lunnan, R. Margutti, A. Miller, P. Milne, M. Nicholl, D. Perley, J. Rastinejad, A. R. Escorial, G. Schroeder, N. Smith, N. Tanvir, and G. Terreran, Short GRB Host Galaxies. I. Photometric and Spectroscopic Catalogs, Host Associations, and Galactocentric Offsets, *Astrophys. J.* **940**, 56 (2022), arXiv:2206.01763 [astro-ph.GA].
- [204] A. E. Nugent, W.-F. Fong, Y. Dong, J. Leja, E. Berger, M. Zevin, R. Chornock, B. E. Cobb, L. Z. Kelley, C. D. Kilpatrick, A. Levan, R. Margutti, K. Paterson, D. Perley, A. R. Escorial, N. Smith, and N. Tanvir, Short GRB Host Galaxies. II. A Legacy Sample of Redshifts, Stellar Population Properties, and Implications for Their Neutron Star Merger Origins, *Astrophys. J.* **940**, 57 (2022), arXiv:2206.01764 [astro-ph.GA].
- [205] B. O’Connor, E. Troja, S. Dichiara, P. Beniamini, S. B. Cenko, C. Kouveliotou, J. B. González, J. Durbak, P. Gatkine, A. Kutyrev, T. Sakamoto, R. Sánchez-Ramírez, and S. Veilleux, A deep survey of short GRB host galaxies over $z \sim 0.2$: implications for offsets, redshifts, and environments, *MNRAS* **515**, 4890 (2022), arXiv:2204.09059 [astro-ph.HE].
- [206] L. Nava, G. Vianello, N. Omodei, G. Ghisellini, G. Ghirlanda, A. Celotti, F. Longo, R. Desiante, and R. Barniol Duran, Clustering of LAT light curves: a clue to the origin of high-energy emission in gamma-ray bursts, *MNRAS* **443**, 3578 (2014), arXiv:1406.6693 [astro-ph.HE].
- [207] P. Beniamini and A. J. van der Horst, Electrons’ energy in GRB afterglows implied by radio peaks, *MNRAS* **472**, 3161 (2017), arXiv:1706.07817 [astro-ph.HE].
- [208] R. A. Duncan, A. J. van der Horst, and P. Beniamini, Constraints on electron acceleration in gamma-ray bursts afterglows from radio peaks, *MNRAS* **518**, 1522 (2023), arXiv:2211.00686 [astro-ph.HE].
- [209] R. Barniol Duran, Constraining the magnetic field in GRB relativistic collisionless shocks using radio data, *MNRAS* **442**, 3147 (2014), arXiv:1311.1216 [astro-ph.HE].
- [210] R. Santana, R. Barniol Duran, and P. Kumar, Magnetic Fields in Relativistic Collisionless Shocks, *Astrophys. J.* **785**, 29 (2014), arXiv:1309.3277 [astro-ph.HE].
- [211] B.-B. Zhang, H. van Eerten, D. N. Burrows, G. S. Ryan, P. A. Evans, J. L. Racusin, E. Troja, and A. MacFadyen, An Analysis of Chandra Deep Follow-up Gamma-Ray Bursts: Implications for Off-axis Jets, *Astrophys. J.* **806**, 15 (2015), arXiv:1405.4867 [astro-ph.HE].
- [212] R. Sari, T. Piran, and J. P. Halpern, Jets in Gamma-Ray Bursts, *The Astrophysical Journal Letters* **519**, L17 (1999), arXiv:astro-ph/9903339 [astro-ph].
- [213] J. E. Rhoads, The Dynamics and Light Curves of Beamed Gamma-Ray Burst Afterglows, *Astrophys. J.* **525**, 737 (1999), arXiv:astro-ph/9903399 [astro-ph].
- [214] D. A. Frail, S. R. Kulkarni, R. Sari, S. G. Djorgovski, J. S. Bloom, T. J. Galama, D. E. Reichart, E. Berger, F. A. Harrison, P. A. Price, S. A. Yost, A. Diercks, R. W. Goodrich, and F. Chaffee, Beaming in Gamma-Ray Bursts: Evidence for a Standard Energy Reservoir, *The Astrophysical Journal Letters* **562**, L55 (2001), arXiv:astro-ph/0102282 [astro-ph].
- [215] G. P. Lamb, J. J. Fernández, F. Hayes, A. K. H. Kong, E.-T. Lin, N. R. Tanvir, M. Hendry, I. S. Heng, S. Saha, and J. Veitch, Inclination Estimates from Off-Axis GRB Afterglow Modelling, *Universe* **7**, 329 (2021), arXiv:2109.00424 [astro-ph.HE].
- [216] J.-N. Li, Y.-Y. Wang, Y. Wang, Z.-P. Jin, S. Covino, and Y.-Z. Fan, The detection prospect of the Counter Jet radiation in the Late Afterglow of GRB 170817A, *arXiv e-prints*, arXiv:2401.17978 (2024), arXiv:2401.17978 [astro-ph.HE].
- [217] P. Beniamini, L. Nava, and T. Piran, A revised analysis of gamma-ray bursts’ prompt efficiencies, *MNRAS* **461**, 51 (2016), arXiv:1606.00311 [astro-ph.HE].
- [218] D. Wanderman and T. Piran, The rate, luminosity function and time delay of non-Collapsar short GRBs, *MNRAS* **448**, 3026 (2015), arXiv:1405.5878 [astro-ph.HE].
- [219] O. S. Salafia, M. E. Ravasio, G. Ghirlanda, and I. Mandel, The short gamma-ray burst population in a quasi-universal jet scenario, *Astronomy & Astrophysics* **680**, A45 (2023), arXiv:2306.15488 [astro-ph.HE].
- [220] R. Gill, J. Granot, and P. Kumar, Linear polarization in gamma-ray burst prompt emission, *MNRAS* **491**, 3343 (2020), arXiv:1811.11555 [astro-ph.HE].
- [221] G. P. Lamb and S. Kobayashi, Low- Γ Jets from Compact Stellar Mergers: Candidate Electromagnetic Counterparts to Gravitational Wave Sources, *Astrophys. J.* **829**, 112 (2016), arXiv:1605.02769 [astro-ph.HE].
- [222] P. Beniamini, R. B. Duran, M. Petropoulou, and D. Giannios, Ready, Set, Launch: Time Interval between a Binary Neutron Star Merger and Short Gamma-Ray Burst Jet Formation, *The Astrophysical Journal Letters* **895**, L33 (2020), arXiv:2001.00950 [astro-ph.HE].
- [223] K. Ioka and T. Nakamura, Can an off-axis gamma-ray burst jet in GW170817 explain all the electromagnetic counter-

- parts?, *Progress of Theoretical and Experimental Physics* **2018**, 043E02 (2018), arXiv:1710.05905 [astro-ph.HE].
- [224] D. Lazzati, A. Deich, B. J. Morsony, and J. C. Workman, Off-axis emission of short γ -ray bursts and the detectability of electromagnetic counterparts of gravitational-wave-detected binary mergers, *MNRAS* **471**, 1652 (2017), arXiv:1610.01157 [astro-ph.HE].
- [225] P. C. Duffell, E. Quataert, D. Kasen, and H. Klion, Jet Dynamics in Compact Object Mergers: GW170817 Likely Had a Successful Jet, *Astrophys. J.* **866**, 3 (2018), arXiv:1806.10616 [astro-ph.HE].
- [226] O. S. Salafia, G. Ghisellini, and G. Ghirlanda, Jet-driven and jet-less fireballs from compact binary mergers, *MNRAS* **474**, L7 (2018), arXiv:1710.05859 [astro-ph.HE].
- [227] O. Bromberg, A. Tchekhovskoy, O. Gottlieb, E. Nakar, and T. Piran, The γ -rays that accompanied GW170817 and the observational signature of a magnetic jet breaking out of NS merger ejecta, *MNRAS* **475**, 2971 (2018), arXiv:1710.05897 [astro-ph.HE].
- [228] O. Gottlieb, E. Nakar, T. Piran, and K. Hotokezaka, A cocoon shock breakout as the origin of the γ -ray emission in GW170817, *MNRAS* **479**, 588 (2018), arXiv:1710.05896 [astro-ph.HE].
- [229] E. Nakar, O. Gottlieb, T. Piran, M. M. Kasliwal, and G. Hallinan, From γ to Radio: The Electromagnetic Counterpart of GW170817, *Astrophys. J.* **867**, 18 (2018), arXiv:1803.07595 [astro-ph.HE].
- [230] T. Matsumoto, E. Nakar, and T. Piran, Constraints on the emitting region of the gamma-rays observed in GW170817, *MNRAS* **483**, 1247 (2019), arXiv:1807.04756 [astro-ph.HE].
- [231] S. Dichiara, E. Troja, B. O'Connor, F. E. Marshall, P. Beniamini, J. K. Cannizzo, A. Y. Lien, and T. Sakamoto, Short gamma-ray bursts within 200 Mpc, *MNRAS* **492**, 5011 (2020), arXiv:1912.08698 [astro-ph.HE].
- [232] D. Band, J. Matteson, L. Ford, B. Schaefer, D. Palmer, B. Teegarden, T. Cline, M. Briggs, W. Paciesas, G. Pendleton, G. Fishman, C. Kouveliotou, C. Meegan, R. Wilson, and P. Lestrade, BATSE Observations of Gamma-Ray Burst Spectra. I. Spectral Diversity, *Astrophys. J.* **413**, 281 (1993).
- [233] L. Nava, G. Ghirlanda, G. Ghisellini, and A. Celotti, Spectral properties of 438 GRBs detected by Fermi/GBM, *Astronomy & Astrophysics* **530**, A21 (2011), arXiv:1012.2863 [astro-ph.HE].
- [234] D. Grupe, D. N. Burrows, S. K. Patel, C. Kouveliotou, B. Zhang, P. Mészáros, R. A. M. Wijers, and N. Gehrels, Jet Breaks in Short Gamma-Ray Bursts. I. The Uncollimated Afterglow of GRB 050724, *Astrophys. J.* **653**, 462 (2006), arXiv:astro-ph/0603773 [astro-ph].
- [235] D. N. Burrows, D. Grupe, M. Capalbi, A. Panaitescu, S. K. Patel, C. Kouveliotou, B. Zhang, P. Mészáros, G. Chincarini, N. Gehrels, and R. A. M. Wijers, Jet Breaks in Short Gamma-Ray Bursts. II. The Collimated Afterglow of GRB 051221A, *Astrophys. J.* **653**, 468 (2006), arXiv:astro-ph/0604320 [astro-ph].
- [236] A. M. Soderberg, E. Berger, M. Kasliwal, D. A. Frail, P. A. Price, B. P. Schmidt, S. R. Kulkarni, D. B. Fox, S. B. Cenko, A. Gal-Yam, E. Nakar, and K. C. Roth, The Afterglow, Energetics, and Host Galaxy of the Short-Hard Gamma-Ray Burst 051221a, *Astrophys. J.* **650**, 261 (2006), arXiv:astro-ph/0601455 [astro-ph].
- [237] A. Nicuesa Guelbenzu, S. Klose, J. Greiner, D. A. Kann, T. Krühler, A. Rossi, S. Schulze, P. M. J. Afonso, J. Elliott, R. Filgas, D. H. Hartmann, A. Küpcü Yoldaş, S. McBreen, M. Nardini, F. Olivares E., A. Rau, S. Schmidl, P. Schady, V. Sudilovsky, A. C. Updike, and A. Yoldaş, Multi-color observations of short GRB afterglows: 20 events observed between 2007 and 2010, *Astronomy & Astrophysics* **548**, A101 (2012), arXiv:1206.1806 [astro-ph.HE].
- [238] E. Berger, B. A. Zauderer, A. Levan, R. Margutti, T. Laskar, W. Fong, V. Mangano, D. B. Fox, R. L. Tunnicliffe, R. Chornock, N. R. Tanvir, K. M. Menten, J. Hjorth, K. Roth, and T. J. Dupuy, The Afterglow and ULIRG Host Galaxy of the Dark Short GRB 120804A, *Astrophys. J.* **765**, 121 (2013), arXiv:1209.5423 [astro-ph.HE].
- [239] W. Fong, E. Berger, R. Margutti, B. A. Zauderer, E. Troja, I. Czekala, R. Chornock, N. Gehrels, T. Sakamoto, D. B. Fox, and P. Podsiadlowski, A Jet Break in the X-Ray Light Curve of Short GRB 111020A: Implications for Energetics and Rates, *Astrophys. J.* **756**, 189 (2012), arXiv:1204.5475 [astro-ph.HE].
- [240] W. Fong, E. Berger, B. D. Metzger, R. Margutti, R. Chornock, G. Migliori, R. J. Foley, B. A. Zauderer, R. Lunnan, T. Laskar, S. J. Desch, K. J. Meech, S. Sonnett, C. Dickey, A. Hellund, and P. Harding, Short GRB 130603B: Discovery of a Jet Break in the Optical and Radio Afterglows, and a Mysterious Late-time X-Ray Excess, *Astrophys. J.* **780**, 118 (2014), arXiv:1309.7479 [astro-ph.HE].
- [241] Z.-P. Jin, X. Li, H. Wang, Y.-Z. Wang, H.-N. He, Q. Yuan, F.-W. Zhang, Y.-C. Zou, Y.-Z. Fan, and D.-M. Wei, Short GRBs: Opening Angles, Local Neutron Star Merger Rate, and Off-axis Events for GRB/GW Association, *Astrophys. J.* **857**, 128 (2018), arXiv:1708.07008 [astro-ph.HE].
- [242] E. Troja, T. Sakamoto, S. B. Cenko, A. Lien, N. Gehrels, A. J. Castro-Tirado, R. Ricci, J. Capone, V. Toy, A. Kutyrev, N. Kawai, A. Cucchiara, A. Fruchter, J. Gorosabel, S. Jeong, A. Levan, D. Perley, R. Sanchez-Ramirez, N. Tanvir, and S. Veilleux, An Achromatic Break in the Afterglow of the Short GRB 140903A: Evidence for a Narrow Jet, *Astrophys. J.* **827**, 102 (2016), arXiv:1605.03573 [astro-ph.HE].
- [243] E. Troja, A. J. Castro-Tirado, J. Becerra González, Y. Hu, G. S. Ryan, S. B. Cenko, R. Ricci, G. Novara, R. Sánchez-Rámirez, J. A. Acosta-Pulido, K. D. Ackley, M. D. Caballero García, S. S. Eikenberry, S. Guziy, S. Jeong, A. Y. Lien, I. Márquez, S. B. Pandey, I. H. Park, T. Sakamoto, J. C. Tello, I. V. Sokolov, V. V. Sokolov, A. Tiengo, A. F. Valeev, B. B. Zhang, and S. Veilleux, The afterglow and kilonova of the short GRB 160821B, *MNRAS* **489**, 2104 (2019), arXiv:1905.01290 [astro-ph.HE].
- [244] G. P. Lamb, N. R. Tanvir, A. J. Levan, A. de Ugarte Postigo, K. Kawaguchi, A. Corsi, P. A. Evans, B. Gompertz, D. B. Malesani, K. L. Page, K. Wiersema, S. Rosswog, M. Shibata, M. Tanaka, A. J. van der Horst, Z. Cano, J. P. U. Fynbo, A. S. Fruchter, J. Greiner, K. E. Heintz, A. Higgins, J. Hjorth, L. Izzo, P. Jakobsson, D. A. Kann, P. T. O'Brien, D. A. Perley, E. Pian, G. Pugliese, R. L. C. Starling, C. C. Thöne, D. Watson, R. A. M. J. Wijers, and D. Xu, Short GRB 160821B: A Reverse Shock, a Refreshed Shock, and a Well-sampled Kilonova, *Astrophys. J.* **883**, 48 (2019), arXiv:1905.02159 [astro-ph.HE].
- [245] R. L. Becerra, S. Dichiara, A. M. Watson, E. Troja, N. Fraija, A. Klotz, N. R. Butler, W. H. Lee, P. Veres, D. Turpin, J. S. Bloom, M. Boer, J. J. González, A. S. Kutyrev, J. X. Prochaska, E. Ramirez-Ruiz, and M. G. Richer, Reverse Shock Emission Revealed in Early Photometry in the Candidate Short GRB 180418A, *Astrophys. J.* **881**, 12 (2019), arXiv:1904.05987 [astro-ph.HE].
- [246] B. O'Connor, E. Troja, S. Dichiara, E. A. Chase, G. Ryan, S. B. Cenko, C. L. Fryer, R. Ricci, F. Marshall, C. Kouve-

- Iliotou, R. T. Wollaeger, C. J. Fontes, O. Korobkin, P. Gatkine, A. Kutyrev, S. Veilleux, N. Kawai, and T. Sakamoto, A tale of two mergers: constraints on kilonova detection in two short GRBs at $z \sim 0.5$, *MNRAS* **502**, 1279 (2021), arXiv:2012.00026 [astro-ph.HE].
- [247] W. Fong, T. Laskar, J. Rastinejad, A. R. Escorial, G. Schroeder, J. Barnes, C. D. Kilpatrick, K. Paterson, E. Berger, B. D. Metzger, Y. Dong, A. E. Nugent, R. Straubbaugh, P. K. Blanchard, A. Goyal, A. Cucchiara, G. Terrian, K. D. Alexander, T. Eftekhar, C. Fryer, B. Margalit, R. Margutti, and M. Nicholl, The Broadband Counterpart of the Short GRB 200522A at $z = 0.5536$: A Luminous Kilonova or a Collimated Outflow with a Reverse Shock?, *Astrophys. J.* **906**, 127 (2021), arXiv:2008.08593 [astro-ph.HE].
- [248] A. Rouco Escorial, W. Fong, P. Veres, T. Laskar, A. Lien, K. Paterson, M. Lally, P. K. Blanchard, A. E. Nugent, N. R. Tanvir, D. Cornish, E. Berger, E. Burns, S. B. Cenko, B. E. Cobb, A. Cucchiara, A. Goldstein, R. Margutti, B. D. Metzger, P. Milne, A. Levan, M. Nicholl, and N. Smith, GRB 180418A: A Possibly Short Gamma-Ray Burst with a Wide-angle Outflow in a Faint Host Galaxy, *Astrophys. J.* **912**, 95 (2021), arXiv:2012.09961 [astro-ph.HE].
- [249] T. Laskar, A. R. Escorial, G. Schroeder, W.-f. Fong, E. Berger, P. Veres, S. Bhandari, J. Rastinejad, C. D. Kilpatrick, A. Tohuvavohu, R. Margutti, K. D. Alexander, J. DeLaunay, J. A. Kennea, A. Nugent, K. Paterson, and P. K. G. Williams, The First Short GRB Millimeter Afterglow: The Wide-angled Jet of the Extremely Energetic SGRB 211106A, *The Astrophysical Journal Letters* **935**, L11 (2022), arXiv:2205.03419 [astro-ph.HE].
- [250] P. Beniamini, R. Gill, and J. Granot, Robust features of off-axis gamma-ray burst afterglow light curves, *MNRAS* **515**, 555 (2022), arXiv:2204.06008 [astro-ph.HE].
- [251] R. Gill, J. Granot, F. De Colle, and G. Urrutia, Numerical Simulations of an Initially Top-hat Jet and the Afterglow of GW170817/GRB170817A, *Astrophys. J.* **883**, 15 (2019), arXiv:1902.10303 [astro-ph.HE].
- [252] G. Ashton, E. Burns, T. D. Canton, T. Dent, H.-B. Eggenstein, A. B. Nielsen, R. Prix, M. Was, and S. J. Zhu, Coincident detection significance in multimessenger astronomy, *The Astrophysical Journal* **860**, 6 (2018).
- [253] A. Palmese, M. Fishbach, C. J. Burke, J. T. Annis, and X. Liu, Do LIGO/Virgo Black Hole Mergers Produce AGN Flares? The Case of GW190521 and Prospects for Reaching a Confident Association, *Astrophys. J. Lett.* **914**, L34 (2021), arXiv:2103.16069 [astro-ph.HE].
- [254] H. Tagawa, S. S. Kimura, Z. Haiman, R. Perna, and I. Bartos, Observable Signature of Merging Stellar-mass Black Holes in Active Galactic Nuclei, *Astrophys. J.* **950**, 13 (2023), arXiv:2301.07111 [astro-ph.HE].
- [255] M. Graham, K. Ford, B. McKernan, N. Ross, D. Stern, K. Burge, M. Coughlin, S. Djorgovski, A. Drake, D. Duev, M. Kasliwal, A. Mahabal, S. van Velzen, J. Belecki, E. Bellm, R. Burruss, S. Cenko, V. Cunningham, G. Helou, S. Kulkarni, F. Masci, T. Prince, D. Reiley, H. Rodriguez, B. Rusholme, R. Smith, and M. Soumagnac, Candidate electromagnetic counterpart to the binary black hole merger gravitational-wave event s190521g, *Physical Review Letters* **124**, 10.1103/physrevlett.124.251102 (2020).
- [256] M. J. Graham, B. McKernan, K. E. S. Ford, D. Stern, S. G. Djorgovski, M. Coughlin, K. B. Burge, E. C. Bellm, G. Helou, A. A. Mahabal, F. J. Masci, J. Purdum, P. Rosnet, and B. Rusholme, A Light in the Dark: Searching for Electromagnetic Counterparts to Black Hole-Black Hole Mergers in LIGO/Virgo O3 with the Zwicky Transient Facility, *Astrophys. J.* **942**, 99 (2023), arXiv:2209.13004 [astro-ph.HE].
- [257] T. Cabrera, A. Palmese, L. Hu, B. O'Connor, K. E. S. Ford, B. McKernan, I. Andreoni, T. Ahumada, A. Am sellem, M. Busmann, P. Clark, M. W. Coughlin, E. Dadiani, V. Diaz, M. J. Graham, D. Gruen, K. Kunnumkai, J. Postiglione, J. S. Sommer, and F. Valdes, Searching for electromagnetic emission in an AGN from the gravitational wave binary black hole merger candidate S230922g, arXiv e-prints , arXiv:2407.10698 (2024), arXiv:2407.10698 [astro-ph.HE].
- [258] C. R. Bom and A. Palmese, Standard siren cosmology with gravitational waves from binary black hole mergers in active galactic nuclei, *Phys. Rev. D* **110**, 083005 (2024).
- [259] H. Wang, R. G. Dastidar, D. Giannios, and P. C. Duffell, jetsimpy: A Highly Efficient Hydrodynamic Code for Gamma-ray Burst Afterglow, arXiv e-prints , arXiv:2402.19359 (2024), arXiv:2402.19359 [astro-ph.HE].
- [260] R. Sari and T. Piran, Predictions for the Very Early Afterglow and the Optical Flash, *Astrophys. J.* **520**, 641 (1999), arXiv:astro-ph/9901338 [astro-ph].
- [261] E. Molinari, S. D. Vergani, D. Malesani, S. Covino, P. D'Avanzo, G. Chincarini, F. M. Zerbi, L. A. Antonelli, P. Conconi, V. Testa, G. Tosti, F. Vitali, F. D'Alessio, G. Malaspina, L. Nicastro, E. Palazzi, D. Guetta, S. Campana, P. Goldoni, N. Masetti, E. J. A. Meurs, A. Monfar dini, L. Norci, E. Pian, S. Piranomonte, D. Rizzato, M. Stefanon, L. Stella, G. Tagliaferri, P. A. Ward, G. Ihle, L. Gonzalez, A. Pizarro, P. Sinclair, and J. Valenzuela, REM ob servations of GRB 060418 and GRB 060607A: the onset of the afterglow and the initial fireball Lorentz factor determina tion, *Astronomy & Astrophysics* **469**, L13 (2007), arXiv:astro-ph/0612607 [astro-ph].
- [262] G. Ghisellini, G. Ghirlanda, L. Nava, and A. Celotti, GeV emission from gamma-ray bursts: a radiative fireball?, *MNRAS* **403**, 926 (2010), arXiv:0910.2459 [astro-ph.HE].
- [263] L. Nava, L. Sironi, G. Ghisellini, A. Celotti, and G. Ghirlanda, Afterglow emission in gamma-ray bursts - I. Pair-enriched ambient medium and radiative blast waves, *MNRAS* **433**, 2107 (2013), arXiv:1211.2806 [astro-ph.HE].
- [264] F. Nappo, G. Ghisellini, G. Ghirlanda, A. Melandri, L. Nava, and D. Burlon, Afterglows from precursors in gamma-ray bursts. Application to the optical afterglow of GRB 091024, *MNRAS* **445**, 1625 (2014), arXiv:1405.3981 [astro-ph.HE].